Title
Under Pressure: The Role of Retinal Astrocytes and the Response to Ocular Hypertension

Author
Cullen, Paul Francis

Publication Date
2021

Peer reviewed|Thesis/dissertation

Under Pressure: The Role of Retinal Astrocytes and the Response to Ocular Hypertension

By

Paul F Cullen

A dissertation submitted in partial satisfaction of the

requirements for the degree of

Doctor of Philosophy

in

Vision Science

in the

Graduate Division

of the

University of California, Berkeley

Committee in charge:
Professor John Flanagan, Chair
Professor Kaoru Saijo
Professor John Flannery

Spring 2021

Abstract

Under Pressure: The Role of Retinal Astrocytes
and the Response to Ocular Hypertension

by

Paul F Cullen

Doctor of Philosophy in Vision Science

University of California, Berkeley

Professor John Flanagan, Chair

The vertebrate retina – a thin layer of photosensitive tissue that forms from a protrusion of the early brain during development – is a highly conserved structure essential for functioning sight. Although there are modest variations from species to species, across taxa the overall structure is largely the same: photoreceptor cells at the back of the retina sense light, multiple types of interneurons in the intermediate layers perform computational comparisons that sharpen the image, and the retinal ganglion cells at the front of the retina aggregate these signals, transmitting them to the brain through their axons, which form the optic nerve. The retina is a highly energy intensive structure, however, and it is in part through their adaptations to provide additional blood flow to this tissue that the retinas of distinct groups of vertebrates differ.

In humans and other mammals, a unique type of astrocyte – a class of non-neuronal support cell that maintains homeostasis in the central nervous system and responds to injury or infection via a process known as reactivity – emerges from the optic nerve head during development to facilitate the direct vascularization of the retina, which is a sharp departure from most other vertebrate species. These astrocytes tile the surface of the retina, and like their counterparts in the optic nerve, are closely associated with both blood vessels and the delicate axons of the retinal ganglion cells, although their full range of functions is yet to be elucidated. During glaucoma, a disease of the retina and optic nerve head that causes progressive and irreversible vision loss, the vulnerable axons of retinal ganglion cells degenerate, leading to the death of these irreplaceable cells. Although some risk factors such as age and elevated intraocular pressure have been identified, and treatments have been developed that can slow this degeneration to an extent, much remains unknown about this condition, which affects tens of millions around the world and is a leading cause of blindness.

Notably, the known risk factors are only modestly predictive of development or progression of glaucoma, suggesting that other elements of the visual pathway may contribute, whether positively or negatively, to retinal ganglion cell survival. A number of studies have indicated a role for retinal and optic nerve head astrocytes in the loss of retinal ganglion cells during the

most common form of glaucoma, primary open angle glaucoma. Recent research has suggested that these astrocytes undergo changes that result in a loss of neuroprotective behavior, a gain of neurotoxic behavior, or some combination of the two. Understanding the contributions of retinal astrocytes to this debilitating disease, and determining whether they are a suitable target for treatment, requires close study of these incompletely understood cells.

As the primary obstacle to investigating these cells has been their sparseness – retinal astrocytes are estimated to represent less than 0.1% of cells in the retina – I have developed a novel method in order to rapidly isolate these cells. This method, which relies on the characteristic layering of the retina, involves directly removing the astrocytes by first treating the retina with an enzyme to breakdown the extracellular matrix, then mechanically removing the astrocyte layer as a single, thin sheet. It possesses a number of advantages, including speed and the versatility of the samples generated, which can be used both for molecular biology techniques as well as immunostaining.

By combining this retinal astrocyte isolation technique – which I termed the 'astrocyte pulloff' in reference to earlier techniques that were attempted on retinal ganglion cells – with an *in vivo* model of ocular hypertension, I investigated the changes undergone by these cells in response to changes in intraocular pressure that mimic some elements of glaucoma, such as the death of retinal ganglion cells. This model, performed by treating the episcleral veins with brief laser pulses to induce photocoagulation, drives an in increase in pressure inside the eye that lasts for approximately one week, during which a significant fraction of retinal ganglion cells are lost. In order to study the changes that retinal astrocytes undergo as a result of this process, I employed a technology called RNA sequencing, which is used to generate a profile of the genes being expressed by cells at the time of isolation. This allowed me to identify key genes that undergo changes in response to this treatment relative to untreated controls.

The initial phase of these results was characterized by a massive amount of information, with expression changes being logged at the sites of nearly 25,000 genes and other genetic loci. After an initial filtering to remove marginal or questionable results, 1129 genes were found to be upregulated, while another 44 were downregulated. Further analysis revealed that many of the upregulated genes had been previously linked to astrocyte reactivity in brain injury and neurodegeneration, and additional clusters of genes had been found in a separate type of cell, known as microglia, in models of Alzheimer's disease. These results were of considerable interest, as they suggested a linkage between other neurodegenerative disorders and glaucoma, which has been speculated on at length but for which the evidence is modest.

The second phase of the experiment was to reprise the laser treatment with immunostaining techniques as the downstream assay. These techniques are fickle and low throughput relative to RNA sequencing, but when done correctly have the major advantage of being able to identify the cell types driving changes in RNA sequencing data. This follow up investigation revealed that many of the observed changes were instead driven by other cell types, including Müller cells, that are typically excluded by this isolation technique; their inclusion, and those of other additional cell types, was driven by focal damage to the retina during *in vivo* treatment,

creating scarring that resisted enzymatic treatment. As one of the chief aims of my approach was to allow for the analysis of the retinal astrocyte response without contributing signals from Müller cells, which are a similar but distinct cell type, this was something of a disappointment. However, the aforementioned versatility of the technique demonstrated a major advantage of this approach, as it was the ability to use identically prepared samples for both phases of the experiment that allowed us to detect this artifact. This was of particular import, as many commonly employed assays would have failed to detect the heterogeneity within the samples, complicating the task of interpretation. In the future, I aim to employ this technique to investigate alternative *in vivo* treatments that may produce clearer retinal astrocyte responses.

Acknowledgements

I would like to thank my committee for their continued support and advice over the years, as well as my collaborators Dr Yujia Yang and Dr Sandra Muroy, without whom the work presented herein would not have been possible.

I would also like to the thank Dr Choi and the staff of the Functional Genomics Laboratory here at Berkeley for their expert handling of our RNA samples.

Most of all, I would like to thank my family and friends for making this all possible and helping me stay sane throughout this long journey.

List of Abbreviations

BBB: Blood brain barrier
BRB: Blood retinal barrier
CNS: Central nervous system
DAM: Disease-associated microglia
DAMP: Damage-associated molecular pattern
DNA: Deoxyribonucleic acid
ECM: Extracellular matrix
FACS: Fluorescence-activated cell sorting
GFAP: Glial fibrillary acidic protein
GFP: Green fluorescent protein
IF: Intermediate filament
ILM: Inner limiting membrane
INL: Inner nuclear layer
IOP: Intraocular pressure
IPL: Inner plexiform layer
LPS: Lipopolysaccharides
MACS: Magnetic-activated cell sorting
MCAO: Mid-cerebral artery occlusion
MGnD: Microglia, neurodegeneration
MHC: Major histocompatibility complex
MMP: Matrix metalloproteinase
MS: Multiple sclerosis
NFL: Nerve fiber layer
OHT: Ocular hypertension
ONH: Optic nerve head
ONL: Outer nuclear layer
OPL: Outer plexiform layer
PAMP: Pathogen-associated molecular pattern
PCR: Polymerase chain reaction
POAG: Primary open angle glaucoma
RGC: Retinal ganglion cell
RNA: Ribonucleic acid
RPE: Retinal pigment epithelium
TBI: Traumatic brain injury
TLR: Toll-like receptor

TABLE OF CONTENTS

Chapter I

The Retina, Glia, and Glaucoma

Introduction

One of the chief characteristics of vertebrates – a group of animals that includes not only humans and other mammals, but birds, reptiles, amphibians, and fish as well – is their well-developed central nervous system. In addition to the brain and spinal cord, which are ubiquitous among these organisms, nearly all possess eyes as well; although these sensory organs have severely atrophied in some species that live their lives in dark caves or underground. Central to the eyes' function is the retina, a thin sheet of light sensitive neural tissue that forms from an extension of the brain during development. Sight occurs when light interacts with photosensitive compounds – opsins – in the specialized photoreceptor cells at the outermost edge of the retina. In response, a cascade of electrochemical signals within and between the cells of the retina culminates at the retinal ganglion cells near the inner retinal surface, which transmit the signals to the brain where it is further processed into a representation of our perceived visual environment, allowing us to see. This sensory adaptation is not without drawbacks, however; as the relative metabolic needs of the retina rival, or even exceed, those of the brain. As such, vertebrates have evolved a variety of specialized adaptations to ensure a steady flow of oxygen and nutrients to the retina.

Another key adaptation found within the central nervous system, or CNS, of vertebrates are cells known as glia. These cells, which emerge from the same population of precursor cells during development as the more widely known neurons, are thought to enable the specialized adaptations of neurons by providing a variety of essential support functions. Although glia are also found in invertebrate models favored by neuroscience such as C. elegans – a flat, worm-like creature composed of fewer than 1,000 cells – the CNS of vertebrates feature a variety of glial cell types, many specialized for particular functional or regional roles. Within the vertebrate retina, specialized glia known as Müller cells provide structural and metabolic support for the variety of neuronal cell types that make up the tissue. However, in many mammals – including humans – an additional glia type emerges from the astrocytes of the optic nerve head during development and enables the growth of blood vessels into the retina itself. These retinal astrocytes are unique to mammals, and in humans are closely associated with both blood vessels and the retinal ganglion cells (RGCs) that transmit information from the retina to the brain.

Although the vertebrate retina consists of a variety of neuronal cell types, as well as supporting glia, only the axons of the RGCs exit the retina to form the optic nerve that conveys visual information to the brain. As such, any damage to or death of these cells can result in partial or complete vision loss, regardless of the integrity of the rest of the tissue. In humans, the death of retinal ganglion cells and accompanying vision loss are known as glaucoma, and it is one of the most common neurodegenerative disorders as well as the leading cause of irreversible

blindness worldwide. Although a variety of conditions within the eye can contribute to glaucoma, in the most common variant – Primary Open Angle Glaucoma – the main risk factors are age and elevated pressure within the eye. While treatment to lower intraocular pressure (IOP) is commonly prescribed, retinal ganglion cell loss is often slowed rather than halted. Recent research has suggested that retinal astrocytes undergo changes in glaucoma that result in a loss of neuroprotective behavior, a gain of neurotoxic behavior, or some combination of the two. Understanding the contributions of retinal astrocytes to this debilitating disease, and determining whether they are a suitable target for treatment, requires close study of these incompletely understood cells.

Part I: The Evolutionary Origins of Retinal Astrocytes and the Vascularized Retina

The retina of the eye, alongside the brain and spinal cord, is a key component of the central nervous system (CNS) of vertebrate animals. Emerging as a projection of the forebrain during development, the retina is a specialized light-sensing structure that is linked to several vision processing regions of the brain by retinal ganglion cell axons, which exit the rear of the eye to form the optic nerve [1]. Owing to the energy intensive tasks it performs, the retina possesses high metabolic needs similar to, and in some cases greater than, the rest of the CNS [2, 3]. The choroid, a specialized vasculature located behind the retina, provides nutrition sufficient for thinner retinas with a thickness of ~150 um or less [4, 5]. However, many vertebrates possess thicker retinas that require supplemental vascularization, including humans [6]. The form this additional vasculature takes varies across taxa, but can be grouped into a limited number of types based on shared morphologies and developmental origins [7, 8]. In mammals, this vasculature is dependent on a subpopulation of glia – retinal astrocytes – that differentiate from optic nerve astrocytes during development and facilitate angiogenesis of the retina [9-14]. The close relationship of these cells with the retinal vasculature, as well as with retinal ganglion cells, makes them an important but insufficiently understood topic in retinopathies involving ischemia, including glaucoma and diabetic retinopathy.

I-A The Interrelationship between Retinal Thickness and Vascularization

Except in the most primitive members of the taxa, the structure of the retina in vertebrates is highly conserved [8]. Neuronal lamination, or layering, during development results in a series of well-defined anatomical layers readily observed in cross section under a microscope [15, 16]. The outermost of these contain the rod and cone photoreceptors, which are nearest the choroid and separated from it by the retinal pigment epithelium (RPE). The middle layers of the retina are home to a variety of interneuron types responsible for aggregating and modifying the signal transduced by these photoreceptors. Finally, in the innermost layers, retinal ganglion cells receive these signals and transmit them to the brain through lengthy axons that form the nerve fiber layer and the optic nerve.

While the choroid is a highly vascularized tissue capable of supporting the metabolic needs of neuronal cells in adjacent layers - particularly the energy intensive photoreceptors in the outer retina – constraints on oxygen and nutrient diffusion through the retina limit the thickness that can be achieved with this sort of vascularization[17, 18]. Calculations made by Dollery et al. approximately 50 years ago suggest an upper limit of 143 um to the thickness of the retina in the absence of additional vasculature [5, 6].

Although certain assumptions about the level of dissolved oxygen in the blood do not hold across taxa (see Section II), this figure is largely consistent with the reported thickness of avascular mammalian retinas, such as that of the guinea pig, as well as avascular regions within the otherwise vascularized human retina [4, 6, 17]. Furthermore, the choroidal vasculature is the only known example in adult mammals of a key blood supply for the central nervous system

that is completely isolated from the tissue it oxygenates, separated as it is from the retina by Bruch's membrane and the RPE [19]. Consequently, the choroid lacks neurovascular coupling, precluding the precise temporal and spatial control required for adjusting the supply of oxygen and nutrients to meet the real time needs of this metabolically demanding tissue [20, 21].

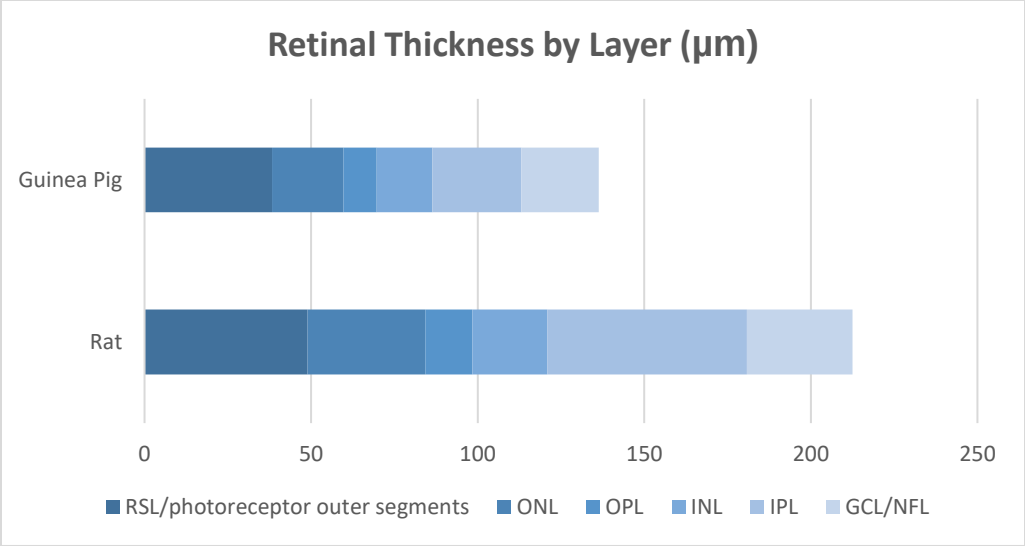

Figure 1: Thickness of layers in the vascularized rat retina versus the un-vascularized guinea pig retina. Adapted from data presented in Buttery et al., 1991[4]

By comparing the retinal thickness of two species of rodents, the rat and the guinea pig, we can gain some measure of insight into the relationship between the vascularization of the retina and its thickness. Both species are considered to have relatively low dependence on vision, but the rat eye has additional vasculature support for the retina while the guinea pig eye does not [22]. As such, the guinea pig retina averages only 136 um thick – below the calculated diffusion limit – while the rat possesses a retina averaging 212 um despite having a considerably smaller eye [4]. The overall reduction in retinal thickness (~36%) is not borne evenly by the various layers of the retina; while the choroid adjacent photoreceptor outer segments are ~22% thinner in the guinea pig eye, the inner plexiform layer (IPL) – an important region of dense synapses – is more than 50% thinner in the guinea pig relative to the rat. Although a thicker retina does involve some drawbacks, most notably the increased distance that light must penetrate the tissue before reaching photoreceptors, the increased retinal volume allows for additional signal processing before visual information exits the retina for the brain [4, 23]. The repeated evolution of thicker retinas across taxa, and the enhanced vasculature to support them, suggests oftentimes this trade-off is evolutionarily advantageous [8].

I-B Comparative Biology of Retinal Blood Supplies across Vertebrates

The need for abundant retinal nutrition is apparent from the wide array of structures that vertebrates have evolved to supply it [8]. Unlike the highly conserved layering of neuronal cell types in the retina, supplemental vascularization in the eye varies widely across and even within taxa [24, 25]. Among teleosts – the category of bony fish that includes nearly half of extant vertebrate species – adaptations have emerged both anterior and posterior to the retina [24]. Posterior to the retina, a modified choroidal structure known as a *rete mirabile* uses a dense capillary bed and countercurrent exchange to generate oxygen 'partial pressure' (PO_2) in excess of atmospheric levels (>250 mm Hg vs ~150 mm Hg); this results in greater tissue perfusion than can be achieved through ordinary vasculature (where the PO_2 is ~85 mm Hg), allowing for a thicker retina [8, 26].

In fish with additional perfusion needs, or those without *rete mirabile*, the falciform process may be present [8, 24]. This intravitreal structure is a protrusion of highly vascularized choroidal tissue, and reaches as anteriorly as the lens in some species. Other species possess a hyaloidal pre-retinal vasculature, in which blood vessels are present directly on the vitreal side of the inner limiting membrane (ILM) but do not actually penetrate the ILM or retina itself [8, 27]. Both the falciform process and pre-retinal vasculature can be found in species with a *rete mirabile*, resulting in a retina with enhanced vascularization on both sides of the retina, although these two vitreal adaptations are not found together [8]. Finally, in at least two species – *A. anguilla* (the European Eel) and *G. petersii* (the elephant nose fish) intra-retinal vessels similar to those found in mammals can be observed; this adaptation appears to have evolved independently in these lineages, not only from mammals but from each other [24, 28].

In lungfish, the living members of the group of fish that gave rise to terrestrial vertebrates, the falciform process is absent and the presence of a *rete mirabile* is only claimed in a single species [29]. Conversely, the presence of pre-retinal hyaloid vessels in most species suggests that these may be the ancestral vasculature strategy of tetrapods [24]. This view is supported by the presence of similar pre-retinal vessels in amphibians of the order Anura (frogs and toads), although Urodeles (salamanders) and Caecilians (snake-like amphibians) lack these and have retinas supported by the choroid only [8, 24].

In reptiles, we see not only a mix of avascular (turtles, crocodilians) and hyaloid supplied retinas (snakes) as in amphibians, but also the emergence of the *conus papillaris* in lizards [24, 30, 31]. Forming after the regression of the hyaloidal vasculature, and supplied by a vessel analogous to the central retinal artery in mammals, this cone-like protrusion of vascularized neuroectoderm projects into the vitreous to supplement retinal nutrition [7, 8]. Birds possess a similar structure, the *pecten oculi*, which is thought to share an evolutionary origin with the *conus papillaris* but has undergone greater morphological radiation [24, 32].

In mammals, the predominant mechanism for providing additional retinal nutrition is a series of blood vessel derived from the central retinal artery and radiating out from the optic disc, although a number of species possess avascular retinas and rely solely on the choroid [22, 24]. Unlike the hyaloid or vitreal vessels that tile the retina superficially during development (and in the adults of many vertebrate taxa) these vessels penetrate intraretinally, producing a series of

vascular plexuses within the retina [14]. This nutritive strategy - the embedding of vessels within the neural parenchyma – mirrors that of the brain and depends on a specialized population of astrocytes. Unlike Müller cells, the endogenous glia in the retina of nearly all vertebrates, these retinal astrocytes emerge from the optic nerve during development (see III) and are found only in the eyes of mammals [10]. Within mammals, they are essential for the formation of intraretinal vasculature; indeed, the strength of this association is such that intraretinal vascularization is considered indicative of astrocyte presence. [13, 33].

The extent of vascularization in the mammalian retina varies considerably between species and is typically sub-categorized into 3 or 4 major variants, which are documented extensively in the work of George Johnson, an ophthalmologist who in 1901 published an influential monograph on comparative eye anatomy in mammals [22]. Featuring dozens of full color illustrations of the fundus across species, his work highlights vascularization strategies from the highly vascularized euangiotic retinas of humans and other primates, to the selectively vascularized merangiotic pattern seen in rabbits, to the paurangiotic and avascular retinas in seemingly unrelated groups such as horses and guinea pigs [6, 7, 34]. These variations raise significant questions about the evolution of intraretinal vasculature in mammals, with regards to not only the evolutionary origin of this innovation but also the circumstances leading to the loss (or gain) of this feature.

Originally, avascular retinas in mammals were thought to represent the taxa's basal state, with vascularized retinas emerging in more 'derived' species [6]. However, a better understanding of the developmental requirements for vascularization – including the role of astrocytes – and modern phylogenetic models showing the concentration of avascularity in small 'clumps' of related groups imply that placental mammals, at least, likely share a common ancestor with vascularized retinas [14, 28]. Because marsupials and placental mammals each present examples of both intraretinally vascularized and avascular retinas, the precise timeline for the evolution of this adaptation remains ambiguous [22, 28, 35-37]. Depending on whether intra-retinal vessels emerged in a common ancestor of these two groups or as a later development, these vessels are thought to have evolved between 1 and 3 times in mammals [28].

Furthermore, ecological adaptations and reproductive strategies appear to play a large part in whether retinal vascularization is present. Predatory mammals (carnivores, cetaceans) and those with highly developed vision (primates) possess intraretinal vascularization, while herbivorous species (odd-toed ungulates, elephants) and those that are highly dependent on alternative sensory modalities (many bat species) are more likely to have avascular retinas [22, 28, 38]. Developmental patterns also appear to play a role – precocial rodents such as guinea pigs lack retinal vascularization, but most rodents reproduce altricially and possess intra-retinal blood vessels [4]. Not all precocial mammals lack retinal vascularization – whales and even-toed ungulates, for example, have vascularized retinas – but nearly every altricial mammal has intra-retinal vasculature [28]. The development of intra-retinal vasculature occurs after birth in most altricial mammals (the exception in this case being primates), and so it may be the case that many mammals with precocial young – such as odd-toed ungulates and some rodents – lost this developmental stage when their ancestors changed reproductive strategies [14, 39].

Ultimately, the evolution of nocturnality in mammals may be responsible for the emergence of retinal astrocytes and intraretinal vascularization. The 'nocturnal bottle-neck' hypothesis, first

suggested by Walls in 1942, holds that the common ancestor of mammals underwent adaptation – particularly with regards to vision – for a nocturnal lifestyle in response to predation by contemporaneous dinosaur species [24, 40, 41]. The resulting changes, such as a dramatic increase in the ratio of rod to cone photoreceptors, thought to be the result of developmental repurposing of S-cones to a rod photoreceptor fate, have persisted even in primarily diurnal species such as humans (20:1 rod to cone ratio, compared to ~1:1 in zebrafish and ~3:2 in chickens) [42-45]. Owing to the higher packing density of rods relative to cones, rod nuclei in the outer nuclear layer are staggered, resulting in thicker ONLs in rod-dominant retinas and an overall increase in retinal thickness [46, 47].

Although the photoreceptors of the outer retina are largely supported by the choroidal vasculature, studies of oxygen pressure in the rat retina suggest a rapid drop over the first 50 µm inward from Bruch's membrane until a plateau is reached near the outermost intraretinal vessels. [17]. While vitreal supplementation, such as the pecten of birds, apparently works equally well for diurnal species with thicker inner retinas, it may be of limited utility in supporting a thicker ONL with increased rod density. While nocturnal avians possess thicker outer nuclear layers than diurnal species (approximately 27 µm for kiwi and owl vs 7 µm for chicken and 11 µm for ostrich), the ONL in nocturnal mammals can exceed 50 µm [48-50]. This suggests that retinal vascularization may have evolved alongside nocturnal lifestyles in order to nourish the denser outer nuclear layer in early common ancestors of placental mammals and marsupials.

Part II: The Developmental History of the Vascularized Retina and the Role of Astrocytes

During early development, the mammalian retina is perfused both posteriorly, by the choroid, and anteriorly, by the hyaloidal vasculature; best known for the hyaloid artery that supplies the growing lens [14, 51]. As development progresses, the lens decouples from this blood supply and the artery regresses along with the other intravitreal vessels [52, 53]. In mammals without intra-retinal vasculature, such as guinea pigs, this leaves the retina completely reliant on the choroidal blood supply. In other species, including humans, the regression of the hyaloid is contemporaneous with the emergence of intra-retinal vasculature from the central retinal artery [14]. The timing of this changeover varies with the developmental strategy of the species in question – in mammals that give birth to blind young, such as carnivores and many rodents, the process begins perinatally. However, in humans, which like other primates give birth to sighted young, this process is completed during gestation [14].

Although the association between retinal vasculature and retinal astrocytes has long been observed, the developmental relationship between the glia and blood vessels was, until relatively recently, poorly understood [9]. Astrocytes are known to be late comers to the retina, derived not from resident neuroglial precursors but emerging from the optic nerve head [10]. Their association with the retinal vasculature - outside of disease state or experimental manipulation, the two are always found to be present or absent in unison – led early researchers to believe the glia followed the blood vessels into the retina [33]. Later experiments demonstrated the inverse to be true; that is, that astrocytes precede, and are required for, retinal vascularization [54, 55]. However, in recent years this understanding has grown more nuanced, as contemporary research shows that the maturation of retinal astrocytes depends on the increased oxygen levels these developing vessels deliver to the retina [56, 57].

Retinal vascularization is a highly conserved trait in eutherian - or placental – mammals, a trend highlighted by modern studies of mammalian evolution [28]. Despite major differences between the primate eye – which possesses an avascular fovea and is relatively developed at birth – and the mouse eye – which is uniformly vascularized and still developing at birth – the progression of development and vascularization is similar. As such, the mouse retina has been used extensively as a model to understand the process of retinal vascularization, and developmental dates in the mouse will be referenced whenever possible when discussing key events in order to provide a clear chronology.

II-A Gross Developmental Anatomy and the Development of the Intrinsic Neuroretina

During development in vertebrates, the eye emerges from complex interactions between a trio of distinct tissue types. Of these, the surface ectoderm and the periocular mesenchyme go on to form external and internal non-neuronal eye structures, such as the lens in the former and the iris and trabecular meshwork in the latter [39, 58]. The third of these elements, a protrusion of neuroectoderm from the forebrain known as the ocular neuroepithelium, goes on to form the retina and the retinal pigment epithelium (RPE) [59, 60]. By embryonic day 11 (E11) in the mouse, these structures assume a concave morphology known as the optic cup, with the developing retina nested within the RPE [58, 61]. It is at the juncture of these structures, at the outer edge of the retina, that retinal precursor cells undergo mitotic division before differentiating and migrating anteriorly [15, 61, 62]. By utilizing radio-labeled thymidine to timestamp the formation of chromosomal DNA, researchers have identified a timeline of proliferation for the various cell types of the neuroretina [62].

Table 1: Cell Types of the Intrinsic Neuroretina

Cell Type	Function	Location	Birth Dates
Retinal Ganglion Cells	Neuron: Aggregation of retinal output, transmission of sensory information to relevant brain regions	Inner Retina	E11 - P0
Amacrine Cells	Neuron: Higher-order feature detection	IPL (Nuclei in INL [and GCL?])	E11 - P1
Horizontal Cells	Neuron: Contrast enhancement, including of color, via lateral inhibition	OPL (Nuclei in INL)	E11 - E13
Bipolar Cells	Neuron: Transmission of signal from photoreceptor(s) to RGCs and amacrine cells, localized contrast detection and adaptation	Transverse (OPL to IPL)	E15 - P7
Cone Photoreceptors	Photoreceptor: specialized for bright light, color vision, and higher temporal sensitivity than rods	Outer Retina	E11 - E16
Rod Photoreceptors	Photoreceptor: specialized for low light conditions; secretes rdCVF, a trophic factor required for cone survival	Outer Retina	E13 - P9
Muller Cells	Glia: Trophic and structural support of neurons, maintenance of intercellular environment, light transmission, and electrical insulation	Transverse (ONL to ILM)	E16 - P9

Of the seven cell types that emerge from these retinal precursors – 6 neuronal, 1 glial – the first to be ‘born’ are the retinal ganglion cells, some of which exit mitosis as early as E11 in the mouse [62]. Following shortly thereafter are amacrine cells, horizontal cells, and cone photoreceptors. Rod photoreceptors follow approximately two days later, on E13, while the bipolar cells and Muller glia are formed last, on E15 and E16 respectively. It bears mentioning that the process of proliferation and differentiation of these cell types goes on for an extended

period, ranging from three days in the horizontal cells to over two weeks in rod photoreceptors, and so there is considerable overlap between the emergences of the disparate cell types [63]. Two additional trends also appear in these developmental studies: firstly, the process of proliferation and differentiation spreads from the central retina to the periphery; secondly, the neurons of the inner retina (RGCs and amacrine cells) are formed almost entirely before birth in the mouse, with only the most peripheral regions showing signs of postnatally formed RGCs [62] [64].

II-B The Hyaloid Vasculature – Blood supply to the embryonic retina

During the earliest stages of its development, the retina receives vascular support entirely through the choroid [25]. However, shortly before the optic fissure closes, an intravitreal network of blood vessels known as the hyaloidal vasculature begins to take shape [60] [51]. This network – consisting of the hyaloid artery, vasculosa hyaloidea propria (VHP), tunica vasculosa lentis (TVL), and pupillary membrane – is entirely arterial, draining via choroidal veins [65, 66]. Although most well-known for the hyaloid artery's role in supplying the developing lens – via the pupillary membrane (anterior) and TVL (equatorial and posterior) – this vasculature also supports the developing retina through the VHP [66] [67]. Its regression later in development (postnatally in mice [52], during gestation in primates [68]) has been shown to be a function of retinal ganglion cell signaling driven in part by exposure to VEGF [53]. Unlike the intraretinal vasculature found in many adult mammals, the hyaloidal vessels are located vitreally to the ILM, suggesting that they may be homologous to the supra-retinal vasculature observed in fish, amphibians and some reptiles [6]. In mammals with vascularized retinas it briefly coexists, but never anastomoses, with the emerging retinal vasculature [52].

In mice, the hyaloid vasculature begins forming shortly after the optic cup on day 11, with the hyaloid artery emerging from the ophthalmic artery through the optic fissure shortly before it closes on E12.5 [60, 69]. From E11-E18 the hyaloid artery grows anteriorly, first branching to form the VHP before ensheathing the lens with the TVL and pupillary membrane; by birth (P0), the VHP radiates outward from the hyaloid artery. Not long after reaching its greatest extent, the hyaloid vasculature begins to regress shortly after birth at P4 [52]. Macrophages are recruited to hasten the disassembly of the vessels, and by the time eyes open at P12 the hyaloid vasculature is almost entirely regressed.

In humans, failed regression of the hyaloid vasculature results in persistent fetal vasculature, a congenital disorder in which the remaining hyaloid vasculature interferes with normal eye growth [70]. Without intervention, the prognosis is poor as the elongation of the eye results in retinal detachment, hemorrhaging and secondary glaucoma. Current surgical interventions enable the preservation of useful vision if administered within the first months of life, although most individuals still suffer from diminished visual acuity in the affected eye.

II-C Emergence and Infiltration of Retinal Astrocytes

Table 2: Non-native Cell Types of the Retina

Cell Type	Function	Location	Arrival in Retina
Retinal Astrocytes & Astrocyte Precursors	Glia: Prime retina for blood vessel infiltration, neurovascular coupling, maintenance of blood retinal barrier, support of RGCs.	Nerve Fiber Layer and RGC Layer	E18 - P0
Microglia	Glia: Immune surveillance, pathogen defense, synaptic pruning	Throughout inner retina	E11 - P1
Pericytes	Mural Cell: Neurovascular coupling, BRB maintenance, regulation of endothelial cells	OPL (Nuclei in INL)	E11 - E13

In vertebrates, the astrocytes of the optic nerve are responsible for ensuring the health and function of retinal ganglion cell axons connecting the retina to the brain. However, in many mammals an additional subpopulation of astrocytes emerges midway through ocular development and spreads across the inner surface of the retina [12, 14]. Initially, the origin of these astrocytes was unclear, in part because Müller cells innate to the retina share morphological similarities with astrocyte precursors (APCs) [71]. Furthermore, these precursors lack the GFAP expression that characterizes adult astrocyte populations in the retina and elsewhere [54]. While developmental studies strongly suggested that cells with astrocytic potential originated from the optic nerve and not the retina itself, the lack of suitable markers meant these cells could not be identified until they appeared en masse as $GFAP^+$ cells in the inner retina during later development, masking their early developmental history [10, 11].

The identification of PDGFRα, a receptor for platelet derived growth factor (PDGF), as a novel marker of retinal astrocyte lineage clarified this crucial developmental process [12, 72]. Elsewhere in the central nervous system, neurons utilize the 'A' isoform of PDGF to recruit a class of glia known as oligodendrocytes that ensheath axons in non-conductive myelin, thereby protecting and insulating them [73-75]. Uniquely among astrocytes, retinal astrocytes and their developmental precursors in the optic nerve express PDGFRα, and developing RGCs in the embryonic retina utilize PDGFA as a chemoattractant to spur retrograde migration from the optic nerve [14, 72]. Observations made using this marker identified the spindle-shaped cells that precede retinal vascularization – previously thought to be endothelial cells – as APCs emerging from the optic nerve; resolving not only the origin of retinal astrocytes but also revealing that the spread of astrocyte-lineage cells precedes vascularization of the retina, rather than the inverse [72].

While PDGFRα positive oligodendrocytes are also present in the developing optic nerve, these are typically absent from the mammalian eye [12, 34]. Although the mechanisms underlying their exclusion remain unclear, optic nerve oligodendrocytes develop at a later date than retinal astrocytes, which may contribute; the lamina cribrosa is also thought to play a role [76]. Curiously, the rabbit retina – unlike those of other mammals – has both oligodendrocytes and

astrocytes in spatially distinct domains [34]. While the astrocytic region of their retina is well vascularized, the remainder is avascular. Partial myelination of the retina has also been observed in humans and is thought to occur in ~0.5-1% of the population [77, 78]. This can result in relative scotoma, although the extent of myelination and corresponding impairment is typically limited.

In addition to RGC driven chemotaxis, the outward migration of astrocytes from the optic disc towards the peripheral retina is also dependent on the inner limiting membrane (ILM), the basement membrane separating the neuroretina from the vitreous. During development, the ILM is formed by a mix of proteins synthesized by the lens and ciliary body - including laminins and collagens – interacting with retina-derived proteoglycans [13, 79, 80]. Disruption of this membrane not only interferes with astrocytic tiling of the retina and subsequent vascularization, but can also result in infiltration of the vitreous by stray glia [81]. Notably, these abnormal vitreal astrocytes have been observed ensheathing the lingering hyaloid vessels in persistent fetal vasculature, suggesting they may play a role in preserving these structures and preventing their normal regression [82].

In mice and rats, astrocyte infiltration of the retina begins just before birth [10, 83]. During development in mice, a subpopulation of optic nerve APCs begins to express PDGFRα around E15 (E14 in rats); shortly thereafter, retinal ganglion cells begin to express PDGF [12, 84]. This change occurs follows the formation of the ILM (E13 in mice) and is contemporaneous with the emergence of APCs and immature astrocytes from the optic nerve head and their migration into the retina [85]. By P0 APCs are found as far as .8mm from the ONH in both mice [57] and rats [10]; as these astrocytes/APCs migrate across the retina - following the gradient of PDGF signaling at a rate of approximately 200-300 microns per day - they create conditions suitable for superficial angiogenesis by depositing fibronectin scaffolding and secreting pro-angiotic VEGF [86-89]. Approximately one day after the emergence of APCs into the retina, blood vessels begin to extend into the retina in response to glial and neuronal VEGF signals.

II-D The Emergence of Retinal Vasculature and Maturation of Retinal Astrocytes

Although retinal astrocyte precursors precede the spread of vasculature into the retina, their maturation to an adult phenotype is dependent on a complex interplay between blood vessels, retinal neurons (especially RGCs) and the APCs themselves [14]. This results in a gradual process of maturation that spreads outward from the ONH in a series of waves, similarly to the maturation of the endogenous retinal cells [57]. Furthermore, once the innermost layer of the retina is tiled with astrocytes and fully vascularized, vessels of the superficial plexus begin to penetrate deeper into the retina, where they establish two additional plexuses [90, 91].

Table 3: Markers of Astrocyte Maturation in the Retina [92, 93]

Maturation Stage	Markers
Astrocyte Precursors (APCs)	$Pax2^+$/ $vimentin^+$/$GFAP^-$/ $S100^-$
Immature Retinal Astrocytes	$Pax2^+$/ $vimentin^+$/$GFAP^+$/ $S100^+$
Mature Retinal Astrocytes	$Pax2^+$/ $vimentin^-$/$GFAP^+$/ $S100^+$

Shortly after retinal APCs first emerge from the optic nerve, those nearest the optic nerve head begin to upregulate GFAP – a marker of astrocyte differentiation and maturation - while those more distal to the ONH retain a mix of APC and immature astrocytic identity [93]. The differentiated but still immature astrocytes travel only a limited distance from the optic nerve head, while the more motile APCs migrate to the distal regions of the retina [57]. These spindle shaped cells were originally believed to be vascular precursor cells until the absence of VEGF receptors and the presence of retinal-astrocyte-specific PDGFRa revealed their glial lineage [54].

The differentiation and maturation of retinal astrocytes – from astrocyte precursors to immature and finally mature astrocytes – is dependent on the approach of developing retinal vasculature. The first transition occurs as the leading edge of vascularization approaches APCs, following the secretion of VEGF, resulting in greater local oxygen perfusion [56]. In response, the oxygen sensing transcription factor HIF-2α undergoes degradation and depletion in astrocyte precursors, resulting in changes – particularly the downregulation of the orphan nuclear receptor TLX – that lower their motility and proliferation and mark their partial maturation to immature astrocytes [14, 94]. As the vascular network continues to expand distally, VEGF signaling from these immature astrocytes upregulates apelin in the endothelial "tip" cells at the leading edge of vascularization [95, 96]. In response, the trailing endothelial "stalk" cells secrete leukemia inhibitory factor (LIF), a cytokine required for the developmental maturation of astrocytes [95, 97, 98]. The binding of LIF to its receptor initiates JAK-STAT mediated intracellular signaling, resulting in the transcription factor STAT3 – known to play major roles in astrocyte behavior and maturation – upregulating the expression of GFAP and inducing the transition to a mature astrocytic phenotype [97, 99, 100].

The result is a series of 3 concentric astrocyte maturation domains, centered on the optic disc [57, 93]. The innermost of these regions is occupied by mature astrocytes - characterized by high GFAP expression and downregulated VEGF - and a well-developed superficial plexus of blood vessels. The intermediate ring surrounding this is populated by immature retinal astrocytes that express low-to-moderate GFAP levels, and developing blood vessels. The outermost ring is avascular and occupied primarily by APCs expressing little to no GFAP.

Disruption of HIF-2α – or exposure to hyperoxic conditions – during this developmental period results in precocious maturation of astrocytes and a halt to their migration towards the periphery, yielding an incomplete or absent vasculature bed [56, 94]. Conversely, hyperoxia after the completion of the superficial plexus results in "a central zone of vaso-obliteration", followed by retinal neovascularization in the affected area when normoxic conditions are resumed [101]. The latter phenomena in particular contributes to retinopathy of prematurity in human infants born before 30 weeks gestation and treated with supplemental oxygen; hyperoxia results in vasculature regression, followed by hypoxia and subsequent neovascularization once oxygen treatment is withdrawn [19, 102]. Careful titration of oxygen levels must be maintained to minimize complications that can include retinal detachment and blindness in the most severe cases.

During normal development, the completion of the superficial vasculature plexus is followed by the penetration of new vessel formation deeper into the retina [90, 103, 104]. Driven by the HIF-1α hypoxia sensing pathway, rather than the HIF-2α pathway regulating astrocytic maturation, horizontal cells secrete VEGF and induce angiotic growth to the outer edge of the inner nuclear layer. After the establishment of this deep plexus, a new wave of VEGF signaling from amacrine cells results in new vessel formation towards the superficial surface of the retina. When these vessels reach the inner edge of the INL, they once more begin to spread laterally, forming the intermediate vascular plexus, completing the broad strokes of the retinal vasculature. Although generation of sufficient vasculature is required for proper development and function of the retina, penetration of intraretinal vessels into the outer retina is associated with pathogenesis and visual impairment [103, 105]. Expression of soluble VEGF receptor 1 (Flt1) by photoreceptors and the RPE acts as a sink for VEGF in the outer retina, inhibiting signaling that can otherwise result in inappropriate vessel formation; neuronal VEGFR2 and microglial Flt1 have also been shown to contribute to this vasculature exclusion [106-108].

As with many aspects of development, the formation of the retina is characterized by the initial overproduction of blood vessels and many cell types, including astrocytes and RGCs. The greatest number of retinal astrocytes are found on P5 in the mouse, as they reach the periphery of the retina [109]. Over the following ~9 days, in excess of 2/3's of retinal astrocytes are lost through what evidence suggests is phagocytosis of living astrocytes by resident microglia. Curiously, experimental efforts to disrupt microglial ablation of astrocytes have revealed a partial compensation by the astrocytes themselves, in which evidence suggests they engulf their neighbors. Furthermore, an excess of surviving astrocytes - induced by microglial ablation or delayed maturation of proliferative astrocytes precursors - results in an elevated density of capillaries in the superficial vasculature [110]. Comparative analysis of markers of angiogenesis and vasculature regression indicate normal vessel formation but impaired pruning

under these conditions, suggesting an ongoing role for astrocytes in the survival of retinal vasculature. This view is lent further support by the association of astrocytes with persistent fetal vasculature, in which portions of the hyaloidal vessels fail to regress. Furthermore, excess retinal astrocytes and superficial vessels are associated with vascular leakage in the microglia ablation model; whether this is directly related to the excess of astrocytes and vessels or a failure of defective vessels to regress remains unclear [109].

Just as the retinal astrocyte network undergoes both pruning and maturation shortly after achieving peak density, so too does the intraretinal vasculature [14]. However, unlike the macrophage-driven disassembly of the hyaloidal vasculature or microglial pruning of excess astrocytes, cell death only plays a minor role in the regression of surplus blood vessels in the retina [111]. Instead, vasculature regression occurs predominantly through the recruitment of endothelial cells from redundant vessels to their surviving neighbors, with cell death relegated to the final stages of removal of non-perfused vessels [112]. Concurrent with vascular pruning is a process of maturation, yielding a net effect of consolidation. Of particular note is the recruitment of pericytes via PDGFB signaling by endothelial cells, which results in vasculature stabilization throughout the retina [113, 114]. Furthermore, pericytes play essential roles in the formation of the blood retinal barrier (BRB) and in neurovascular coupling in the retina; in addition to close interactions with astrocytes in both retina and brain, both cell types are among the first casualties of diabetic retinopathy [20, 113, 115-117].

In mice, retinal astrocyte precursors emerge from the optic nerve head circa E17/18 [14, 83]. At P0 these cells have spread ~700 um distally, while immature and mature astrocytes (distinguished by low and high GFAP positivity) are found up to 300 um and 100 um from the ONH, respectively, in concentric circles [57]. By P5 astrocyte precursors have migrated to the peripheral edge of the retina, with the arrival of the superficial vasculature and the accompanying transition of APCs to immature astrocytes occurring roughly two days later on P7 [54]. Shortly after, endothelial ‘stalk-tips’ begin extending from the superficial plexus towards the outer retina, reaching as far as the INL/OPL interface before they resume spreading parallel to the retinal surface, forming the deep plexus over the next several days [104]. As this outermost capillary bed reaches completion during P11/12, new vascular spreading turns inward, and a final, intermediate plexus is formed midway between the superficial and deep ones by P17 [101].

As the deep plexus forms within the retina, astrocytes at the vitreoretinal surface continue maturing in response to elevated oxygen levels and endothelial cell secreted LIF; this wave of maturation spreads outward from the optic nerve head and reaches the periphery around P9 [14, 57]. Throughout this process, these maturing astrocytes are subject to pruning by microglia and possibly other astrocytes, with population density stabilizing by day P14 [109]. Maturation of the retinal vasculature occurs concurrently, with the superficial and deep plexi being largely complete by P15, while the intermediate plexus continues maturing through at least P21 [101]. Mouse pups open their eyes at approximately P12, thus while the maturation of retinal astrocytes and the superficial plexus is largely complete by the time eye opening occurs, the development of the intermediate plexus and the final maturation of the retinal vasculature continues for 1 – 2 weeks after.

Part III: Mature Astrocytes in Physiological Conditions

While retinal astrocytes in particular are readily identifiable by their developmental origin and location, the broader category of astrocytes resists easy classification [118]. They are neither restricted to a particular region of the of the central nervous system – like the Bergmann glia of the cerebellum – nor are they readily defined by a single behavioral or morphological feature like the myelin-forming oligodendrocytes [119, 120]. Furthermore, many of their most well-known characteristics, such as non-excitability, are true of glia as a whole and not just astrocytes. Instead, these cells are characterized by their heterogeneity as a category, rendering a clear and concise definition of astrocyte identity elusive [121]. As research on glia has progressed, the heterogeneity of astrocytes within, and particularly between, regions of the central nervous system have become central to our understanding [122, 123]. However, despite variation between astrocyte populations, certain behaviors, markers, and morphological elements are widely – if not universally – shared among these cells [124]. In part due to the study of their migration from optic nerve to retina, the developmental role may be the most completely elucidated aspect of retinal astrocytes, and the only area in which their behavior is more fully understood than the behavior of astrocytes in general. As such, to parse our current knowledge of mature retinal astrocytes we must first cover the common behaviors and markers typical of most – but perhaps not all – astrocytes before delving into the somewhat more limited knowledge of retinal astrocytes in particular.

III-A Categorization by Morphology and Niche

Although the presence of astrocytes, including retinal astrocytes, has been observed and documented in the central nervous system from the earliest days of cellular neuroscience, much remains unknown about these cells [125, 126]. As the development of modern electrophysiology made possible the real-time measurement of activity from individual neurons, the lack of equivalent techniques to study glial behavior left investigators to classify astrocytes by morphology, location, and their association with other cell types and structures, along with the expression of a limited set of cellular markers such as GFAP [127-130]. Only in 1990, nearly four decades after Hodgkin and Huxley's Noble-prize-winning work measuring the depolarization of nerve axons in the giant squid, did the documentation of glial calcium signaling, first in cell culture, then later in intact tissue including the retina, allow for the real time detection of astrocyte activity [131, 132]. While increasingly eclipsed by this and other modern approaches such as transcriptomics, the older methods of characterization retain some utility, as the type, localization and quantity of cell-cell connections made by astrocytes can give many clues to their roles within the CNS.

One of the oldest categorizations of astrocytes, published by the pathologist W. Lloyd Andriezen in 1893, divides the cells into fibrous (originally "fibrillary") and protoplasmic subtypes [127]. Despite modifications to this schema in the ensuing years, the categorization remains largely the same: protoplasmic astrocytes are "bushy" with highly branched processes and found in the so-called "gray matter" of CNS, while fibrous astrocytes inhabit the "white

matter" and are slender with longer, less branching processes [124, 126, 133]. Perhaps more relevantly, with regards to the specialization of each subtype, protoplasmic astrocytes extend their processes to the synapses between neurons, while fibrous astrocytes contact the exposed neuronal axons at the nodes of Ranvier; both subtypes additionally contact blood vessels [133-136]. Owing to their association with synapses, protoplasmic astrocytes are sometimes referred to as perisynaptic, while fibrous astrocyte with processes at the nodes of Ranvier are similarly termed perinodal [134, 137].

However, although the divergence of forms indeed seems to align with functional specialization, an increased understanding of the heterogeneity of astrocyte populations between regions of the central nervous system has begun to expose the limitations of morphology-based classification [122]. There is also the issue of mature radial glia – Bergmann glia and Muller cells – that retain morphologies that resemble those of immature astrocytes but fulfill astrocyte-like roles. Indeed, the distinction between these cell types and astrocytes is based largely on morphology and localization, and some authors refer to them as astrocytes or astroglia [126, 133]. For the sake of clarity, we will continue to refer to the radial glia of the retina as Müller cells or Müller glia, and the term retinal astrocytes will be reserved to the distinct population of glia that emerge from the optic nerve during development rather than the retina. For the purpose of classification by Andriezen's criteria, retinal astrocytes have been classified as fibrous due to their association with retinal ganglion cell axons in addition to their morphology [133]. Conversely, due to bushy processes that spread from Müller cells to the retinal synapses of the inner and outer plexiform layers, these cells have described as protoplasmic/perisynaptic [126, 137].

III-B Astrocytes Provide Structural Support in the Central Nervous System

One of the earliest proposed functions for glia, credited to the pioneering German pathologist Rudolf Virchow, was that of the connective tissue of the central nervous system [138, 139]. Although this is an oversimplification of the role of astrocytes that modern researchers have spent their careers trying to dispel, the inferences of early neuroscientists was at least partially correct. Depending on type and brain region, astrocytes typically express intermediate filaments consisting of GFAP and/or vimentin, although these may be augmented with nestin and symenin during development and reactivity [140, 141]. These filaments do not pervade the smallest branching elements of astrocyte processes but are instead thought to provide overall structure and polarity to the cell and have long been thought to in turn provide structural support to the brain.

Since its discovery in 1969 by Lawrence Eng, GFAP has been used as something of a canonical marker of astrocyte identity, although its low expression in some brain regions has led to increased use of the more recently identified protein Aldh1l1 [122, 142] Although vimentin and GFAP are differentially expressed, the two are similar enough that in GFAP -/- knock out mice, vimentin can fulfill some of the same roles as GFAP, occluding the functional significance of GFAP [143]. However, GFAP has a critical role in protecting the central nervous system from

sudden trauma, as revealed by experiments in rodents. When wild-type, GFAP+ mice were anesthetized and placed on a foam support before having a 20g weight dropped on their heads, the animals suffered minor injuries but recovered rapidly; however, when the experiment was repeated with GFAP null mice, 12 of the 15 knockout animals died within 2-3 minutes [144]. Although skeletal injuries were absent upon postmortem investigation, the knockout animals were found to have suffered widespread hemorrhaging within their spinal cords. When the experiments were repeated, except with the heads of the mice resting on a wooden surface to prevent rapid motion at the moment of impact, both wild type and null mice survived, highlighting the role of astrocytic GFAP in protecting the CNS from sudden shear forces.

In the retina, where astrocytes and (to a lesser degree) Müller cells both express GFAP, a related phenomenon has been observed in the retinas of GFAP -/- Vim -/- double knockout mice. While the retinas of wild type mice remain structurally intact when isolated, the retinas of the double knockout mice underwent complete detachment of the ILM and nerve fiber layer, and intermittent detachment of the underlying retinal ganglion cell layer [145]. Beyond their role in protecting the nervous system from trauma, evidence suggests that intermediate filaments are also involved in trafficking secretory vesicles to their targets at the cell membrane and are also instrumental in astrocyte motility; the former will be revisited in the section on signaling while the later will be discussed in greater detail alongside reactivity [146, 147].

III-C The Functional Syncytium: Direct Coupling between Glia

In addition to their contribution to the structural integrity of the nervous system, the processes of astrocytes – projections from the cell soma analogous to neuronal axons – form a variety of functional connections with the neurons they support, nearby vasculature, and other glia. As with neurons, astrocytes can display subcellular compartmentalization when responding to stimuli, and express key functional proteins at the distal ends of their processes [148, 149]. These phenomena – known as microdomains and polarity – partially explain the correlation between the morphology of astrocytes and their physiological functions, as they facilitate the restriction of behavioral responses to a particular region of the cell. In particular, astrocytes are frequently ‘coupled’ to other cell types; coupling is a class of behavior in which two or more cells act in rough synchrony as a single functional unit. Examining the nature of these connections has proven a useful approach for elucidating, both generally and specifically, the functions these cells are performing.

At sites where astrocytes contact neighboring glia – including other astrocytes – the membranes of these cells do not directly touch, as at a tight junction, but remain separated by a 2-3 nm gap continuous with extracellular space [150]. However, by the time the structure of these ‘gap junctions’ was first described, it was already established that electrical coupling could occur between such cells despite their physical separation [151]. By combining electron microscopy and x-ray diffraction studies, the fine structure responsible for this apparent contradiction – the connexon – was identified [152, 153]. Composed of a hexamer of proteins

known as connexins, connexons are hemi-channels protruding from the cell surface; at gap junction 'plaques' between apposed cells, connexons from both cells meet and form channels that allow for the flow of small molecules (< 1 kD) and ions [153, 154]. Flow through these channels occurs via passive diffusion and allows the passage of signaling molecules such as cAMP and IP_3, while larger biological molecules like nucleic acids and proteins are excluded [155].

Furthermore, connexons are voltage gated – meaning that they can open or close in response to charge-mediated signaling – with the specifics of this behavior being a function of the constituent connexins [156]. At least 21 connexin genes have been documented in vertebrates, and individual connexons can consist of one or more types [153]. Additionally, the channels formed by connexons may consist of a pair of matching hemi-channels or two distinct ones, referred to as homotypic or heterotypic, respectively. While a given cell type only expresses a limited number of connexins and only certain connexon pairings are possible, the combinatorial aspect is thought to add selectivity and structure to networks of coupled cells [153, 157].

Although gap junctions can be found in solid tissues throughout the body, the networks formed by coupled astrocytes have long been of particular interest [150]. Astrocytes are known to express connexin 43 (hereafter referred to as Cx43), and to a lesser extent connexin 30 (Cx30); astrocyte-astrocyte coupling relies on homotypic Cx43:Cx43 junctions to form localized instances of functional syncytium as first observed by Quigley in the optic nerve of rats [157-161]. Although not a true syncytium – a continuous, acellular network akin to the since disproven 'reticular' model of the nervous system proposed by Nobel laureate Camillo Golgi – astrocytes in the central nervous system form extensive networks which can be directly visualized through the process of dye-coupling, in which a single cell is injected with a membrane non-permeable marker that then spreads to adjacent coupled cells via gap junctions [161, 162].

Intriguingly, while the gap junctions between astrocytes are symmetrical, the same is not true for the heterotypic connections formed between astrocytes and other glia [163]. Both oligodendrocytes in the brain and Muller cells in the retina form heterotypic gap junctions with astrocytes, resulting in the unidirectional flow of permeable small molecules and ions from an astrocytic network into individual oligodendrocytes and Muller cells [164, 165]. This leads to particularly striking results from coupling experiments in the mammalian retinas, where the densely-packed Muller cells are coupled to astrocytes but not each other: injection of neurobiotin – a low molecular weight tracer – into a single astrocyte resulted in spread of the marker into nearby astrocytes and the hundreds of Muller cells coupled to them [165, 166]. Injection of a single Muller cell, conversely, resulted in no spread, instead trapping the marker within the targeted cell's cytoplasm.

While our understanding of the role of these astroglial networks remains incomplete, a number of crucial functions have been previously elucidated, such as buffering of ion concentrations and the synchronization of astrocyte behavior [157, 161, 167]. These functions will be discussed in greater detail below.

III-C1 Homeostatic Buffering

After structural support, perhaps the longest recognized function of the astrocytic network is to maintain homeostasis in the CNS via ionic and osmotic buffering [168]. One challenge these cells face is that the parenchyma of the brain, retina and spinal cord is a site of sudden change while simultaneously being especially vulnerable to these changes. Neuronal signaling leads to sudden effluxes of K^+ and glutamate into the extracellular space, leading to a disruption of neuron function if not cleared rapidly and, in the case of glutamate, excitotoxicity [169, 170]. Although individual astrocytes remove these byproducts from extracellular space – particularly through the K^+ channel Kir 4.1 and the glutamate transporters GLAST and GLT-1 – and possess the ability to metabolize glutamate, it is the ability of these cells to subsequently diffuse them through the syncytium that prevents individual astrocytes in high activity regions from being overwhelmed and exhausting their buffering capacity [171-173]. Indeed, disruption of the glial syncytium in mice via astrocyte-specific knockout of Cx30 and Cx43 leads not only to reduced glutamate clearance by GLT-1 and a prolonged half-life for extracellular K^+, but also swelling of astrocytes as the increase in ion concentrations forces them to take in water to maintain osmolarity [174]. Relatedly, astrocytes in many regions of the CNS also express the water channel AQP4, particularly on endfeet contacting perivascular space; this is thought to facilitate the transport of solutes like K^+ out of the neural parenchyma by alleviated osmotic stress [175].

In the retina, AQP4 is expressed in Muller cells – particularly where their endfeet contact the ILM – and on the vitreal side of retinal astrocytes, as well as in the processes of both cell types where they ensheath the retinal vasculature [176, 177]. Although the distribution of Kir 4.1 in the retina largely mirrors that of AQP4 with regards to Muller cells, with channel density on the endfeet being roughly an order of magnitude higher than across the cell surface overall, retinal astrocytes appear not to express the K^+ channel [177, 178]. This may be the result of retinal ganglion cell axons being able to 'vent' their K+ efflux directly into the vitreous, or it may represent one of the functions of the previously described retinal glia circuit. That is, the gap junction coupling between retinal astrocytes and Muller cells allows for the unidirectional flow of small molecules and ions from the former into the latter; it may be that retinal astrocytes utilize the highly specialized Muller cells to dispose of excess K^+.

III-C2 Astrocyte Ca^{2+} Signaling

Since its discovery in the 1990s, Ca^{2+} signaling in astrocytes has been a source of much progress in the field of glia research, but also much conjecture and consternation [131, 179, 180]. Prior to this discovery, astrocytes were thought to be relatively inert due to their lack of electrical activity, but Ca^{2+} signaling provided a mechanism by which these cells could participate in the rapid activities that characterize the central nervous system [181-183]. As a result, astrocytic roles were proposed for neurovascular coupling, coordination of cell behavior, and even participation in synaptic transmission between neurons [163, 184, 185]. However, in the aftermath of these initial claims, various groups published studies with starkly divergent, difficult to reconcile results [180, 186, 187]. In the past decade, as more precise tools have emerged to dissect the Ca^{2+} dependent behavior of astrocytes from those of adjacent neurons,

a more nuanced picture of astrocytic Ca^{2+} signaling has developed [148, 188-190]. Indeed, recent evidence suggests that astrocytes, both as a category and as individual cells, can make use of multiple sources of calcium and mechanisms of signaling, at several overlapping scales, to modulate a variety of behaviors [191-195].

What is Calcium Signaling?

One of the chief sources of disagreement on the topic of calcium signaling in astrocytes appears to be over-generalization of experimental outcomes, resulting from a failure to appreciate the complexity of Ca^{2+} signaling as a behavior [180, 186]. Fundamentally, calcium signaling entails a sudden rise in cytoplasmic Ca^{2+} that alters the biochemistry within a cell, resulting in a rapid change in functional behavior on the scale of milliseconds to seconds [196]. In astrocytes, Ca^{2+} mediated functions include synthesis of the PGE_2-precursor arachidonic acid (AA) by phospholipase as a necessary step in neurovascular coupling at the capillary level (see 'Functional Hyperemia'), as well as vesicular exocytosis of signaling molecules ('Astrocyte Signaling') [193, 197-199]. Free intracellular calcium is aggressively regulated by cells; sequestration of Ca^{2+} in the endoplasmic reticulum results in cytosolic [Ca^{2+}] of ~100nM, approximately 4-5 orders of magnitude lower than in the extracellular space of the nervous system [181, 200]. Even when channels are opened to extracellular space or endoplasmic Ca^{2+} stores, the influx is spatially restricted by buffering, such that [Ca^{2+}] increases are largely limited to sub-micron distances from the point of entry [201]. This spatial restriction, along with rapid clearance of cytosolic Ca^{2+}, is an essential function of calcium signaling in light of the ion's ubiquitous role in modulating cellular functions [202]. However, due to the limited sensitivity of early techniques used to detect calcium signaling in astrocytes, only the most widespread and long lasting Ca2+ fluxes could be studied while these restricted but physiologically relevant signaling events remained essentially invisible.

Types of Ca^{2+} Signaling in Astrocytes

While changes in [Ca^{2+}] can occur at very different scales, relatively imprecise methods were initially used to study calcium signaling, which allowed for the effective detection of large-scale fluxes within the soma of astrocytes but not those in the finer processes of these cells [179, 181]. This contributed in part to an initial research focus on the most dramatic calcium fluxes, such as the Ca^{2+} "waves" that propagate locally through the gap-junction coupled syncytium [203, 204]. However, these large-scale changes are comparatively slow, occurring on the scale of seconds, resulting in the conclusion of some researchers that astrocyte calcium signaling was too slow to be involved in relatively rapid processes such as neurovascular coupling [205, 206]. In parallel, early work on the mechanics of astrocyte Ca^{2+} signaling focused on IP_3-mediated release of Ca^{2+} from the endoplasmic reticulum, as this was the primary source of calcium for somatic and wave signaling [183, 207]. This too was found to be incompatible with a Ca^{2+} mediated role for astrocytes in key neuronal functions, as astrocyte-specific genetic ablation of IP_3R2, the receptor mediating IP_3 dependent release of Ca^{2+} from the endoplasmic reticulum, abolished large-scale calcium signaling in astrocyte but did not appear to alter the function of

the CNS [206, 208]. Nevertheless, experimental outcomes continued to suggest a role for astrocytic Ca^{2+} signaling in a variety of functions [209-212].

Eventually, improved instrumentation and more precise markers of Ca^{2+} activity allowed for detection of smaller scale fluxes within the subcellular compartments of astrocytes, confirming the hypotheses of researchers that suspected that rapid Ca^{2+} signals were present but going undetected [188, 191, 211]. Additionally, recent research has shown that, particularly in these smaller signaling events, influx of extracellular Ca^{2+} is more crucial than IP_3R2 mediated release from the ER [191, 193]. Although something of a simplification, Ca^{2+} fluxes in astrocytes take place at three levels of scale – restricted, somatic, and intercellular wave – with the time scales involved growing longer as the affected area expands [194, 202, 204]. Likewise, the mechanisms of signal induction and sources of Ca^{2+} vary between these scales [180, 202]. Therefore, it may prove useful to treat astrocytic Ca^{2+} functioning not as a unified phenomenon, but rather three or more interrelated functions all utilizing the same effector: Ca^{2+}.

- Restricted or localized Ca^{2+} signaling takes place on astrocyte endfeet or in processes. Work in mice showed a subset of these restricted signaling events occurring on time scales of 100-200ms after local synaptic activity, in a model of waking perception [194]. Other studies utilizing different stimuli and measurement approaches detected less rapid changes, but nonetheless found Ca^{2+} signaling in astrocyte processes preceding – and required for – vasodilation in models of neurovascular coupling [193, 213]. Spatially restricted signaling is primarily dependent on extracellular sources of Ca^{2+}, which enters the cell through transmembrane channels such as the ATP gated P2X1 receptor, rather than intracellular stores [191, 193, 211].

- Somatic Ca2+ signaling takes place in the main body, or soma, of the astrocyte. Although this category has an outsized role in the literature, modern studies suggest it may represent less than 10% of Ca2+ signaling in astrocytes [148, 214]. Somatic signals are slower, on the scale of seconds, and primarily dependent on IP_3R2-mediated Ca^{2+} release, being greatly attenuated in IP_3R2-KO animals [205, 208]. It remains an open question as to whether somatic signaling represents the summation of multiple localized signaling events, or a discrete phenomenon [195, 202]. Astrocyte Ca^{2+} influxes are required for vesicular exocytosis (see section III-E), and some evidence suggests that these slower, more widespread signaling events play a major role in this function [197, 215, 216].

- Wave Ca2+ signals are both the most dramatic manifestation of astrocyte calcium signaling and the most mysterious. These intercellular waves occur on the scale of 10s of seconds to a minute or more, and have been shown to propagate both through gap junctions – apparently by IP_3 diffusion – as well through extracellular ATP release [192, 217]. Similarly to the relationship between restricted and somatic Ca^{2+}, it is unclear to what degree somatic and wave signals represent gradations of the same phenomenon

versus separate classes of event. *In vivo* work with genetically encoded calcium indicators has made clear that these events occur under physiological conditions in live animals, and are not simply an artifact induced by experimental stimulation methods [191, 218, 219]. While the function of these waves remains less well understood than smaller scale Ca^{2+} signaling, experimental results have indicated a role in mediating neuronal synchronization, such as in sleep and waking [220, 221].

Calcium Signaling in the Retina

One of the earliest documentations of glial calcium signaling *in situ* came from studies of Ca^{2+} waves in the retina by Newman and Zahs in 1997 in which they established the rate at which these waves propagate through both astrocytes and Muller cells in the living retina and identified a role for intracellular calcium stores [179]. The following year, they determined that proximity to these signaling waves could dampen subsequent neuronal activity in the retina, although this may not represent a typical physiological response [132]. Several years later, Newman demonstrated that retinal Ca^{2+} waves propagate both through gap junctions and via extracellular ATP signals [203]. Years later, Newman's group published one of two papers that finally and unequivocally demonstrated a role for glia in neurovascular coupling, showing that the loss of IP_3 mediated Ca^{2+} signals in Muller cells abrogated light-induced vasodilation in retinal capillaries [222]. However, the choice of the GLAST promoter to drive their genetically encoded calcium indicator left retinal astrocytes functionally invisible in their study, as they do not express this glutamate transporter.

Muller cell calcium signaling has also been demonstrated in retinal development by the Feller and Flannery labs, with wave propagation occurring both spontaneously and in response to stimulation with neurotransmitters [223]. However, they too utilized mice with a GLAST driven reporter of calcium signaling, leaving the potential role of retinal astrocytes unknown.

III-D Functional Hyperemia and the Neurovascular Unit

Direct coupling via gap junctions provides a powerful mechanism for coordinated glial activity, yet astrocytes must also act in concert with other cell types, primarily neurons and cells of the vasculature, with which they are not directly linked. This requires the release or uptake of various factors from the extracellular space, as well as response on a physiologically relevant timescale. As such, although these interactions are distinct from the gap junction mediated type, they too are considered a form of coupling. Although these include the recycling of metabolic factors and neurotransmitters – such as glutamate – from neurons, and gliovascular coupling with blood vessels, our focus in this review will be on a phenomenon known as functional hyperemia, in which the coupling of neurons, glia, and the vasculature modulates blood flow to active tissue in the central nervous system [224-227].

Functional Hyperemia

Functional hyperemia, the capacity of tissue to draw increased blood flow in response to elevated need, is well documented in the central nervous system, where it is also referred to as neurovascular coupling [228]. While the brain represents approximately 2% of the body's mass, it is responsible for ~20% of systemic oxygen consumption, and studies suggest that the energetic needs of the retina may be even higher on a gram-for-gram basis [17, 229, 230]. This creates immense pressure to not only ensure an adequate blood supply to the tissue but to also direct blood flow to active regions where it is needed most.

Although a modern hot topic – it forms the basis for the BOLD signal in functional MRI – study of the phenomena dates to at least 1890, when Roy and Sherrington investigated the relationship between blood flow and activity in the brain [231, 232]. Among their observations were that extracts from ischemic neural tissue could induce vasodilation in the brain upon injection into a healthy animal; evidence, they concluded, that the mechanism inducing increased blood flow was secretory in nature and "well fitted to provide for a local variation of the blood-supply in accordance with local variations of the functional activity" [233]. Nearly 100 years later, less invasive techniques including positron emission topography (PET) and, later, fMRI made it possible to investigate the link between neuronal activity and blood flow in awake, task performing human subjects [234]. Since then, researchers have begun studying the response of the retinal vasculature to direct visual stimuli in both animal and human subjects, an approach that allows for precise control of stimulus conditions [20, 235, 236].

In its original conception, the functional unit of neurovascular coupling consisted only of neuronal signal – either passive, in the form of metabolic byproducts, or active, in the form of vasodilatory nitric oxide – and a vascular response [198]. However, experimental stimulation of brain slices later showed an essential intermediary role for astrocytes, dependent on Ca^{2+} signaling, without which vasodilation disappears [184]. Crucially, astrocytes simultaneously contact neurons and ensheath the vasculature of the neural parenchyma, and secrete vasodilators such as prostaglandin E2 (PGE_2) and K^+, making them excellent candidates for mediating neurovascular coupling [198]. Early versions of this astrocyte-mediated neurovascular coupling proposed K^+ syphoning; that is, astrocytic uptake of K^+ released by neuronal signaling, with the ion traveling through the astrocyte syncytium to be released onto the vasculature, triggering vasodilation [237]. However, later experimental results suggest K^+ syphoning is neither necessary nor sufficient to mediate vasodilation [238].

Despite years of additional research on the topic, the specific mechanisms undergirding astrocytic modulation of neurovascular coupling remain highly debated [231, 239]. Multiple groups have reported that Ca^{2+} signaling in astrocytes is required to induce vasodilation and can do so independently of neuronal signaling, while other have concluded that this same Ca^{2+} mediated astrocytic signaling is dispensable [205, 206, 212, 213]. Recent attempts to resolve these seeming contradictions suggest that neurovascular signaling mechanisms differ between CNS regions and among vasculature types [193, 222, 240]. In particular, it is now thought that vasodilation in the capillary beds is mediated by Ca^{2+} dependent signaling in astrocytes, while dilation of the larger arterioles is not [229].

In this model, astrocytes detect signals of neuronal activity – such as the neurotransmitter glutamate – via receptors at the cell surface, resulting in release of the intracellular second messenger inositol trisphosphate (IP_3) into the cytoplasm [198]. IP_3 then binds its receptor, IP_3R2, triggering the release of stored Ca^{2+} from within the endoplasmic reticulum. This influx of Ca^{2+} into the cytosol results in arachidonic acid (AA) synthesis by PLA2, with astrocytes then using this AA to generate vasodilators such as PGE_2, which are released into perivascular space to induce vasodilation [180, 198]. At least in some brain regions, Ca^{2+} may also originate extracellularly, as activation of the transmembrane ATP receptor P2X1 has been shown to lead to an influx of Ca^{2+} [193]. Although the source of Ca^{2+} is different under these conditions, the downstream elements are generally similar, and Ca^{2+} induced generation and secretion of PGE_2 from astrocytes has been shown to be both necessary and sufficient for vasodilation at the level of the capillaries.

In the retina, Muller cells and pericytes – capillary associated contractile cells – have been shown to partner in mediating vasodilation in response to photic stimuli, particularly in the intermediate plexus where the change in capillary dilation is greatest, [222, 241]. Furthermore, direct stimulation of Muller cells to evoke ATP-mediated Ca^{2+} waves also induced vessel dilation in this layer, and in both cases these responses were IP_3 dependent, implicating intracellular stores as the source of Ca^{2+}. However, the authors did not investigate potential vasodilatory response to Ca^{2+} waves originating in astrocytes, despite having previously demonstrated that these waves propagate to nearby Muller cells *en masse* via gap junctions permeable to IP_3 [165, 179]. More recently, networks of gap-junction coupled pericytes in the superficial layer have been shown to mediate retinal capillary vasodilation in direct response to nitric oxide, a signaling molecule generated by neurons but not glia [115]. Intriguingly, these networks are coupled by Cx43, the same connexin linking retinal astrocytes, but the two cell types show little to no crossover in dye-coupling experiments despite their close proximity, suggesting they form separate but parallel networks.

Currently, the mechanisms underpinning the dilation of the larger superficial arterioles remains unknown, as it has been shown to be independent of the IP_3 dependent Ca^{2+} mediated Muller cell response seen in the intermediate plexus; direct vasodilatory stimulus by neuron derived nitric oxide has been proposed as a candidate, as has K^+ mediated signaling from retinal astrocytes [222, 242]. Whether retinal astrocytes directly contribute to arteriole dilation, and whether they mediate the Ca2+ dependent response in “downstream” Muller cells, remains to be elucidated.

III-E Astrocyte Signaling & Secretion

While small, permeable molecules can spread freely through the astrocyte syncytium via gap junctions, interactions with other cell types such as neurons and endothelial cells require the secretion of factors into extracellular space. In addition to releasing stored ions such as K^+, astrocytes secrete signaling molecules such as glutamate at the synaptic cleft to modulate neuronal signaling and PGE_2 and other vasodilators into the perivascular space to increase local blood flow [180, 198, 199, 243]. They also engage in the more gradual release of signaling

molecules - such as cytokines, growth factors, and lipid mediators – that can act on immediately adjacent cells (juxtracrine signaling) or those that are more distant but still nearby (paracrine). These signaling functions are distinct from the previously discussed coupling functions in that they primarily convey *information* between cells, rather than inducing coupled cells to act as a single functional unit. Astrocytes also secrete key elements of the extracellular matrix of the CNS, which can perform signaling roles in addition to acting as structural elements. Factors secreted by astrocytes play critical roles in both maintaining homeostasis in the neural parenchyma and in responding to external stimuli, and enter extracellular space by one of three mechanisms.

Mechanisms of Astrocyte Secretion

The first of these mechanisms, diffusion, occurs primarily through transmembrane channels at the astrocyte surface [244, 245]. These membrane-bound channels operate passively, driven by existing electrochemical gradients, but are typically "gated", such that they open or close in response to local membrane potential or the binding of an appropriate ligand [244]. Many of these are typical ion channels, displaying selectivity for size and for specific electrical charges; the most well-known of these in astrocytes are the K^+ channels like Kir4.1 [149, 245]. However other astrocytic channels such as Best1 have been shown to release the neurotransmitters GABA and glutamate under physiological conditions [246, 247]. Furthermore, unapposed hemichannels form large and relatively non-selective pores when open, as does the purinergic P2X7 receptor [248, 249]. In astrocytes, these hemichannels are formed by Cx43 or the pannexin Panx1, and their opening to extracellular space is mediated by elevations in intracellular [Ca^{2+}], as in Ca^{2+} signaling [243, 250]. The opening of these channels then allows the release of ATP and previously up-taken neurotransmitters including glutamate from astrocytes at the synaptic cleft, a process sometimes referred to as gliotransmission and one that, like the specifics of neurovascular coupling, remains contentious [180, 199, 251]. Conversely, the P2X7 receptor is ligand mediated and opens in response to elevated concentrations of ATP in extracellular space; it too has been shown to secrete glutamate from astrocytes [252].

The second mechanism utilized by astrocytes to move factors across their cell membrane is active transport, which typically involves the movement of ions and signaling molecules against their natural diffusion gradient [197]. This "uphill" movement requires energy, which can be supplied by the breakdown of ATP or by allowing a second ion to move down a favorable gradient, thus offsetting the "cost" of the transport. This category of action includes several essential and well documented elements of astrocytic function, such as the sodium-potassium pump and the glutamate transporters GLAST1 and GLT-1, which are often used as cell surface markers to identify astrocytes [253]. However, the activity of the sodium potassium pump is constitutive, while glutamate transporters are typically restricted to astrocytic uptake under physiological conditions, meaning that neither of these activities constitute astrocrine signaling; this is characteristic of the majority of well documented membrane transporters studied in astrocytes [244]. The less well-known transporter MRP4 is both expressed in astrocytes and implicated in the secretion of eicosanoids, including PGE2 [254, 255]. Although this category of secretory signaling is less well investigated in astrocytes, evidence also suggests that the lipid

mediator sphingosine 1‐phosphate is produced by astrocytes and exits via the ABCA1 transporter [256].

Although passive diffusion through open channels allows cells to rapidly secrete factors with minimal metabolic cost, for most proteins and other molecules used for intercellular signaling the path from the cytosol to extracellular space is considerably more complex [197, 257]. Vesicular exocytosis, in which molecules – especially proteins and peptides – destined for export are packaged in small lipid vesicles and subsequently released across the plasma membrane, allows for the regulated secretion of factors that are too large for channel transport. Exocytosis relies on a heterogeneous array of mechanisms – even within an individual cell – that include multiple vesicle types of different sizes and a variety of sorting mechanisms [257]. This sophistication allows for the stockpiling of vesicles in advance of a particular release-triggering stimuli, as well as the delivery of vesicle types to particular regions of the cell membrane for more targeted release from polarized cells.

Although essentially all cells engage in this form of exocytosis to some degree, neurons have particularly sophisticated mechanisms allowing for rapid release of stored vesicles in response to stimuli, which forms the basis of synaptic transmission [257, 258]. As with gliotransmission, the degree to which astrocytes utilize this more responsive vesicular system is highly debated. Among the key differences are the rate at which stimuli, such as a sudden local rise in [Ca^{2+}], induce fusion of vesicles with the membrane, triggering the release of their contents into the extracellular space. In neurons, this occurs at the millisecond or sub-millisecond scale, while the same process takes hundreds of milliseconds or even seconds in astrocytes [197, 259]. Although astrocytes and neurons utilize some of the same cellular machinery, such as the vesicle associated membrane protein VAMP2, astrocytes appear to lack the optimized vesicular arrangement that makes the rapid response at neuronal synapses possible [197, 260, 261].

These differences likely reflect the different roles vesicular transport plays in astrocytes and neurons. While synaptic vesicle release in neurons is optimized for rapid signaling to minimalize delays in neurotransmission, in astrocytes at least five classes of secretory vesicles utilize overlapping signaling and transport elements [197]. The smallest of these, the glutamate and d-serine transporting synaptic-like microvesicles (SLMVs), are reported to respond to Ca^{2+} signaling that differs from that which triggers exocytosis of the larger secretory lysosomes, which contain ATP and have been shown to contribute to ATP mediated Ca^{2+} signaling between astrocytes [197, 262]. This suggests the possibility that different patterns of intracellular Ca^{2+} signaling within astrocytes leads to functionally distinct outcomes regarding signals propagated to nearby cells. Further alluding to this possibility, experiments indicating the utilization of the intermediate filaments GFAP and vimentin for directional transport of astrocyte vesicles also showed that glutamate containing SLMVs underwent acceleration when exposed to elevated intracellular [Ca^{2+}], while secretory lysosomes and dense core vesicles (which carry BDNF and other peptides) decelerated instead [146, 210]. In addition to these three secretory vesicle types, which merge with the cell membrane and dissipate when releasing their cargo, astrocytes also produce two classes of extracellular vesicles that retain their structure for a time in the extracellular space – exosomes and ectosomes/microvesicles – and either release their

cargo there or merge with the membranes of other cells to deliver their load directly [197, 257, 263].

Categories of Factors Secreted by Astrocytes

Due to the overlapping mechanisms by which astrocytes secrete factors, and the considerable experimental challenges that frequently attend efforts to elucidate a given secretory pathway's role in cell behavior, many well studied astrocyte-derived factors lack clear pathways for exocytosis. However, discussing the important signaling roles of these molecules may be undertaken without knowing the precise mechanism by which these factors exit the cell. Three categories of signaling molecules will be briefly reviewed below: gliotransmitters, 'astrocrine' factors, and ECM components.

Gliotransmitters

As alluded to previously, the topic of gliotransmission is a contentious one; however, a review of the literature suggests that the debate stems at least in part from disagreements about the implications of glia signaling to neurons [180, 186, 187, 251]. As those implications are outside of the scope of this work, however, the term is included as a useful category for classifying a group of signaling molecules that are characterized by their overlap with conventional neurotransmitters and which appear to be released by astrocytes in a spatially restricted way at synapses. In addition to glutamate, a fast-acting excitatory neurotransmitter, astrocytes have also been shown to release the inhibitory neurotransmitter GABA, the neuromodulator D-serine, and broad-acting ATP [264]. Unlike astrocrine signaling, which includes specialized molecules such as growth factors, gliotransmitters are commonly utilized signaling molecules in the CNS and so their functions are likely to be heavily context dependent. One example of astrocyte to neuron signaling can be found in the brainstem, where vasculature ensheathing astrocytes have been shown to detect CO_2 related changes in blood pH and release ATP, directly modulating neuronal activity and inducing elevated breathing [265].

Astrocrine

Astrocrine or gliocrine signaling refers to a wide variety of factors originating from astrocytes that can target neurons, vasculature, and other glia, and which are characterized as occurring on a slower time scale than neurotransmission or even gliotransmission [197, 266]. These factors typically have greater specificity than gliotransmitters, targeting a restricted range of cell types via a specific receptor or receptors. Unlike endocrine signaling, in which signals are carried systemically via the blood, astrocyte-secreted molecules typically target nearby (paracrine) or even adjacent cells (juxtracrine).These include neurotrophic factors such as BDNF, which are expressed at relatively low levels in the healthy adult CNS but which can be highly upregulated in reactivity [267]. Astrocytes also secrete the synaptic regulators hevin and SPARC, the former promotes synaptogenesis while the later inhibits it, providing these cells with a measure of control over synapse development [268, 269]. Astrocyte-secreted APOE – a major target in Alzheimer's research – contributes to the development of functional pre-synaptic elements, while glypicans 4 & 6, also secreted by astrocytes, promote the functionality of post-synaptic elements [268, 270-272]. With regards to blood vessels, Apelin, a regulator of

vascular tone, is secreted by retinal astrocytes and plays a prominent role in retinal vasculature development [95, 98, 273]. Additionally, recent research has found a role for lipid mediators derived from astrocytes, such as LXA_4 and LXB_4, in promoting neuronal survival in the retina and *in vitro* [274].

Extracellular Matrix Components

A related mechanism by which astrocytes signal nearby cells is the incorporation of secreted factors into the extracellular matrix. The extracellular space of the CNS is actually quite small, with restricted volume for the diffusion of soluble factors. Instead, many signaling molecules are embedded in the ECM, including factors secreted by astrocytes; the synapse promoting Thrombospondins (Tsp -1, -2) fall into this category [275, 276]. Astrocytes are also in part responsible for the broader formation of the ECM in the central nervous system, such as through the deposition of fibronectin for vascular patterning on the surface of the developing retina or secreting Tenascin C in development and injury, however these are generally down-regulated in the mature nervous system under homeostatic conditions [86, 277]. Indeed, the full range of astrocyte secretions is considerable and exceeds the scope of this document (although additional reactivity specific secretions will be covered in section IV-D). For a fuller review, please see Jha et al., 2018 [278].

Part IV: Astrocyte Reactivity

Although astrocytes are masters of maintaining homeostasis in the central nervous system, they are – alongside microglia – first responders when that homeostasis is disrupted [124, 279, 280]. Physical and ischemic injuries (such as traumatic brain injury or stroke), pathogen infiltration, and even aging related neurodegenerative disorders (glaucoma and AD) all trigger response behavior in astrocytes known as "reactivity" [281-285]. A recent consensus statement, authored by a number of leading figures in astrocyte research, defined reactivity in astrocytes as "morphological, molecular, and functional changes in response to pathological situations in surrounding tissue"[286]. The lack of specificity illustrates how broad a topic astrocyte reactivity is, which is a function of both the wide range of injuries the central nervous system can suffer – from the mild to the devastating – and the extensive behavioral repertoire of astrocytes [287-290].

However, despite the breadth of behaviors that exist under the banner of reactivity, the vast majority can be understood as modifications of quiescent behaviors or recapitulations of developmental ones. For example, major neurological trauma – induced by physical injuries such as penetrating wounds or TBI – can induce a particularly severe reactive phenotype in astrocytes, in which typically non-proliferative mature astrocytes near the site of injury undergo low levels of proliferation as they form a glial scar [291-293]. One exception to this trend is that reactive astrocytes also often take on elements of immune cells during acute inflammatory states, which will be covered separately [283, 294]. Otherwise, astrocyte reactivity will be reviewed in a similar arrangement to the section reviewing mature astrocytes in the healthy CNS. Owing to the larger focus on reactivity in much of retinal astrocyte research, there will be greater emphasis on this particular population in this section.

IV-A Classification of Reactive Astrocytes

Historically, particularly during the period in which glia were thought of as primarily structural elements in the CNS, astrocyte reactivity was treated as a unidimensional phenomenon. In this model, the astrocyte response to myriad pathological stimuli varied only in severity, with the most severe form – often referred to as gliosis – characterized by the formation of permanent 'glial scars' [291, 295]. These scars were observed to be barriers to potential regeneration in the nervous system, and so astrocyte reactivity was considered a primarily harmful behavior [296, 297]. However, as improved research techniques began to allow for the ablation or even prevention of gliosis and scarring, these phenomena were found to not only <u>not</u> inhibit regrowth, but to be key to averting even worse outcomes such as neurotoxic immune responses [298, 299]. Simultaneously, as available models of reactivity diversified from acute injury models to include more subtle models that came closer to recapitulating aspects of neurodegenerative disease, signs began to emerge that reactivity was a complex, multidimensional phenomena, and that elements of this behavior that were neuroprotective in

one model of disease might be neurotoxic in others, and vice versa [300-302]. However, research in astrocyte reactivity remained largely 'silo-ed', with groups researching a given disease using highly specific sets of markers sharing little overlap with those used by researchers of other diseases.

More recently, as increasingly robust transcriptomic studies made it possible to go beyond studying reactivity one marker at a time, broad trends began to emerge in the patterns of genes expressed by astrocytes [300]. Eventually, an accumulation of *in vivo* studies began to resolve two highly divergent phenotypes of astrocyte reactivity: one resulting from exposure to bacterial lipopolysaccharide (LPS) – a marker of pathogen infiltration – and the other from mid-cerebral artery occlusion, an ischemic injury mimicking stroke [303-307]. Although the use of these two phenotypes was in part an artifact of the inducible *in vivo* models of reactivity used at the time and represents an oversimplification, the results were robust and transferrable enough that they became the basis of a reactivity classification schema [288, 300]. This classification scheme, borrowing from one used for macrophage activation, termed the LPS-induced phenotype A1, and the MCAO phenotype A2. Particular attention was paid to the A1 phenotype, and in vitro experiments demonstrated that the response was mediated by microglia, which detected the bacteria derived LPS and in turn secreted a milieu of reactivity inducing factors. A set of three of these factors, Il-1a, TNF-a, and C1q were found to be necessary and sufficient to induce the A1 phenotype, and the classification schema found widespread adoption[307].

However, Liddelow et al. took their investigations a step further, and found that, the factors secreted by these A1 astrocytes were harmful to cultured neurons *in vitro*. Although their *in vivo* results were less conclusive, they termed the A1 phenotype neurotoxic [288, 308, 309]. This overreach might have been ignored had the A1 phenotype been less ubiquitous in disease models, but the rapid adoption of the naming convention and the frequency with which their proposed markers were found in models of neurodegeneration eventually led to the above mentioned 'consensus statement' from a number of leading reactivity researchers, including the first author of the original neurotoxic A1 astrocytes paper [286]. However, although the model led to overreach and is an oversimplification – the reactivity state of astrocytes is increasingly thought of as composite of multiple inter-related functional behaviors – like the original classification of astrocytes by morphology it does have value in representing the broad counters of two common reactive phenotypes. Further investigation into the underlying behaviors that make up the phenotype to determine to what extent they are interlinked through common pathways vs occurring concurrently due to experimental design remain to be done. Some evidence suggests that these phenotypes may more accurately represent phases of reactivity than discrete types, but this too requires further investigation [287].

An additional, insufficiently explored aspect of astrocyte classification is whether different types of astrocytes undergo reactivity differently. In the eye, retinal astrocytes are fibrous and express GFAP at high levels during homeostatic conditions, as a result they show relatively

limited upregulation of GFAP during reactivity. However, the protoplasmic Muller cells express low levels of GFAP under normal conditions and greatly upregulate when exposed to reactivity inducing stimuli. A limited body of research done primarily in the brain suggests that these two categories of astrocytes may have distinct repertoires of functional changes in reactivity [301, 310]. In glaucoma, both in animal models and human derived retinal tissue, many markers of reactivity are expressed in retinal astrocytes, including the proposed A1 marker C3, part of the compliment cascade used to target tissue for pruning and removal [311, 312]. Liddelow et al. have documented A1 reactivity markers in the retina of mice after optic nerve crush, and by using their TNF, Il-1a, C1q triple knock out animals, have asserted that A1 astrocyte reactivity drives RGC death [309]. However, they did not separate retinal astrocytes for transcriptomics but rather used whole retina with a panel of their chosen markers, meaning that any glial signal detected likely originated in Muller cells, which outnumber retinal astrocytes in the mouse by a factor of 40 to 1. Finally, their use of axotomized RGCs, which were rescued in their knockout mouse, may reveal key factors involved in the elimination of catastrophically injured neurons, but also illustrates why their characterization of the astrocytes involved as neurotoxic was considered overreach by others in the field.

IV-B Morphology, Structure, and Recapitulating Development

A common element among various astrocyte reactivity states is structural remodeling. This remodeling, which relies on the upregulation of intermediate filaments (IF) including GFAP, vimentin, and nestin, occurs most prominently in response to localized stimuli, such as penetrating wounds, ischemic infarcts, and amyloid plaques in Alzheimer's disease [281, 284, 285]. However certain aspects, such as hypertrophy – in which the processes of astrocytes thicken as they incorporate larger amounts of GFAP and other IFs – occur even in cases of generalized neuroinflammation [124]. Hypertrophy is a graded response that may reflect the severity of neurological insult, and in the case of the localized injury tends to increase in relationship with proximity to the injury site. Contrary to long held assumptions about the nature of hypertrophy, work in the cortex has shown that the restriction of astrocytes to non-overlapping domains – a hallmark of so called quiescent or homeostatic astrocytes – persists even in cases acute injury [313].

In addition to hypertrophy-induced breakdown of domain exclusivity, reactive astrocytes – particularly in response to severe insults – were thought to migrate to the site of injury and undergo proliferation. As homeostatic mature astrocytes exhibit little to no motility or proliferation, this partial recapitulation of developmental phenotype was considered a hallmark of reactive astrocytes [292, 314]. However, it now largely accepted these assumptions stem from artifacts resulting from the reliance on GFAP as an astrocyte marker. Briefly, astrocytes in many brain regions, and protoplasmic astrocytes of the cortex in particular, express low levels of GFAP under homeostatic conditions, rendering them essentially invisible under many tissue imaging approaches. Reactivity-induced hypertrophy results in an upregulation of GFAP,

however, and in rendering a larger population of astrocytes in a given region visible gives the general impression of a larger total astrocyte population [124]. This increase was attributed to migration and extensive proliferation, as both behaviors could be observed with isolated astrocytes in vitro.

Although the breakdown of domains and the re-emergence of motility are no longer considered elements of astrocyte reactivity *in vivo*, structural changes relying on an upregulation of astrocyte intermediate filaments – including the developmentally expressed IFs vimentin and nestin – are indeed present [141]. In addition to general hypertrophy, astrocytes near the site of a localized injury may show signs of reoriented processes, with these structures repositioning to surround the core of amyloid plaques in tissue taken from Alzheimer's patients [315]. In the case of particularly severe localized insult, they may form a glial scar [291]. Furthermore, although the broader narrative of extensive migration and proliferation in reactivity has been largely eroded, evidence does suggest that a limited sub-population of reactive astrocytes does proliferate, although the percentage of astrocyte observed to proliferate in vivo is small [292]. This proliferation is observed primarily in severe cause of neuropathology and is associated with the formation of a permanent glial scar.

In the retina, Müller cell hypertrophy is more readily discernable than that of astrocytes, as the upregulation of GFAP in these cells contrasts sharply with the low level of expression in healthy tissue [47, 316]. Scar formation in the retina is characteristic of Müller cell response to focal injuries, such as photocoagulation induced by laser exposure [317]. Astrocytic hypertrophy, conversely, is a major avenue of investigation in glaucomatous degeneration, particularly at the optic nerve head and in the optic nerve [285, 318-320]. Of note, diseases such as diabetic retinopathy that are characterized by a breakdown of the blood retinal barrier can induce proliferation in Müller cells, likely due to their exposure to factors in serum [47]. Additionally, retinal detachment may also induce proliferation in Müller cells and their partial migration to the outer retina, in a process that mimics some elements of retinal development [321].

IV-C A Breakdown of Order: Changes to Astrocytic Coupling in Reactivity

Although certain assumptions about the individual behavior of reactive astrocytes have not held up, reactivity can induce major changes in the functionality of the astrocyte syncytium that effect both global and local changes in astrocyte function. As previously discussed, Cx43 has dual roles in astrocytes: it, along with Cx30, can form gap junctions that allow for direct coupling between astrocytes; however, it (and the pannexin Panx1) may also form hemichannels at the cell surface that are capable of opening a pore to extracellular space under certain conditions [243, 250]. In the case of the former, this connectivity is essential for large scale astrocyte connectivity, with metabolites, regulators of Ca2+ signaling, water and ions flowing freely between astrocytes, while the later are involved in the indirect coupling of astrocytes to neurons and the vasculature and provide a route by which glutamate, ATP, PGE_2

and other signaling molecules can exit the cell [158, 161, 322]. However, under conditions that induce astrocyte reactivity, the delicate balance between these functions can be disrupted, leading to a decrease in astrocyte network function and a simultaneous increase in hemichannels activity [323]. In particular, exposure to media conditioned by LPS treated microglia has been shown to reduced gap-junction coupling of astrocytes *in vitro* while increasing Cx43-mediated hemichannels activity, as did treatment with TNFα and Il-1B.

Although the clearest results showing a role for pathological over-activity of Cx43 hemichannels in astrocytes comes from *in vitro* work, abundant *in vivo* and *in situ* work, including medical investigation of living human patients, shows clear astrocyte gap junction dysfunction in a variety of neurological disorders, such as epilepsy, while histological studies show alteration of Cx43 expression in human glaucoma and Alzheimer's disease [324-326]. Furthermore, in a mouse model of LPS induced astrocyte reactivity, reactivity induced uncoupling of in vivo astrocytes and a concomitant disruption of K^+ buffering, leading to seizures and the apoptotic death of neurons [324]. In addition to the above-mentioned roles of Cx43 in reactivity, changes in astrocytic gap junctions may contribute to Ca^{2+} signaling dysregulation observed in astrocytes in a number of disease states [327]. Likewise, as some elements of neurovascular coupling are mediated through astrocytes, the breakdown of astrocyte coupling behavior is of considerable interest with regard to the neurovascular dysregulation that is observed in diseases such as Alzheimer's [328].

In the retina and optic nerve, where neurovascular coupling has been extensively demonstrated in response to sensory stimuli, neurodegenerative conditions associated with the induction of astrocyte reactivity are also associated with disruption of neurovascular coupling [329, 330]. In particular, patients with primary open angle glaucoma experienced dysregulation of neurovascular coupling in response to flicker stimuli, with a diminished response compared to healthy age matched controls [331, 332]. Likewise, in tissue from deceased glaucomatous patients, Cx43 was upregulated in the retina and at the lamina cribrosa relative to non-glaucomatous controls [326]. Studies in monkeys have further indicated that elevated intraocular pressure, the hallmark of glaucoma and a key component driving neurodegeneration in the disease, induces phosphorylation and relocation of Cx43 in the optic nerve, potentially contributing to astrocyte reactivity and axonal degradation [333]. However, although evidence points to the relevance of dysfunctional astrocyte coupling in glaucomatous degeneration, the specific mechanism by which this is mediated – whether through a specific role for retinal or ONH astrocytes in diminished neurovascular coupling or a general disruption of the astrocyte syncytium – remains to be elucidated.

Ca^{2+} Signaling Dysregulation in Astrocyte Reactivity

Given the increasingly recognized role of Ca^{2+} signaling in regulating astrocyte behavior, it should come as little surprise that reactive astrocytes exhibit measurable alterations in their Ca^{2+} signaling relative to homeostatic astrocytes [327]. Indeed, because Ca^{2+} signaling mediates rapid behavioral changes in astrocytes, it may be an early indicator of the induction of

reactivity; a kainic acid-based model of seizures, for example, triggers an IP_3R2-dependent elevation in astrocytic Ca^{2+} signaling that precedes the neuronal response [334]. Additionally, a murine model of Alexander disease – a genetic disorder in which a mutated GFAP gene results in pathogenic accumulation of intracellular fibers in astrocytes - showed abnormally large Ca^{2+} signals coupled with upregulation of GFAP and the reactive astrocyte markers Lcn2 and C3; abrogation of elevated Ca^{2+} signals by IP_3R2 deletion had the additional effect of largely abolishing upregulation of Lcn2 and C3 [335]. Mouse models of common neuropathologies, including Alzheimer's and stroke, are also characterized by elevated astrocyte Ca^{2+} signaling, while spontaneous Ca^{2+} signaling was instead reduced in a mouse model of Huntington's disease [336-338].

Given the ongoing efforts to understand the complexity of the Ca^{2+} signaling "code" in astrocytes, however, it is difficult to ascertain the precise implications of a given change in signaling patterns. Furthermore, the transient nature of these signals makes their role more difficult to assess in human derived tissue than more stable changes at the mRNA and protein level. Finally, although a number of groups have investigated glial Ca^{2+} signaling in healthy retinas, to our knowledge the changes this signaling undergoes in retinal neurodegeneration, specifically OHT induced / glaucomatous neurodegeneration, remains unknown.

IV-D Reactive Astrocyte Signaling and Secretions

Under homeostatic conditions, astrocytes have a major role as secretory cells, and this remains true under reactivity inducing conditions as well [197, 278]. However, the nature of reactive astrocyte secretions can differ dramatically from those of homeostatic astrocytes; in addition to upregulating mediators of inflammation, reactivity can decrease astrocytic expression of homeostatic factors, exacerbating damage during extended or chronic insult [274, 287, 307]. Furthermore, the relationship between astrocytes and the extracellular matrix can change dramatically under these conditions, with astrocytes both contributing to ECM remodeling and inhibiting it [339, 340]. Finally, reactive astrocytes secrete chemo-attractive cytokines, known as chemokines, that can recruit microglia and peripheral immune cells to the site of insult [341]. However, the review of chemokines is presented in section IV-E, "Immune Functions of Reactive Astrocytes".

Gain of Inflammatory Signaling, Loss of Homeostatic Signals

Although the particular secretory changes undergone by reactive astrocytes depends largely on the nature and severity of the activating insult, and can vary along the time course of the pathology, reactive astrocytes are well known for expressing inflammatory mediators [278, 286, 287]. Evidence suggests that A1-type reactivity may represent a pro-inflammatory mode of response, while A2-type reactivity may represent the contribution of astrocytes to dampening or resolution of inflammation, but there are a number of secreted factors that can be found in multiple models and states of astrocyte reactivity [288]. Perhaps the most ubiquitous of the

proteins secreted by reactive astrocytes, Lipocalin-2 (LCN2) is upregulated in both A1 and A2 reactivity models, as well as Alzheimer's disease and stroke [307, 342-344]. Part of a family of extracellular transporters, LCN2 has been suggested to act as a protective carrier for MM9 – a matrix metallopeptidase involved in the breakdown of ECM – and to mediate the propagation of reactivity throughout astrocyte populations via the receptor 24p3R; it is additionally known to have antibacterial activity via its iron sequestering properties [345-347]. While the full range of factors secreted by reactive astrocytes is beyond the scope of this review, several additional noteworthy examples are covered below.

Complement factor 3 (C3), the proposed marker of A1 astrocytes, is a component of the innate immune system associated with phagocytosis of both cellular debris and pathogens [348]. Secreted C3 binds to the surface of cells and debris, targeting them for removal, and is highly upregulated in the human retina in glaucoma, as well as the brain in Alzheimer's and other neurodegenerative diseases [307, 311, 312]. The Alzheimer's biomarker CHI3L1, also referred to as YKL-40, is secreted by reactive astrocytes, and recent research suggests it may control the phagocytic activity of glia in a circadian rhythm dependent manner [349-351]. Conversely, Clcf1 – which is highly upregulated in A2 astrocytes – binds both the CNTF and ApoE receptor and is neurotrophic [300, 352]. Although factors downregulated in reactive astrocytes are less well investigated, Apelin – secreted by astrocytes during development to promote vascular maturation and expressed constitutively thereafter – is downregulated in reactivity [353].

Secretions from Reactive Astrocytes Mediate Extracellular Matrix Remodeling

Just as astrocytes play a major role in the formation of the extracellular matrix during development, so to do reactive astrocytes mediate the remodeling of the ECM that occurs during neuropathologies. Whether in response to chronic neurodegeneration or acute physical trauma, major changes to the central nervous system are accompanied by extracellular matrix remodeling, a process that prioritizes restoration of the blood brain barrier and structural support, but can inhibit functional regeneration and recovery of function [354-356]. Accordingly, astrocytes both mediate the breakdown of the existing ECM – promoting or inhibiting it accordingly – and secrete crucial elements to rebuild the extracellular matrix during recovery [339, 340].

Particularly during the acute phase of neurological insult, reactive astrocytes secrete both proteases – in part to facilitate the infiltration of pathogen hunting and debris clearing immune cells into the neural parenchyma – and proteinase inhibitors to restrict this potentially damaging activity [340, 357, 358]. Two of the most well studied astrocyte proteinases – MMP2 and MMP9 – are members of the matrix metalloproteinase family, with major roles in ECM remodeling and disruption of the blood brain barrier [359]. During acute neuroinflammation, MMPs from astrocytes and peripheral immune cells such as leukocytes combine to disrupt the endothelial cell derived basement membrane around blood vessels, degrading it from both sides to disrupt tight junctions and facilitate the extravasation of blood borne immune cells. However, this activity is not without risk – not only can this disrupted BBB become "leaky",

allowing both cells and soluble factors that should not be present in the CNS to pass through – but the enzymes involved can damage intact CNS cells, including the astrocytes themselves, as well as triggering neuropathic pain [360]. Prior studies suggest that this risk may be managed in part by differential roles for the proteases involved, with MMP2 activity associated with temporary and reversible changes to the BBB and MMP9 being associated with permanent degradation of BBB components [359].

To further mitigate the risk of excess damage, astrocytes secrete a number of protease inhibitors to block widespread degradation of the ECM and BBB. Two of these, Timp1 and Serpina3n, are considered markers of generalized astrocyte reactivity and upregulated in a variety of neuropathologies, including Alzheimer's [286, 307]. Timp1 is most well-known as an inhibitor of MMPs, but both it and Serpina3n are able to inhibit a variety of proteases, and the loss of either has been implicated in the progression of neuropathic pain induced by immune infiltration [357, 360, 361].

During and after acute insult in the CNS, reactive astrocytes respond by repairing and remodeling the extracellular matrix, but chronic conditions can also trigger astrocyte driven remodeling [339]. Tenascin C, a glycoprotein secreted by astrocytes during development but downregulated in homeostatic mature astrocytes, is a major component of the extracellular matrix of the brain and spinal cord [277]. Severe acute trauma, such as found in penetrative injury models, can cause reactive astrocytes to express and secrete tenascin C [362]. However, upregulation by reactive astrocytes also results in increased levels of tenascin C at the optic nerve of head in glaucomatous eyes, suggesting it additionally plays a role in strengthening and repairing the ECM in response to slower, chronic insults [363, 364]. Astrocytes also secrete multiple members of the lectican family of proteoglycans, which help bind tenascin and neuronally derived hyaluronan and stabilize the extracellular matrix of the CNS [365, 366]. After injury, reactive astrocytes upregulate secretion of these proteoglycans, which tightly bind the remodeled ECM and are thought to contribute to the inability of neuronal axons to regrow through the glial 'scar' [356, 367, 368]. Finally, in addition to secreting structural elements of the extracellular matrix, reactive astrocytes also seed the ECM with signaling molecules that promote or inhibit regrowth, migration, and specific cell behaviors. These include synapse promoting thrombospondins 1 & 2, and the synaptic regulators hevin and sparc [339].

IV-E Immune Functions of Astrocytes

In addition to their other functions in CNS development, homeostasis, and reactivity, astrocytes have a complex role in both immune surveillance and response. The brain and central nervous system are frequently described as “immune-privileged”, referring to the relatively limited infiltration of the CNS by peripheral immune cells, particularly in the healthy animal [369]. Contrary to popular conception this privilege is far from absolute, but it does mean that astrocytes and microglia have enhanced roles in detecting and responding to microbial threats and physical injuries of the CNS [370-372]. Although elements of this behavior, such as immune surveillance and some degree of phagocytosis, appear to be found in homeostatic astrocytes, these are best understood in the context of reactivity and so are presented here. Curiously, many factors expressed by reactive astrocytes even in the context of “sterile” neuroinflammation (in which there is little evidence of pathogen infiltration of the CNS) are associated with antimicrobial inflammatory response [288, 307]. One possibility is that these factors, which can hinder CNS recovery from trauma, are expressed prophylactically due to the potentially fatal consequences of microbial infiltration of the CNS [370].

Immune Surveillance by Astrocytes

Alongside microglia, astrocytes contribute to immune surveillance functions in the CNS. Throughout evolution, multicellular organisms have developed a range of conserved receptors that are specialized for detecting disease associated molecular patterns (DAMPs) and pathogen associated molecular patterns (PAMPs) [373, 374]. These receptors react to stereotyped elements of pathogens – such as lipopolysaccharide (LPS) from bacteria and double-stranded RNA from viruses – or byproducts of injury and allow for a more precise immune response [375]. The most well studied group of these sensory receptors are the Toll-like receptor (TLR) family, several of which are expressed by astrocytes including TLRs 2, 3 and 4 [287, 370]. Of these, TLR2 and TLR3 are relatively specific, with TLR2 responding primarily to PAMPS derived from bacteria while TLR3 detects signals of viral replication [376]. However, TLR4 responds not only to bacterial LPS but also a variety of DAMPs – including heparan sulfate, fibronectin, and hyaluronic acid – released by breakdown of the extracellular matrix of the CNS [377-379]. Furthermore, TLR4 has the widest range of intracellular signaling pathways induced by its activation, activating MyD88/NFkB- , JNK- , and ERK- mediated pathways in astrocytes [376, 380]. This may represent a partial explanation for the overlap of the response to CNS injury with potentially neurotoxic anti-microbial behavior and chemokine secretion.

Beyond the TLR family of pattern receptors, astrocytes also express NOD-2 receptors, which play a key role in detecting intracellular pathogens and contribute to an augmented response by astrocytes to both gram positive and gram negative bacteria, including *S. aureus*, which can cause brain abscess and fatality in infected individuals [370, 381]. Likewise, the scavenger receptor SR-MARCO has been linked to the response of astrocytes to both bacterial meningitis and Alzheimer’s [382, 383]. Finally, in addition to their ability to directly sense several classes of PAMPs and DAMPs, astrocytes can also respond to signals secreted by activated microglia,

which have a greater role in immune surveillance in the central nervous system [371, 384]. This modulates astrocyte reactivity (A1[307], TIMP1[358]) and may enhance chemokine secretion and peripheral immune cell recruitment by reactive astrocytes.

Immune Cell Recruitment: Chemokine Signaling and Antigen Presentation

Whether detecting signs of pathogenesis directly or in response to microglial signals, astrocytes play an essential role in mediating the subsequent immune response. Throughout the body, nearly all cells express major histocompatibility complex class I (MHC I) on their surface in order to participate in immune surveillance through a process known as antigen presentation, in which they externalize peptide fragments from intracellular proteins, "presenting" them for immune detection [385]. In healthy individuals this function is responsible for training the immune system to recognize the body's own cells and reducing the risk of auto-immune response, while the presentation of unfamiliar peptides can indicate an infected cell [386]. In addition to MHC I mediated surveillance, specialized antigen presenting cells – such as the dendritic cells of the immune system – also express class II MHC molecules, which display fragments from extracellular threats [387]. Antigens bound by either class of MHC are assessed by T cells – a roaming class of immune lymphocyte – that evaluate the threat and may act to destroy infected cells or mount a broader immune response [386]. However, T cells are rare in the healthy central nervous system – a function of the tissue's (relative) immune privilege – and dendritic cells are completely absent in the CNS parenchyma [384, 388, 389]. Instead, reactive astrocytes play a key role in recruiting immune cells and antigen presentation during infection or injury of the central nervous system.

Chemokine Signaling

Chemokines – a class of cytokine responsible for inducing chemotaxis, particularly of immune cells – are secreted by reactive astrocytes under a variety of neuropathological conditions, which can attract both resident microglia and peripheral immune cells [390-392]. The chemokine signaling system includes a variety of ligands and receptors, with receptor expression varying by immune cell type, and both *in vivo* and *in vitro* studies suggest that the mix of secreted chemokines may be pathogen specific [370, 393]. For example, when stimulated with markers of bacterial infection such as LPS, astrocytic secretions are dominated by monocyte chemoattractant protein 1 (MCP-1/CCL2), which can induce monocyte/macrophage recruitment; however, when poly I:C – a synthetic analog of double-stranded virus RNA that triggers TLR3 activation – is used as a stimulus instead, astrocytes primarily secrete CXCL10, which can recruit T-cells to eliminate infected cells [394-396]. Chemokine signaling by astrocytes is not limited to these factors; both categories of stimuli induce the secretion of additional factors in lesser quantities, and additional chemokine signaling motifs may exist. In addition to generating chemotactic signals to immune cells, reactive astrocytes also participate in the blood brain/retina barrier disruption that allows these cells to infiltrate into the neural parenchyma [397]. Although this can enhance neurological damage, it is essential for survival of the organism in the case of microbial presence in the CNS;

furthermore these reactive astrocytes also act to “corral” infiltrating immune cells at the site of damage, limiting the spread of harmful neuroinflammation [398].

Antigen Presentation

After recruiting peripheral immune cells to the site of injury and facilitating their extravasation to the neural parenchyma, reactive astrocytes can then directly act as antigen presenting cells. The response of T-cells to microbial antigens depends in large part on whether they are presented by MHC I or MHC II; in the case of the former, CD8+ “killer” T-cells induce apoptosis of the infected cell, while presentation by the later instead primes CD4+ “helper” T-cells to recruit additional immune resources [386]. Originally, in line with earlier interpretations of immune privilege in the tissue, MHC I was thought to be absent in the CNS [399, 400]. While this is not strictly true, MHC I expression on neurons and glia is limited and shows unusual patterns: *in vivo*, astrocytes display low MHC I expression even in the case of viral infection, while neuronal MHC I appears to be restricted to synaptic processes where evidence suggests it may play a role in plasticity [400-404]. This altered MHC I expression may play a role in the survival of virally infected neurons, and infected astrocytes show considerable resistance to T-cell mediated apoptosis as well; an adaption that makes sense given the constrained ability of either cell population to proliferate in mature animals [399, 401].

Unlike dendritic cells, astrocytes do not express MHC II constitutively, leading to early controversy over their role in antigen presentation; however the inflammatory cytokine interferon gamma (IFN-γ) has been shown to induce cell surface MHC II on astrocytes *in vitro*, and astrocytic MHC II expression has been detected *in vivo* in neurodegenerative disorders including multiple sclerosis (MS) and Parkinson’s disease (PD), as well as experimentally induced ocular hypertension [405-408]. Furthermore, several endogenous cytokines – including IFN-β and TGF-β – are known to reduce MHC II expression in astrocytes; the former is utilized as a treatment for MS [406, 409, 410]. Intriguingly, exposure to the neurotransmitter glutamate has been shown to suppress expression of astrocytic MHC II, potentially limiting the intensity of immune response in regions with intact neural function [411].

Phagocytosis

Phagocytosis – the engulfment and destruction of pathogens, damaged cells, and debris – is a necessary function in multicellular organisms, and the central nervous system is not exempt [412, 413]. During development, more neurons and glia are formed than required, and a significant fraction die and are removed as part of normal developmental processes [109, 414]. Likewise, clearance of debris, destruction of pathogens, and removal of dead and dying cells are required in response to injury and disease [415-417]. More recent work has shown that phagocytic clearance even plays key roles in the maintenance of function and homeostasis [418, 419].

Although microglia are the primary phagocytic cell of the central nervous system, astrocytes have also shown a more restricted version of these functions [109, 294, 420]. In a mouse model

of stroke – MCAO – reactive astrocytes at the periphery of the injury showed upregulation of the phagocytic marker galectin-3 and lysosomal marker LAMP2, as well as internalization of neuronal debris [294]. Additionally, astrocytes in human tissue isolated from MS patients showed engulfment of myelin fragments, while reactive astrocytes have been documented phagocytosing damaged synaptic elements in tissue from Alzheimer's patients [421, 422]. Intriguingly, the Alzheimer's risk associated allele APOE4 has been linked to diminished phagocytosis by astrocytes in an in vivo animal model, while the protective allele APOE2 is conversely associated with an increase in this activity [423].

Beyond their role in debris clearance in pathological states, mature homeostatic astrocytes engage in phagocytosis of protrusions from retinal ganglion cell axons at the optic nerve head, which were later shown to contain damaged mitochondria, and have been implicated in synaptic pruning in the brain [268, 419]. Finally, as part of development astrocytes have been shown to participate both in synaptic elimination – a key component of mediating plasticity – and in removal of excess glia, although the latter case involved microglial inactivation and may not reflect typical astrocyte activity in healthy animals [109, 420]. Reviews of the available evidence suggest that the phagocytic activity of astrocytes is generally positive, and its upregulation in disease states may reflect an aging associated decline in microglia phagocytosis [424].

Part V: Glaucoma

Glaucoma, a neuropathology of the retina characterized by the death of retinal ganglion cells and an accompanying loss of visual field function, is estimated to affect roughly 76,000,000 individuals globally as of 2020, making it both a common neurodegenerative disease and the leading cause of irreversible blindness worldwide [425, 426]. Although the net results of all unchecked glaucomas are similar – death of retinal ganglion cells accompanied by progressive visual field loss – there are a number of variants with a range of contributing factors, prognoses, and treatments [427]. Of the various subtypes, primary open angle glaucoma (POAG) is the most prevalent, and unlike rarer subtypes - such as corticosteroid induced glaucoma or exfoliation glaucoma - POAG lacks a clear causative factor; that is, it is 'primary' because it is not known to be secondary to another etiology [320, 428, 429]. The designation 'open angle' also distinguishes POAG from closed angle glaucoma, which derives its name from the measurable obstruction of aqueous outflow from the eye that can induce a much more rapid onset, which may be accompanied by more pronounced symptoms including pain [427].

One of the most significant factors in the development and progression of POAG is an increase in intraocular pressure (IOP), which is thought to induce strain on the axons of retinal ganglion cells at the optic nerve head where they exit the retina, as well as at the lamina cribrosa, a reticular network composed of cells and extracellular matrix that is known to undergo remodeling in glaucoma and under conditions of ocular hypertension [430-432]. The optic nerve and optic nerve head, which are key sites of RGC axon damage in glaucoma, are heavily populated by astrocytes, which demonstrate considerable upregulation of reactive markers in human glaucoma and a number of animal models [285, 319, 333]. Additionally, the somas of RGCs and the retinal portion of their axons are in close association with the astrocytes of the inner retina [433-435]. Although POAG can be slowed with treatment, there is no cure, and so these circumstances have made retinal and optic nerve head astrocytes subjects of significant research for their role in glaucomatous degeneration, as astrocyte behavior is closely tied to neuronal survival [320, 333, 436, 437].

V-A Epidemiology

Of the estimated 76 million individuals worldwide suffering from glaucoma in 2020, roughly 44 million cases (nearly 60%) are projected to be affected by primary open angle glaucoma, making it by far the most common variant [425]. Of these individuals, historical evidence suggests that up to 10% – or 4.4 million individuals – may be bilaterally blinded, although this ratio may rely on outdated or regionally specific estimates [438, 439]. Regardless, this represents an enormous population of individuals with partial or complete vision loss, and direct medical costs alone for US patients was estimated to be approximately $2.9 billion in 2004 dollars [440]. Owing to inflation, an aging population, under-diagnosis, lost productivity,

and the burdens on unpaid caregivers, this is likely to be a significant underestimate of the current actual cost [441].

Primary open angle glaucoma is a complex disease, with environmental factors, sex, age, and ancestry all contributing to risk, although individual genetic variation has only been shown to play a modest part [320]. Among all populations, increasing age – particularly after 60 – was associated with a rise in disease prevalence, and when adjusted for age, males were at a ~30% increased risk [320, 425]. Individuals with African ancestry, whether they lived in Africa or elsewhere, had an elevated risk of POAG relative to other groups (5.4% prevalence compared to a global prevalence of 3.05%) [425]. Comorbidities associated with a higher risk of glaucoma include hypertension and type 2 diabetes, along with so-called 'high myopia' [442-444]. However, the most well-known risk factor – elevated intraocular pressure – is also one of the largest, with every additional mmHg of pressure increasing risk of disease progression by 5% [445].

V-B Disease Mechanisms and Progression

Although a variety of criteria have been used over time to define and diagnose glaucoma, the functional units of pathology in the disease are the degeneration of retinal ganglion cell axons and the death of RGCs themselves [320, 446]. The precise cause or causes of this neurodegeneration remain elusive, as a variety of relevant factors have been found to induce RGC death or provide neuroprotective effects in animal models; it is likely that the loss of retinal ganglion cells is the result of multifactorial stress and loss of trophic support [320, 447]. Elevated IOP is thought to contribute through multiple mechanisms by driving deformation and remodeling at the optic nerve head and lamina cribrosa – exposing RGC axons to shear forces – while also reducing perfusion pressure, resulting in the impairment of blood flow to the retina and optic nerve and a reduction in the axonal transport of survival factors from the brain to the retina [448-451]. Additional evidence supports the conclusion that the primary sites of damage are the ONH and lamina, including the correlation between the scotomas that characterize visual field loss in human patients and the laminar pores through which axons pass; *i.e.,* the progressive loss of retinal ganglion cells is better predicted by proximity of cell axons at the lamina than by the proximity of somas in the retina [431, 452, 453]. A large body of evidence indicates that axonal degeneration both precedes and precipitates the apoptotic death of retinal ganglion cells, which occurs at the site of the RGC somas in the inner retina.

Perhaps surprisingly for a population of cells that are both essential and non-proliferating, neurons rapidly undergo apoptosis – programmed cell death – under a variety of circumstances, including ischemia, loss of trophic factors, disrupted connectivity and even overstimulation (excitotoxicity). Apoptotic death of RGCs has been shown both in animal models and human glaucoma, and all of the above factors may contribute [447, 454, 455]. Although the programmed death of irreplaceable neurons may seem undesirable, it prevents

the release of intracellular components that accompany more chaotic forms of cell death, such as necrosis, that can trigger localized inflammation and precipitate the loss of additional nearby neurons through the spread of neurotoxic conditions [456]. Accompanying cell death, phagocytosis of dead cells is required to clear cytotoxic debris and allow for remodeling of the surrounding tissue to minimize functional deficit; in the glaucomatous retina, as in development, microglia are the primary phagocytic cell type, although astrocytes also display a limited capacity to contribute to this activity. Well the contribution of non-neuronal cell types to the death and removal of RGCs is occasionally described as neurotoxic, ablation or knockout of these cells and/or their functions typically worsens the progression of neurodegeneration, demonstrating that efforts to blame glial cell 'dysfunction' are largely misplaced [286, 436].

While attributing a causative role to glia for the loss of retinal ganglion cells in glaucoma misrepresents the process of neurodegeneration, astrocytes in the retina and optic nerve do undergo major changes in ocular hypertension and POAG, which can both positively and negatively influence the survival of RGCs [333, 436]. The role of astrocytes at the optic nerve head – where the optic nerve and retina intersect in a roughly perpendicular fashion – is a particular focus of research into the role of glia in glaucoma, although specific elements of astrocytes in the retina will be discussed as well.

V-C The Optic Nerve Head

Although the retina and optic nerve may appear as a continuous tissue under many histological preparation methods, during development they form as adjacent structures, with the retina containing a mix of neuronal and glial cells and the optic nerve being primarily glial. This distinction is not merely semantic; mutations in Pax6 (the retinal homeobox gene) or Pax2 (the optic nerve homeobox gene) can disrupt the joining of these two structures during development, resulting in varying degrees of visual impairment depending on the severity of the disruption [457]. In normal development, however, the projection of RGC axons through the optic fissure and the emergence of astrocyte precursors and vasculature into the retina functionally fuses these tissues, resulting in the optic nerve head [57, 458]. This makes retinal ganglion cell axons and the astrocyte syncytium, along with the ophthalmic vasculature, the only structures that transverse this retina – optic nerve boundary region.

A number of unique characteristics distinguish the optic nerve head region – which for the purpose of this review begins anteriorly at the edge of the optic disc and extends posteriorly to myelination transition zone – and may contribute to its vulnerability. These include dense unmyelinated axon bundles (which are under greater metabolic strain than their myelinated counterparts), a ~90 degree bend that renders axons susceptible to physical strain, and a structural seal at the lamina cribrosa that exposes axons and the vasculature to pressure differentials that may interfere with vascular perfusion and retrograde transport of trophic factors [459-461]. During glaucoma, the optic nerve head undergoes a characteristic

deformation referred to as “cupping”, in which the normally shallow optic disc bulges posteriorly, potentially exacerbating these aforementioned vulnerabilities [320].

As the primary glial cell type of the optic nerve head, astrocytes play a major role in supporting the axons of retinal ganglion cell as they exit the retina. These astrocytes can be classified as fibrous/peri-axonal and are linked in a gap junction coupled network; under physiological conditions they engage in comparable homeostatic roles to those described in section III [160]. Optic nerve head astrocytes also provide particularly extensive structural support via secretion of ECM factors and the arrangement of their processes to form a honeycomb-like network through which axon bundles are guided [462]. Additionally, a sub-population of these astrocytes constitutively Lgals3, a marker of phagocytic cells, and engage in a form of homeostatic phagocytosis not seen in their counterparts elsewhere – the engulfment and elimination of damaged mitochondria from neighboring RGC axons [419, 463].

V-D Changes to Retinal and Optic Nerve Head Astrocytes in Glaucoma

In both human glaucoma and animal models, astrocytes of the optic nerve head and retina show clear signs of reactivity. Upregulation of GFAP is readily apparent at both the optic nerve head and in the retina in human glaucoma, and the ECM component tenascin C is upregulated by ONH astrocytes as well, implying an increase in the structural support provided [311, 363, 464]. Furthermore, optic nerve head astrocytes are observed to undergo morphological changes including hypertrophy in both human glaucoma and animal models, and in mouse models these changes involve an alteration in process orientation [285, 318, 436]. Studies in a monkey model of glaucoma also demonstrated changes to the localization of the gap junction component Cx43, suggesting that intracellular coordination between astrocytes may be a casualty of the ongoing neurodegenerative state [333]. The upregulation of complement factor 3 (C3), considered a key marker of one subtype of reactive astrocytes, has also shown to be upregulated at the optic nerve head and inner retina in human tissue, likely expressed by the resident astrocytes in these locations [311, 465]. At the glaucomatous optic nerve head, astrocytes in human and animal tissue show upregulation of the nitric oxide synthase NOS-2; while the nitric oxide generated by this activity can act as a potent mediator of vasodilation, among other key functions, excess levels can be toxic and have been implicated in neurodegeneration [466-468]. Finally, increased expression of EGFR, a major regulator of cell behavior and receptor for the astrocyte trophic factor HB-EGF, has been shown in optic nerve head astrocytes in human glaucoma. EGFR plays a major role in cell behaviors including survival and proliferation, and is a perennial target in oncology; previous research suggests that it may modulate the transition of astrocytes to a reactive state and a number of studies have correlated EGFR inhibition with improved recovery from acute neurological injury [302, 469, 470].

However, to date the broader behavior of retinal and optic nerve head astrocytes in both glaucoma and animal models of glaucoma remains incompletely understood, making it difficult to interpret what elements of reactivity may be protective or harmful and stymieing efforts to modulate reactivity to improve RGC survival and functional outcomes. Owing to the sparsity of the cells, cell culture is often utilized in order to produce an enriched population of these astrocytes. Although this can provide certain insights, astrocytes are particularly adaptable to cell culture conditions, and can rapidly change elements of their phenotype in order to better survive *in vitro*; this is in contrast to most neurons, which either retain their phenotype or die when cultured.

Some recent studies have looked into the transcriptional state of rapidly isolated astrocytes from the retina, but these present their own problems. One class of studies, single cell RNA-seq, provides astrocyte specific data by running entire dissociated retinas and compartmentalizing the data from each cell, allowing for post-hoc cell sorting *in silico*. However, as astrocytes only represent .06% of cells in the retina, running enough cells to generate a meaningful retinal astrocyte transcriptome is cost prohibitive for all but the most well-funded of groups. Conversely, others have utilized bulk RNA sequencing or custom microarrays of the entire retina, but even with bioinformatic sorting to isolate glial cell signals, retinal astrocytes are outnumbered 40:1 by the related-but-distinct Muller cells. Therefore, in order to study the response of astrocytes in a mouse model of ocular hypertension, a new approach was required, the development of which is described in length in Chapter II.

References

1. von Baer, C.E., *Über Entwicklungsgeschichte der Thiere. Beobachtung und Reflexion*. 1828: Gebrüder Bornträger.
2. Anderson, B., Jr. and H.A. Saltzman, *Retinal Oxygen Utilization Measured by Hyperbaric Blackout.* Arch Ophthalmol, 1964. **72**: p. 792-5.
3. Wong-Riley, M.T., *Energy metabolism of the visual system.* Eye Brain, 2010. **2**: p. 99-116.
4. Buttery, R.G., et al., *How thick should a retina be? A comparative study of mammalian species with and without intraretinal vasculature.* Vision Research, 1991. **31**(2): p. 169-187.
5. Dollery, C.T., C.J. Bulpitt, and E.M. Kohner, *Oxygen supply to the retina from the retinal and choroidal circulations at normal and increased arterial oxygen tensions.* Invest Ophthalmol, 1969. **8**(6): p. 588-94.
6. Chase, J., *The Evolution of Retinal Vascularization in Mammals.* Ophthalmology, 1982. **89**(12): p. 1518-1525.
7. Bellhorn, R.W., *Retinal nutritive systems in vertebrates.* Seminars in Avian and Exotic Pet Medicine, 1997. **6**(3): p. 108-120.
8. Yu, C.Q., I.R. Schwab, and R.R. Dubielzig, *Feeding the vertebrate retina from the Cambrian to the Tertiary.* Journal of Zoology, 2009. **278**(4): p. 259-269.
9. Schnitzer, J., *Retinal Astrocytes - Their Restriction to Vascularized Parts of the Mammalian Retina.* Neuroscience Letters, 1987. **78**(1): p. 29-34.
10. Watanabe, T. and M.C. Raff, *Retinal astrocytes are immigrants from the optic nerve.* Nature, 1988. **332**(6167): p. 834-7.
11. Ling, T.L., J. Mitrofanis, and J. Stone, *Origin of retinal astrocytes in the rat: evidence of migration from the optic nerve.* J Comp Neurol, 1989. **286**(3): p. 345-52.
12. Mudhar, H.S., et al., *PDGF and its receptors in the developing rodent retina and optic nerve.* Development, 1993. **118**(2): p. 539-52.
13. Tao, C. and X. Zhang, *Retinal Proteoglycans Act as Cellular Receptors for Basement Membrane Assembly to Control Astrocyte Migration and Angiogenesis.* Cell Rep, 2016. **17**(7): p. 1832-1844.
14. Selvam, S., T. Kumar, and M. Fruttiger, *Retinal vasculature development in health and disease.* Prog Retin Eye Res, 2018. **63**: p. 1-19.
15. Amini, R., M. Rocha-Martins, and C. Norden, *Neuronal Migration and Lamination in the Vertebrate Retina.* Front Neurosci, 2017. **11**: p. 742.
16. Hoon, M., et al., *Functional architecture of the retina: development and disease.* Prog Retin Eye Res, 2014. **42**: p. 44-84.
17. Yu, D.-Y. and S.J. Cringle, *Oxygen Distribution and Consumption within the Retina in Vascularised and Avascular Retinas and in Animal Models of Retinal Disease.* Progress in Retinal and Eye Research, 2001. **20**(2): p. 175-208.
18. Linsenmeier, R.A. and L. Padnick-Silver, *Metabolic dependence of photoreceptors on the choroid in the normal and detached retina.* Invest Ophthalmol Vis Sci, 2000. **41**(10): p. 3117-23.
19. Chan-Ling, T. and J. Stone, *Chapter 7 Retinopathy of prematurity: Origins in the architecture of the retina.* Progress in Retinal Research, 1993. **12**: p. 155-178.
20. Newman, E.A., *Functional hyperemia and mechanisms of neurovascular coupling in the retinal vasculature.* J Cereb Blood Flow Metab, 2013. **33**(11): p. 1685-95.
21. Stone, J., et al., *The locations of mitochondria in mammalian photoreceptors: relation to retinal vasculature.* Brain Res, 2008. **1189**: p. 58-69.

22. Johnson, G.L., *I. Contributions to the comparative anatomy of the mammalian eye, chiefly based on ophthalmoscopic examination.* Philosophical Transactions of the Royal Society of London. Series B, Containing Papers of a Biological Character, 1901. **194**(194-206): p. 1-82.
23. Country, M.W., *Retinal metabolism: A comparative look at energetics in the retina.* Brain Res, 2017. **1672**: p. 50-57.
24. Walls, G.L., *The vertebrate eye and its adaptive radiation [by] Gordon Lynn Walls*. 1942.
25. Michaelson, I., *Retinal Circulation in Man and Animals*. 1954: C.C. Thomas.
26. Wittenberg, J.B. and B.A. Wittenberg, *The choroid rete mirabile of the fish eye. I. Oxygen secretion and structure: comparison with the swimbladder rete mirabile.* Biol Bull, 1974. **146**(1): p. 116-36.
27. Kaufman, R., et al., *Development and origins of zebrafish ocular vasculature.* BMC Dev Biol, 2015. **15**: p. 18.
28. Damsgaard, C., et al., *Retinal oxygen supply shaped the functional evolution of the vertebrate eye.* Elife, 2019. **8**.
29. Bailes, H.J., et al., *Morphology, characterization, and distribution of retinal photoreceptors in the Australian lungfish Neoceratodus forsteri (Krefft, 1870).* J Comp Neurol, 2006. **494**(3): p. 381-97.
30. Alfayate, M.C., et al., *Ontogeny of the conus papillaris of the lizard Gallotia galloti and cellular response following transection of the optic nerve: an immunohistochemical and ultrastructural study.* Cell Tissue Res, 2011. **344**(1): p. 63-83.
31. Bellairs, A.D. and G. Underwood, *The origin of snakes.* Biol Rev Camb Philos Soc, 1951. **26**(2): p. 193-237.
32. MANN, I.C., *The Pecten of Gallus Domesticus.* Quarterly Journal of Microscopical Science, 1924. **s2-68**(271): p. 413-442.
33. Stone, J. and Z. Dreher, *Relationship between Astrocytes, Ganglion-Cells and Vasculature of the Retina.* Journal of Comparative Neurology, 1987. **255**(1): p. 35-49.
34. Schnitzer, J., *The development of astrocytes and blood vessels in the postnatal rabbit retina.* J Neurocytol, 1988. **17**(4): p. 433-49.
35. Sunderland, S., *The vascular pattern in the central nervous system of the monotremes and Australian marsupials.* The Journal of Comparative Neurology, 1941. **75**(1): p. 123-129.
36. McMenamin, P.G., et al., *The Unique Paired Retinal Vessels of the Gray Short-Tailed Opossum (Monodelphis domestica) and Their Relationship to Astrocytes and Microglial Cells.* Anat Rec (Hoboken), 2017. **300**(8): p. 1391-1400.
37. Buttery, R.G., J.R. Haight, and K. Bell, *Vascular and avascular retinae in mammals. A funduscopic and fluorescein angiographic study.* Brain Behav Evol, 1990. **35**(3): p. 156-75.
38. Mass, A.M. and A.Y. Supin, *Adaptive features of aquatic mammals' eye.* Anat Rec (Hoboken), 2007. **290**(6): p. 701-15.
39. Van Cruchten, S., et al., *Pre- and Postnatal Development of the Eye: A Species Comparison.* Birth Defects Res, 2017. **109**(19): p. 1540-1567.
40. Heesy, C.P. and M.I. Hall, *The nocturnal bottleneck and the evolution of mammalian vision.* Brain Behav Evol, 2010. **75**(3): p. 195-203.
41. Gerkema, M.P., et al., *The nocturnal bottleneck and the evolution of activity patterns in mammals.* Proc Biol Sci, 2013. **280**(1765): p. 20130508.
42. Curcio, C.A., et al., *Human photoreceptor topography.* The Journal of Comparative Neurology, 1990. **292**(4): p. 497-523.
43. Raymond, P.A., et al., *Patterning the cone mosaic array in zebrafish retina requires specification of ultraviolet-sensitive cones.* PLoS One, 2014. **9**(1): p. e85325.
44. Meyer, D.B. and H.C. May, Jr., *The topographical distribution of rods and cones in the adult chicken retina.* Exp Eye Res, 1973. **17**(4): p. 347-55.

45. Kim, J.W., et al., *Recruitment of Rod Photoreceptors from Short-Wavelength-Sensitive Cones during the Evolution of Nocturnal Vision in Mammals.* Dev Cell, 2016. **37**(6): p. 520-32.
46. Solovei, I., et al., *Nuclear architecture of rod photoreceptor cells adapts to vision in mammalian evolution.* Cell, 2009. **137**(2): p. 356-68.
47. Reichenbach, A. and A. Bringmann, *Müller Cells in the Healthy and Diseased Retina*. Müller Cells in the Healthy and Diseased Retina. Vol. 25. 2010. 1-417.
48. Corfield, J.R., et al., *Retinal anatomy of the New Zealand kiwi: structural traits consistent with their nocturnal behavior.* Anat Rec (Hoboken), 2015. **298**(4): p. 771-9.
49. Noh, G.M., et al., *Analysis of Changes in Retinal Photoreceptors Using Optical Coherence Tomography in a Feline Model of Iodoacetic Acid-induced Retinal Degeneration.* Korean J Ophthalmol, 2019. **33**(6): p. 547-556.
50. Hernandez-Merino, E., et al., *Spectral domain optical coherence tomography (SD-OCT) assessment of the healthy female canine retina and optic nerve.* Vet Ophthalmol, 2011. **14**(6): p. 400-5.
51. Balazs, E.A., L.Z. Toth, and V. Ozanics, *Cytological Studies on the Developing Vitreous as Related to the Hyaloid Vessel System.* Albrecht Von Graefes Archiv Fur Klinische Und Experimentelle Ophthalmologie, 1980. **213**(2): p. 71-85.
52. Ito, M. and M. Yoshioka, *Regression of the hyaloid vessels and pupillary membrane of the mouse.* Anat Embryol (Berl), 1999. **200**(4): p. 403-11.
53. Yoshikawa, Y., et al., *Developmental regression of hyaloid vasculature is triggered by neurons.* J Exp Med, 2016. **213**(7): p. 1175-83.
54. Fruttiger, M., *Development of the Mouse Retinal Vasculature: Angiogenesis Versus Vasculogenesis.* Investigative Ophthalmology & Visual Science, 2002. **43**(2): p. 522-527.
55. Miyawaki, T., et al., *Tlx, an orphan nuclear receptor, regulates cell numbers and astrocyte development in the developing retina.* J Neurosci, 2004. **24**(37): p. 8124-34.
56. West, H., W.D. Richardson, and M. Fruttiger, *Stabilization of the retinal vascular network by reciprocal feedback between blood vessels and astrocytes.* Development, 2005. **132**(8): p. 1855-62.
57. Duan, L.J., et al., *Retinal Angiogenesis Regulates Astrocytic Differentiation in Neonatal Mouse Retinas by Oxygen Dependent Mechanisms.* Sci Rep, 2017. **7**(1): p. 17608.
58. Heavner, W. and L. Pevny, *Eye development and retinogenesis.* Cold Spring Harb Perspect Biol, 2012. **4**(12).
59. Fuhrmann, S., C. Zou, and E.M. Levine, *Retinal pigment epithelium development, plasticity, and tissue homeostasis.* Exp Eye Res, 2014. **123**: p. 141-50.
60. Pei, Y.F. and J.A. Rhodin, *The prenatal development of the mouse eye.* Anat Rec, 1970. **168**(1): p. 105-25.
61. Stone, J., *Chapter 1 The origins of the cells of vertebrate retina.* Progress in Retinal Research, 1988. **7**: p. 1-19.
62. Sidman, R.L., *Histogenesis of mouse retina studied with thymidine-H3*, in *Structure of the Eye*, G.K. Smelser, Editor. 1961, Academic Press: New York. p. 487-506.
63. Cepko, C., *Intrinsically different retinal progenitor cells produce specific types of progeny.* Nat Rev Neurosci, 2014. **15**(9): p. 615-27.
64. Young, R.W., *Cell differentiation in the retina of the mouse.* Anat Rec, 1985. **212**(2): p. 199-205.
65. Cairns, J.E., *Normal development of the hyaloid and retinal vessels in the rat.* Br J Ophthalmol, 1959. **43**: p. 385-93.
66. Saint-Geniez, M. and P.A. D'Amore, *Development and pathology of the hyaloid, choroidal and retinal vasculature.* Int J Dev Biol, 2004. **48**(8-9): p. 1045-58.

67. Anand-Apte, B. and J.G. Hollyfield, *Developmental Anatomy of the Retinal and Choroidal Vasculature*, in *Encyclopedia of the Eye*. 2010. p. 9-15.
68. Zhu, M., et al., *The human hyaloid system: cell death and vascular regression.* Exp Eye Res, 2000. **70**(6): p. 767-76.
69. Patel, A. and J.C. Sowden, *Genes and pathways in optic fissure closure.* Semin Cell Dev Biol, 2019. **91**: p. 55-65.
70. Chen, C., H. Xiao, and X. Ding, *Persistent Fetal Vasculature.* Asia Pac J Ophthalmol (Phila), 2019. **8**(1): p. 86-95.
71. Reichenbach, A. and F. Wohlrab, *Morphometric Parameters of Muller (Glial) Cells Dependent on Their Topographic Localization in the Nonmyelinated Part of the Rabbit Retina - a Consideration of Functional-Aspects of Radial Glia.* Journal of Neurocytology, 1986. **15**(4): p. 451-459.
72. Fruttiger, M., et al., *PDGF mediates a neuron-astrocyte interaction in the developing retina.* Neuron, 1996. **17**(6): p. 1117-31.
73. Yeh, H.J., et al., *Pdgf a-Chain Gene Is Expressed by Mammalian Neurons during Development and in Maturity.* Cell, 1991. **64**(1): p. 209-216.
74. Armstrong, R.C., L. Harvath, and M.E. Dubois-Dalcq, *Type 1 astrocytes and oligodendrocyte-type 2 astrocyte glial progenitors migrate toward distinct molecules.* J Neurosci Res, 1990. **27**(3): p. 400-7.
75. Domingues, H.S., et al., *Oligodendrocyte, Astrocyte, and Microglia Crosstalk in Myelin Development, Damage, and Repair.* Front Cell Dev Biol, 2016. **4**: p. 71.
76. Skoff, R.P., *Gliogenesis in Rat Optic-Nerve - Astrocytes Are Generated in a Single Wave before Oligodendrocytes.* Developmental Biology, 1990. **139**(1): p. 149-168.
77. Kodama, T., S. Hayasaka, and T. Setogawa, *Myelinated retinal nerve fibers: prevalence, location and effect on visual acuity.* Ophthalmologica, 1990. **200**(2): p. 77-83.
78. Straatsma, B.R.F., R.Y.; Heckenlively, J.R.; Taylor, G.N., *Myelinated Retinal Nerve Fibers.* American Journal of Ophthalmology, 1981. **92**(6): p. 883-888.
79. Halfter, W., et al., *Origin and turnover of ECM proteins from the inner limiting membrane and vitreous body.* Eye (Lond), 2008. **22**(10): p. 1207-13.
80. Dong, L.J. and A.E. Chung, *The expression of the genes for entactin, laminin A, laminin B1 and laminin B2 in murine lens morphogenesis and eye development.* Differentiation, 1991. **48**(3): p. 157-72.
81. Zhou, M., et al., *Large is required for normal astrocyte migration and retinal vasculature development.* Cell Biosci, 2017. **7**: p. 18.
82. Zhang, C., et al., *A developmental defect in astrocytes inhibits programmed regression of the hyaloid vasculature in the mammalian eye.* Eur J Cell Biol, 2011. **90**(5): p. 440-8.
83. Huxlin, K.R., A.J. Sefton, and J.H. Furby, *The origin and development of retinal astrocytes in the mouse.* J Neurocytol, 1992. **21**(7): p. 530-44.
84. Dakubo, G.D., et al., *Retinal ganglion cell-derived sonic hedgehog signaling is required for optic disc and stalk neuroepithelial cell development.* Development, 2003. **130**(13): p. 2967-2980.
85. Clements, R., et al., *Dystroglycan Maintains Inner Limiting Membrane Integrity to Coordinate Retinal Development.* J Neurosci, 2017. **37**(35): p. 8559-8574.
86. Stenzel, D., et al., *Integrin-dependent and -independent functions of astrocytic fibronectin in retinal angiogenesis.* Development, 2011. **138**(20): p. 4451-63.
87. Stone, J., et al., *Development of Retinal Vasculature Is Mediated by Hypoxia-Induced Vascular Endothelial Growth-Factor (Vegf) Expression by Neuroglia.* Journal of Neuroscience, 1995. **15**(7): p. 4738-4747.
88. Jiang, B., et al., *Astrocytes Modulate Retinal Vasculogenesis - Effects on Fibronectin Expression.* Journal of Cell Science, 1994. **107**: p. 2499-2508.

89. Rattner, A., J. Williams, and J. Nathans, *Roles of HIFs and VEGF in angiogenesis in the retina and brain.* J Clin Invest, 2019. **130**: p. 3807-3820.
90. Engerman, R.L. and R.K. Meyer, *Development of retinal vasculature in rats.* Am J Ophthalmol, 1965. **60**(4): p. 628-41.
91. Fruttiger, M., *Development of the retinal vasculature.* Angiogenesis, 2007. **10**(2): p. 77-88.
92. Mi, H. and B.A. Barres, *Purification and characterization of astrocyte precursor cells in the developing rat optic nerve.* J Neurosci, 1999. **19**(3): p. 1049-61.
93. Chan-Ling, T., et al., *In vivo characterization of astrocyte precursor cells (APCs) and astrocytes in developing rat retinae: differentiation, proliferation, and apoptosis.* Glia, 2009. **57**(1): p. 39-53.
94. Duan, L.J., K. Takeda, and G.H. Fong, *Hypoxia inducible factor-2alpha regulates the development of retinal astrocytic network by maintaining adequate supply of astrocyte progenitors.* PLoS One, 2014. **9**(1): p. e84736.
95. Audigier, Y., L. van den Berghe, and B. Masri, *Apelin Signaling in Retinal Angiogenesis*, in *Molecular Mechanisms of Angiogenesis: From Ontogenesis to Oncogenesis*, J.-J. Feige, G. Pagès, and F. Soncin, Editors. 2014, Springer Paris: Paris. p. 121-148.
96. Gerhardt, H., et al., *VEGF guides angiogenic sprouting utilizing endothelial tip cell filopodia.* J Cell Biol, 2003. **161**(6): p. 1163-77.
97. Kubota, Y., et al., *Leukemia inhibitory factor regulates microvessel density by modulating oxygen-dependent VEGF expression in mice.* J Clin Invest, 2008. **118**(7): p. 2393-403.
98. Sakimoto, S., et al., *A role for endothelial cells in promoting the maturation of astrocytes through the apelin/APJ system in mice.* Development, 2012. **139**(7): p. 1327-35.
99. Bonni, A., et al., *Regulation of gliogenesis in the central nervous system by the JAK-STAT signaling pathway.* Science, 1997. **278**(5337): p. 477-83.
100. Ceyzeriat, K., et al., *The complex STATes of astrocyte reactivity: How are they controlled by the JAK-STAT3 pathway?* Neuroscience, 2016. **330**: p. 205-18.
101. Stahl, A., et al., *The mouse retina as an angiogenesis model.* Invest Ophthalmol Vis Sci, 2010. **51**(6): p. 2813-26.
102. Hellström, A., L.E.H. Smith, and O. Dammann, *Retinopathy of prematurity.* The Lancet, 2013. **382**(9902): p. 1445-1457.
103. Dorrell, M.I. and M. Friedlander, *Mechanisms of endothelial cell guidance and vascular patterning in the developing mouse retina.* Prog Retin Eye Res, 2006. **25**(3): p. 277-95.
104. Usui, Y., et al., *Neurovascular crosstalk between interneurons and capillaries is required for vision.* J Clin Invest, 2015. **125**(6): p. 2335-46.
105. Sun, Y. and L.E.H. Smith, *Retinal Vasculature in Development and Diseases.* Annu Rev Vis Sci, 2018. **4**: p. 101-122.
106. Luo, L., et al., *Photoreceptor avascular privilege is shielded by soluble VEGF receptor-1.* Elife, 2013. **2**: p. e00324.
107. Okabe, K., et al., *Neurons limit angiogenesis by titrating VEGF in retina.* Cell, 2014. **159**(3): p. 584-96.
108. Stefater, J.A., 3rd, et al., *Regulation of angiogenesis by a non-canonical Wnt-Flt1 pathway in myeloid cells.* Nature, 2011. **474**(7352): p. 511-5.
109. Punal, V.M., et al., *Large-scale death of retinal astrocytes during normal development is non-apoptotic and implemented by microglia.* PLoS Biol, 2019. **17**(10): p. e3000492.
110. Duan, L.J. and G.H. Fong, *Developmental vascular pruning in neonatal mouse retinas is programmed by the astrocytic oxygen-sensing mechanism.* Development, 2019. **146**(8).
111. Franco, C.A., et al., *Dynamic endothelial cell rearrangements drive developmental vessel regression.* PLoS Biol, 2015. **13**(4): p. e1002125.

112. Watson, E.C., et al., *Apoptosis regulates endothelial cell number and capillary vessel diameter but not vessel regression during retinal angiogenesis.* Development, 2016. **143**(16): p. 2973-82.
113. Park, D.Y., et al., *Plastic roles of pericytes in the blood-retinal barrier.* Nat Commun, 2017. **8**: p. 15296.
114. Lindblom, P., et al., *Endothelial PDGF-B retention is required for proper investment of pericytes in the microvessel wall.* Genes Dev, 2003. **17**(15): p. 1835-40.
115. Kovacs-Oller, T., et al., *The pericyte connectome: spatial precision of neurovascular coupling is driven by selective connectivity maps of pericytes and endothelial cells and is disrupted in diabetes.* Cell Discovery, 2020. **6**(1).
116. Bonkowski, D., et al., *The CNS microvascular pericyte: pericyte-astrocyte crosstalk in the regulation of tissue survival.* Fluids Barriers CNS, 2011. **8**(1): p. 8.
117. Ly, A., et al., *Early inner retinal astrocyte dysfunction during diabetes and development of hypoxia, retinal stress, and neuronal functional loss.* Invest Ophthalmol Vis Sci, 2011. **52**(13): p. 9316-26.
118. Kimelberg, H.K., *The problem of astrocyte identity.* Neurochem Int, 2004. **45**(2-3): p. 191-202.
119. Rowitch, D.H. and A.R. Kriegstein, *Developmental genetics of vertebrate glial-cell specification.* Nature, 2010. **468**(7321): p. 214-22.
120. Michalski, J.P. and R. Kothary, *Oligodendrocytes in a Nutshell.* Front Cell Neurosci, 2015. **9**: p. 340.
121. Ben Haim, L. and D.H. Rowitch, *Functional diversity of astrocytes in neural circuit regulation.* Nat Rev Neurosci, 2017. **18**(1): p. 31-41.
122. Zhang, Y. and B.A. Barres, *Astrocyte heterogeneity: an underappreciated topic in neurobiology.* Curr Opin Neurobiol, 2010. **20**(5): p. 588-94.
123. Emsley, J.G. and J.D. Macklis, *Astroglial heterogeneity closely reflects the neuronal-defined anatomy of the adult murine CNS.* Neuron Glia Biol, 2006. **2**(3): p. 175-86.
124. Sofroniew, M.V. and H.V. Vinters, *Astrocytes: biology and pathology.* Acta Neuropathol, 2010. **119**(1): p. 7-35.
125. Ramón y Cajal, S., *La rétine des vertébrés.* La cellule, 1893. **9**: p. 119-259.
126. Barres, B.A., *The mystery and magic of glia: a perspective on their roles in health and disease.* Neuron, 2008. **60**(3): p. 430-40.
127. Andriezen, W.L., *The Neuroglia Elements in the Human Brain.* Br Med J, 1893. **2**(1700): p. 227-30.
128. Hodgkin, A.L. and A.F. Huxley, *A quantitative description of membrane current and its application to conduction and excitation in nerve.* J Physiol, 1952. **117**(4): p. 500-44.
129. Vaughn, J.E., *An electron microscopic analysis of gliogenesis in rat optic nerves.* Z Zellforsch Mikrosk Anat, 1969. **94**(3): p. 293-324.
130. Bignami, A., et al., *Localization of the glial fibrillary acidic protein in astrocytes by immunofluorescence.* Brain Research, 1972. **43**(2): p. 429-435.
131. Cornell-Bell, A.H., et al., *Glutamate induces calcium waves in cultured astrocytes: long-range glial signaling.* Science, 1990. **247**(4941): p. 470-3.
132. Newman, E.A. and K.R. Zahs, *Modulation of neuronal activity by glial cells in the retina.* J Neurosci, 1998. **18**(11): p. 4022-8.
133. Sun, D. and T.C. Jakobs, *Structural remodeling of astrocytes in the injured CNS.* Neuroscientist, 2012. **18**(6): p. 567-88.
134. Black, J.A. and S.G. Waxman, *The perinodal astrocyte.* Glia, 1988. **1**(3): p. 169-83.
135. Spacek, J., *Three-dimensional reconstructions of astroglia and oligodendroglia cells.* Z Zellforsch Mikrosk Anat, 1971. **112**(3): p. 430-42.

136. De Robertis, E.D.P., *Some New Electron Microscopical Contributions to the Biology of Neuroglia*, in *Biology of Neuroglia*. 1965. p. 1-11.
137. Reichenbach, A., A. Derouiche, and F. Kirchhoff, *Morphology and dynamics of perisynaptic glia.* Brain Res Rev, 2010. **63**(1-2): p. 11-25.
138. Parpura, V. and A. Verkhratsky, *Neuroglia at the crossroads of homoeostasis, metabolism and signalling: evolution of the concept.* ASN Neuro, 2012. **4**(4): p. 201-5.
139. Virchow, R., *Gesammelte Abhandlungen zyr wissenschaftlischen Medizin.* Verlag von Meidinger Sohn & Comp, Frankfurt, 1856.
140. Schiweck, J., B.J. Eickholt, and K. Murk, *Important Shapeshifter: Mechanisms Allowing Astrocytes to Respond to the Changing Nervous System During Development, Injury and Disease.* Front Cell Neurosci, 2018. **12**: p. 261.
141. Potokar, M., et al., *The Diversity of Intermediate Filaments in Astrocytes.* Cells, 2020. **9**(7).
142. Eng, L.F., et al., *An acidic protein isolated from fibrous astrocytes.* Brain Research, 1971. **28**(2): p. 351-354.
143. Brenner, M., *Role of GFAP in CNS injuries.* Neurosci Lett, 2014. **565**: p. 7-13.
144. Nawashiro, H., et al., *High susceptibility to cerebral ischemia in GFAP-null mice.* J Cereb Blood Flow Metab, 2000. **20**(7): p. 1040-4.
145. Lundkvist, A., et al., *Under stress, the absence of intermediate filaments from Muller cells in the retina has structural and functional consequences.* J Cell Sci, 2004. **117**(Pt 16): p. 3481-8.
146. Potokar, M., et al., *Intermediate filaments attenuate stimulation-dependent mobility of endosomes/lysosomes in astrocytes.* Glia, 2010. **58**(10): p. 1208-19.
147. Lepekhin, E.A., et al., *Intermediate filaments regulate astrocyte motility.* J Neurochem, 2001. **79**(3): p. 617-25.
148. Shigetomi, E., et al., *Imaging calcium microdomains within entire astrocyte territories and endfeet with GCaMPs expressed using adeno-associated viruses.* J Gen Physiol, 2013. **141**(5): p. 633-47.
149. Higashi, K., et al., *An inwardly rectifying K(+) channel, Kir4.1, expressed in astrocytes surrounds synapses and blood vessels in brain.* Am J Physiol Cell Physiol, 2001. **281**(3): p. C922-31.
150. Brightman, M.W. and T.S. Reese, *Junctions between intimately apposed cell membranes in the vertebrate brain.* J Cell Biol, 1969. **40**(3): p. 648-77.
151. Kuffler, S.W., J.G. Nicholls, and R.K. Orkand, *Physiological properties of glial cells in the central nervous system of amphibia.* J Neurophysiol, 1966. **29**(4): p. 768-87.
152. Caspar, D.L., et al., *Gap junction structures. I. Correlated electron microscopy and x-ray diffraction.* J Cell Biol, 1977. **74**(2): p. 605-28.
153. Goodenough, D.A. and D.L. Paul, *Gap junctions.* Cold Spring Harb Perspect Biol, 2009. **1**(1): p. a002576.
154. Bennett, M.V., et al., *Gap junctions: new tools, new answers, new questions.* Neuron, 1991. **6**(3): p. 305-20.
155. Kumar, N.M. and N.B. Gilula, *The Gap Junction Communication Channel.* Cell, 1996. **84**(3): p. 381-388.
156. Brink, P., *Gap junction voltage dependence. A clear picture emerges.* J Gen Physiol, 2000. **116**(1): p. 11-2.
157. Giaume, C., et al., *Astroglial networks: a step further in neuroglial and gliovascular interactions.* Nat Rev Neurosci, 2010. **11**(2): p. 87-99.
158. Giaume, C. and K.D. McCarthy, *Control of gap-junctional communication in astrocytic networks.* Trends Neurosci, 1996. **19**(8): p. 319-25.
159. Dermietzel, R., et al., *Differential expression of three gap junction proteins in developing and mature brain tissues.* Proc Natl Acad Sci U S A, 1989. **86**(24): p. 10148-52.

160. Quigley, H.A., *Gap Junctions between Optic-Nerve Head Astrocytes.* Investigative Ophthalmology & Visual Science, 1977. **16**(6): p. 582-585.
161. Scemes, E. and D.C. Spray, *The astrocytic syncytium*, in *Non-Neuronal Cells of the Nervous System: Function and Dysfunction*. 2003. p. 165-179.
162. Konietzko, U. and C.M. Muller, *Astrocytic dye coupling in rat hippocampus: topography, developmental onset, and modulation by protein kinase C.* Hippocampus, 1994. **4**(3): p. 297-306.
163. Robinson, S.R., et al., *Unidirectional Coupling of Gap-Junctions between Neuroglia.* Science, 1993. **262**(5136): p. 1072-1074.
164. Fasciani, I., et al., *Directional coupling of oligodendrocyte connexin-47 and astrocyte connexin-43 gap junctions.* Glia, 2018. **66**(11): p. 2340-2352.
165. Zahs, K.R. and E.A. Newman, *Asymmetric gap junctional coupling between glial cells in the rat retina.* Glia, 1997. **20**(1): p. 10-22.
166. Huang, Q., D. Zhou, and M. DiFiglia, *Neurobiotin™, a useful neuroanatomical tracer for in vivo anterograde, retrograde and transneuronal tract-tracing and for in vitro labeling of neurons.* Journal of Neuroscience Methods, 1992. **41**(1): p. 31-43.
167. Ma, B., et al., *Gap junction coupling confers isopotentiality on astrocyte syncytium.* Glia, 2016. **64**(2): p. 214-26.
168. Simard, M. and M. Nedergaard, *The neurobiology of glia in the context of water and ion homeostasis.* Neuroscience, 2004. **129**(4): p. 877-96.
169. Anderson, C.M. and R.A. Swanson, *Astrocyte glutamate transport: Review of properties, regulation, and physiological functions.* Glia, 2000. **32**(1): p. 1-14.
170. Bellot-Saez, A., et al., *Astrocytic modulation of neuronal excitability through K(+) spatial buffering.* Neurosci Biobehav Rev, 2017. **77**: p. 87-97.
171. Kofuji, P. and E.A. Newman, *Potassium buffering in the central nervous system.* Neuroscience, 2004. **129**(4): p. 1045-56.
172. Norenberg, M.D. and A. Martinez-Hernandez, *Fine structural localization of glutamine synthetase in astrocytes of rat brain.* Brain Research, 1979. **161**(2): p. 303-310.
173. Bergles, D.E. and C.E. Jahr, *Synaptic Activation of Glutamate Transporters in Hippocampal Astrocytes.* Neuron, 1997. **19**(6): p. 1297-1308.
174. Pannasch, U., et al., *Astroglial networks scale synaptic activity and plasticity.* Proc Natl Acad Sci U S A, 2011. **108**(20): p. 8467-72.
175. Amiry-Moghaddam, M. and O.P. Ottersen, *The molecular basis of water transport in the brain.* Nat Rev Neurosci, 2003. **4**(12): p. 991-1001.
176. Nagelhus, E.A., et al., *Aquaporin-4 water channel protein in the rat retina and optic nerve: polarized expression in Muller cells and fibrous astrocytes.* J Neurosci, 1998. **18**(7): p. 2506-19.
177. Nagelhus, E.A., et al., *Immunogold evidence suggests that coupling of K+ siphoning and water transport in rat retinal Mller cells is mediated by a coenrichment of Kir4.1 and AQP4 in specific membrane domains.* Glia, 1999. **26**(1): p. 47-54.
178. Kofuji, P., et al., *Genetic Inactivation of an Inwardly Rectifying Potassium Channel (Kir4.1 Subunit) in Mice: Phenotypic Impact in Retina.* The Journal of Neuroscience, 2000. **20**(15): p. 5733-5740.
179. Newman, E.A. and K.R. Zahs, *Calcium waves in retinal glial cells.* Science, 1997. **275**(5301): p. 844-7.
180. Bazargani, N. and D. Attwell, *Astrocyte calcium signaling: the third wave.* Nat Neurosci, 2016. **19**(2): p. 182-9.
181. Finkbeiner, S.M., *Glial calcium.* Glia, 1993. **9**(2): p. 83-104.
182. Dani, J.W., A. Chernjavsky, and S.J. Smith, *Neuronal activity triggers calcium waves in hippocampal astrocyte networks.* Neuron, 1992. **8**(3): p. 429-440.

183. Agulhon, C., et al., *What is the role of astrocyte calcium in neurophysiology?* Neuron, 2008. **59**(6): p. 932-46.
184. Zonta, M., et al., *Neuron-to-astrocyte signaling is central to the dynamic control of brain microcirculation.* Nat Neurosci, 2003. **6**(1): p. 43-50.
185. Araque, A., et al., *Tripartite synapses: glia, the unacknowledged partner.* Trends Neurosci, 1999. **22**(5): p. 208-15.
186. Savtchouk, I. and A. Volterra, *Gliotransmission: Beyond Black-and-White.* J Neurosci, 2018. **38**(1): p. 14-25.
187. Fiacco, T.A. and K.D. McCarthy, *Multiple Lines of Evidence Indicate That Gliotransmission Does Not Occur under Physiological Conditions.* J Neurosci, 2018. **38**(1): p. 3-13.
188. Kanemaru, K., et al., *In vivo visualization of subtle, transient, and local activity of astrocytes using an ultrasensitive Ca(2+) indicator.* Cell Rep, 2014. **8**(1): p. 311-8.
189. Akerboom, J., et al., *Genetically encoded calcium indicators for multi-color neural activity imaging and combination with optogenetics.* Front Mol Neurosci, 2013. **6**: p. 2.
190. Srinivasan, R., et al., *New Transgenic Mouse Lines for Selectively Targeting Astrocytes and Studying Calcium Signals in Astrocyte Processes In Situ and In Vivo.* Neuron, 2016. **92**(6): p. 1181-1195.
191. Srinivasan, R., et al., *Ca(2+) signaling in astrocytes from Ip3r2(-/-) mice in brain slices and during startle responses in vivo.* Nat Neurosci, 2015. **18**(5): p. 708-17.
192. Fujii, Y., S. Maekawa, and M. Morita, *Astrocyte calcium waves propagate proximally by gap junction and distally by extracellular diffusion of ATP released from volume-regulated anion channels.* Sci Rep, 2017. **7**(1): p. 13115.
193. Mishra, A., et al., *Astrocytes mediate neurovascular signaling to capillary pericytes but not to arterioles.* Nat Neurosci, 2016. **19**(12): p. 1619-1627.
194. Stobart, J.L., et al., *Cortical Circuit Activity Evokes Rapid Astrocyte Calcium Signals on a Similar Timescale to Neurons.* Neuron, 2018. **98**(4): p. 726-735 e4.
195. Guerra-Gomes, S., et al., *Functional Roles of Astrocyte Calcium Elevations: From Synapses to Behavior.* Front Cell Neurosci, 2017. **11**: p. 427.
196. Clapham, D.E., *Calcium signaling.* Cell, 2007. **131**(6): p. 1047-58.
197. Verkhratsky, A., et al., *Astrocytes as secretory cells of the central nervous system: idiosyncrasies of vesicular secretion.* EMBO J, 2016. **35**(3): p. 239-57.
198. Attwell, D., et al., *Glial and neuronal control of brain blood flow.* Nature, 2010. **468**(7321): p. 232-43.
199. Mayorquin, L.C., et al., *Connexin-Mediated Functional and Metabolic Coupling Between Astrocytes and Neurons.* Front Mol Neurosci, 2018. **11**: p. 118.
200. Verkhratsky, A., *Calcium ions and integration in neural circuits.* Acta Physiol (Oxf), 2006. **187**(3): p. 357-69.
201. Roberts, W.M., *Spatial calcium buffering in saccular hair cells.* Nature, 1993. **363**(6424): p. 74-6.
202. Volterra, A., N. Liaudet, and I. Savtchouk, *Astrocyte Ca(2)(+) signalling: an unexpected complexity.* Nat Rev Neurosci, 2014. **15**(5): p. 327-35.
203. Newman, E.A., *Propagation of intercellular calcium waves in retinal astrocytes and Muller cells.* J Neurosci, 2001. **21**(7): p. 2215-23.
204. Hirase, H., et al., *Calcium dynamics of cortical astrocytic networks in vivo.* PLoS Biol, 2004. **2**(4): p. E96.
205. Nizar, K., et al., *In vivo stimulus-induced vasodilation occurs without IP3 receptor activation and may precede astrocytic calcium increase.* J Neurosci, 2013. **33**(19): p. 8411-22.

206. Bonder, D.E. and K.D. McCarthy, *Astrocytic Gq-GPCR-linked IP3R-dependent Ca2+ signaling does not mediate neurovascular coupling in mouse visual cortex in vivo.* J Neurosci, 2014. **34**(39): p. 13139-50.
207. Fiacco, T.A., et al., *Selective stimulation of astrocyte calcium in situ does not affect neuronal excitatory synaptic activity.* Neuron, 2007. **54**(4): p. 611-26.
208. Petravicz, J., T.A. Fiacco, and K.D. McCarthy, *Loss of IP3 receptor-dependent Ca2+ increases in hippocampal astrocytes does not affect baseline CA1 pyramidal neuron synaptic activity.* J Neurosci, 2008. **28**(19): p. 4967-73.
209. Navarrete, M., et al., *Astrocytes mediate in vivo cholinergic-induced synaptic plasticity.* PLoS Biol, 2012. **10**(2): p. e1001259.
210. Stenovec, M., et al., *Ca2+-dependent mobility of vesicles capturing anti-VGLUT1 antibodies.* Exp Cell Res, 2007. **313**(18): p. 3809-18.
211. Di Castro, M.A., et al., *Local Ca2+ detection and modulation of synaptic release by astrocytes.* Nat Neurosci, 2011. **14**(10): p. 1276-84.
212. Gordon, G.R., et al., *Brain metabolism dictates the polarity of astrocyte control over arterioles.* Nature, 2008. **456**(7223): p. 745-9.
213. Otsu, Y., et al., *Calcium dynamics in astrocyte processes during neurovascular coupling.* Nat Neurosci, 2015. **18**(2): p. 210-8.
214. Bindocci, E., et al., *Three-dimensional Ca(2+) imaging advances understanding of astrocyte biology.* Science, 2017. **356**(6339).
215. Liu, T., et al., *Calcium triggers exocytosis from two types of organelles in a single astrocyte.* J Neurosci, 2011. **31**(29): p. 10593-601.
216. Parpura, V., V. Grubisic, and A. Verkhratsky, *Ca(2+) sources for the exocytotic release of glutamate from astrocytes.* Biochim Biophys Acta, 2011. **1813**(5): p. 984-91.
217. Newman, E.A., *Calcium signaling in retinal glial cells and its effect on neuronal activity.* Prog Brain Res, 2001. **132**: p. 241-54.
218. Dombeck, D.A., et al., *Imaging large-scale neural activity with cellular resolution in awake, mobile mice.* Neuron, 2007. **56**(1): p. 43-57.
219. Ding, F., et al., *alpha1-Adrenergic receptors mediate coordinated Ca2+ signaling of cortical astrocytes in awake, behaving mice.* Cell Calcium, 2013. **54**(6): p. 387-94.
220. Szabo, Z., et al., *Extensive astrocyte synchronization advances neuronal coupling in slow wave activity in vivo.* Sci Rep, 2017. **7**(1): p. 6018.
221. Foley, J., et al., *Astrocytic IP3/Ca(2+) Signaling Modulates Theta Rhythm and REM Sleep.* Front Neural Circuits, 2017. **11**: p. 3.
222. Biesecker, K.R., et al., *Glial Cell Calcium Signaling Mediates Capillary Regulation of Blood Flow in the Retina.* J Neurosci, 2016. **36**(36): p. 9435-45.
223. Rosa, J.M., et al., *Neuron-glia signaling in developing retina mediated by neurotransmitter spillover.* Elife, 2015. **4**.
224. Filosa, J.A., et al., *Beyond neurovascular coupling, role of astrocytes in the regulation of vascular tone.* Neuroscience, 2016. **323**: p. 96-109.
225. De Bock, M., L. Leybaert, and C. Giaume, *Connexin Channels at the Glio-Vascular Interface: Gatekeepers of the Brain.* Neurochem Res, 2017. **42**(9): p. 2519-2536.
226. Mishra, A., *Binaural blood flow control by astrocytes: listening to synapses and the vasculature.* J Physiol, 2017. **595**(6): p. 1885-1902.
227. Weber, B. and L.F. Barros, *The Astrocyte: Powerhouse and Recycling Center.* Cold Spring Harb Perspect Biol, 2015. **7**(12).
228. Iadecola, C. and M. Nedergaard, *Glial regulation of the cerebral microvasculature.* Nat Neurosci, 2007. **10**(11): p. 1369-76.

229. Nippert, A.R., K.R. Biesecker, and E.A. Newman, *Mechanisms Mediating Functional Hyperemia in the Brain.* Neuroscientist, 2018. **24**(1): p. 73-83.
230. Ames, A., 3rd, *Energy requirements of CNS cells as related to their function and to their vulnerability to ischemia: a commentary based on studies on retina.* Can J Physiol Pharmacol, 1992. **70 Suppl**: p. S158-64.
231. Iadecola, C., *The Neurovascular Unit Coming of Age: A Journey through Neurovascular Coupling in Health and Disease.* Neuron, 2017. **96**(1): p. 17-42.
232. Hillman, E.M., *Coupling mechanism and significance of the BOLD signal: a status report.* Annu Rev Neurosci, 2014. **37**: p. 161-81.
233. Roy, C.S. and C.S. Sherrington, *On the Regulation of the Blood-supply of the Brain.* J Physiol, 1890. **11**(1-2): p. 85-158 17.
234. Raichle, M.E., *Behind the scenes of functional brain imaging: a historical and physiological perspective.* Proc Natl Acad Sci U S A, 1998. **95**(3): p. 765-72.
235. Formaz, F., C.E. Riva, and M. Geiser, *Diffuse luminance flicker increases retinal vessel diameter in humans.* Curr Eye Res, 1997. **16**(12): p. 1252-7.
236. Riva, C.E., et al., *Flicker evoked increase in optic nerve head blood flow in anesthetized cats.* Neuroscience Letters, 1991. **128**(2): p. 291-296.
237. Paulson, O.B. and E.A. Newman, *Does the release of potassium from astrocyte endfeet regulate cerebral blood flow?* Science, 1987. **237**(4817): p. 896-8.
238. Metea, M.R., P. Kofuji, and E.A. Newman, *Neurovascular coupling is not mediated by potassium siphoning from glial cells.* J Neurosci, 2007. **27**(10): p. 2468-71.
239. Petzold, G.C. and V.N. Murthy, *Role of astrocytes in neurovascular coupling.* Neuron, 2011. **71**(5): p. 782-97.
240. Rungta, R.L. and S. Charpak, *Astrocyte endfeet march to the beat of different vessels.* Nat Neurosci, 2016. **19**(12): p. 1539-1541.
241. Attwell, D., et al., *What is a pericyte?* J Cereb Blood Flow Metab, 2016. **36**(2): p. 451-5.
242. Filosa, J.A., et al., *Local potassium signaling couples neuronal activity to vasodilation in the brain.* Nat Neurosci, 2006. **9**(11): p. 1397-1403.
243. Lapato, A.S. and S.K. Tiwari-Woodruff, *Connexins and pannexins: At the junction of neuro-glial homeostasis & disease.* J Neurosci Res, 2018. **96**(1): p. 31-44.
244. Verkhratsky, A., et al., *Physiology of Astroglia.* Adv Exp Med Biol, 2019. **1175**: p. 45-91.
245. Olsen, M.L., et al., *New Insights on Astrocyte Ion Channels: Critical for Homeostasis and Neuron-Glia Signaling.* J Neurosci, 2015. **35**(41): p. 13827-35.
246. Lee, S., et al., *Channel-mediated tonic GABA release from glia.* Science, 2010. **330**(6005): p. 790-6.
247. Woo, D.H., et al., *TREK-1 and Best1 channels mediate fast and slow glutamate release in astrocytes upon GPCR activation.* Cell, 2012. **151**(1): p. 25-40.
248. Wei, L., et al., *ATP-induced P2X Receptor-Dependent Large Pore Formation: How Much Do We Know?* Front Pharmacol, 2016. **7**: p. 5.
249. Cheung, G., O. Chever, and N. Rouach, *Connexons and pannexons: newcomers in neurophysiology.* Front Cell Neurosci, 2014. **8**: p. 348.
250. Thompson, R.J. and B.A. Macvicar, *Connexin and pannexin hemichannels of neurons and astrocytes.* Channels (Austin), 2008. **2**(2): p. 81-6.
251. Araque, A., et al., *Gliotransmitters travel in time and space.* Neuron, 2014. **81**(4): p. 728-39.
252. Duan, S., et al., *P2X7 receptor-mediated release of excitatory amino acids from astrocytes.* J Neurosci, 2003. **23**(4): p. 1320-8.
253. Danbolt, N.C., *Glutamate uptake.* Progress in Neurobiology, 2001. **65**(1): p. 1-105.

254. Nies, A.T., et al., *Expression and immunolocalization of the multidrug resistance proteins, MRP1-MRP6 (ABCC1-ABCC6), in human brain.* Neuroscience, 2004. **129**(2): p. 349-60.
255. Russel, F.G., J.B. Koenderink, and R. Masereeuw, *Multidrug resistance protein 4 (MRP4/ABCC4): a versatile efflux transporter for drugs and signalling molecules.* Trends Pharmacol Sci, 2008. **29**(4): p. 200-7.
256. Sato, K., et al., *Critical role of ABCA1 transporter in sphingosine 1-phosphate release from astrocytes.* J Neurochem, 2007. **103**(6): p. 2610-9.
257. van Niel, G., G. D'Angelo, and G. Raposo, *Shedding light on the cell biology of extracellular vesicles.* Nat Rev Mol Cell Biol, 2018. **19**(4): p. 213-228.
258. Sudhof, T.C. and J. Rizo, *Synaptic vesicle exocytosis.* Cold Spring Harb Perspect Biol, 2011. **3**(12).
259. Neher, E., *Introduction: regulated exocytosis.* Cell Calcium, 2012. **52**(3-4): p. 196-8.
260. Wilhelm, A., et al., *Localization of SNARE proteins and secretory organelle proteins in astrocytes in vitro and in situ.* Neurosci Res, 2004. **48**(3): p. 249-57.
261. Bergersen, L.H., et al., *Immunogold detection of L-glutamate and D-serine in small synaptic-like microvesicles in adult hippocampal astrocytes.* Cereb Cortex, 2012. **22**(7): p. 1690-7.
262. Verderio, C., et al., *TI-VAMP/VAMP7 is the SNARE of secretory lysosomes contributing to ATP secretion from astrocytes.* Biol Cell, 2012. **104**(4): p. 213-28.
263. Cocucci, E. and J. Meldolesi, *Ectosomes and exosomes: shedding the confusion between extracellular vesicles.* Trends Cell Biol, 2015. **25**(6): p. 364-72.
264. Bezzi, P. and A. Volterra, *A neuron–glia signalling network in the active brain.* Current Opinion in Neurobiology, 2001. **11**(3): p. 387-394.
265. Gourine, A.V., et al., *Astrocytes control breathing through pH-dependent release of ATP.* Science, 2010. **329**(5991): p. 571-5.
266. Vardjan, N. and R. Zorec, *Excitable Astrocytes: Ca(2+)- and cAMP-Regulated Exocytosis.* Neurochem Res, 2015. **40**(12): p. 2414-24.
267. Poyhonen, S., et al., *Effects of Neurotrophic Factors in Glial Cells in the Central Nervous System: Expression and Properties in Neurodegeneration and Injury.* Front Physiol, 2019. **10**: p. 486.
268. Chung, W.S., N.J. Allen, and C. Eroglu, *Astrocytes Control Synapse Formation, Function, and Elimination.* Cold Spring Harb Perspect Biol, 2015. **7**(9): p. a020370.
269. Kucukdereli, H., et al., *Control of excitatory CNS synaptogenesis by astrocyte-secreted proteins Hevin and SPARC.* Proc Natl Acad Sci U S A, 2011. **108**(32): p. E440-9.
270. Liu, C.C., et al., *Apolipoprotein E and Alzheimer disease: risk, mechanisms and therapy.* Nat Rev Neurol, 2013. **9**(2): p. 106-18.
271. Mauch, D.H., et al., *CNS synaptogenesis promoted by glia-derived cholesterol.* Science, 2001. **294**(5545): p. 1354-7.
272. Allen, N.J., et al., *Astrocyte glypicans 4 and 6 promote formation of excitatory synapses via GluA1 AMPA receptors.* Nature, 2012. **486**(7403): p. 410-4.
273. Mughal, A. and S.T. O'Rourke, *Vascular effects of apelin: Mechanisms and therapeutic potential.* Pharmacol Ther, 2018. **190**: p. 139-147.
274. Livne-Bar, I., et al., *Astrocyte-derived lipoxins A4 and B4 promote neuroprotection from acute and chronic injury.* J Clin Invest, 2017. **127**(12): p. 4403-4414.
275. Barros, C.S., S.J. Franco, and U. Muller, *Extracellular matrix: functions in the nervous system.* Cold Spring Harb Perspect Biol, 2011. **3**(1): p. a005108.
276. Hillen, A.E.J., J.P.H. Burbach, and E.M. Hol, *Cell adhesion and matricellular support by astrocytes of the tripartite synapse.* Prog Neurobiol, 2018. **165-167**: p. 66-86.
277. Wiese, S., M. Karus, and A. Faissner, *Astrocytes as a source for extracellular matrix molecules and cytokines.* Front Pharmacol, 2012. **3**: p. 120.

278. Jha, M.K., et al., *Functional dissection of astrocyte-secreted proteins: Implications in brain health and diseases.* Prog Neurobiol, 2018. **162**: p. 37-69.
279. Streit, W.J., S.A. Walter, and N.A. Pennell, *Reactive microgliosis.* Progress in Neurobiology, 1999. **57**(6): p. 563-581.
280. Pekny, M. and M. Pekna, *Reactive gliosis in the pathogenesis of CNS diseases.* Biochim Biophys Acta, 2016. **1862**(3): p. 483-91.
281. Burda, J.E., A.M. Bernstein, and M.V. Sofroniew, *Astrocyte roles in traumatic brain injury.* Exp Neurol, 2016. **275 Pt 3**: p. 305-315.
282. Liu, Z. and M. Chopp, *Astrocytes, therapeutic targets for neuroprotection and neurorestoration in ischemic stroke.* Prog Neurobiol, 2016. **144**: p. 103-20.
283. Dong, Y. and E.N. Benveniste, *Immune function of astrocytes.* Glia, 2001. **36**(2): p. 180-90.
284. Verkhratsky, A., et al., *Astrocytes in Alzheimer's disease.* Neurotherapeutics, 2010. **7**(4): p. 399-412.
285. Hernandez, M.R., *The optic nerve head in glaucoma: role of astrocytes in tissue remodeling.* Progress in Retinal and Eye Research, 2000. **19**(3): p. 297-321.
286. Escartin, C., et al., *Reactive astrocyte nomenclature, definitions, and future directions.* Nat Neurosci, 2021.
287. Sofroniew, M.V., *Astrocyte Reactivity: Subtypes, States, and Functions in CNS Innate Immunity.* Trends Immunol, 2020. **41**(9): p. 758-770.
288. Liddelow, S.A. and B.A. Barres, *Reactive Astrocytes: Production, Function, and Therapeutic Potential.* Immunity, 2017. **46**(6): p. 957-967.
289. Ben Haim, L., et al., *Elusive roles for reactive astrocytes in neurodegenerative diseases.* Front Cell Neurosci, 2015. **9**: p. 278.
290. Pekny, M., U. Wilhelmsson, and M. Pekna, *The dual role of astrocyte activation and reactive gliosis.* Neurosci Lett, 2014. **565**: p. 30-8.
291. Sofroniew, M.V., *Molecular dissection of reactive astrogliosis and glial scar formation.* Trends Neurosci, 2009. **32**(12): p. 638-47.
292. Bardehle, S., et al., *Live imaging of astrocyte responses to acute injury reveals selective juxtavascular proliferation.* Nat Neurosci, 2013. **16**(5): p. 580-6.
293. Sirko, S., et al., *Reactive glia in the injured brain acquire stem cell properties in response to sonic hedgehog. [corrected].* Cell Stem Cell, 2013. **12**(4): p. 426-39.
294. Morizawa, Y.M., et al., *Reactive astrocytes function as phagocytes after brain ischemia via ABCA1-mediated pathway.* Nat Commun, 2017. **8**(1): p. 28.
295. Hatten, M.E., et al., *Astroglia in CNS injury.* Glia, 1991. **4**(2): p. 233-43.
296. Windle, W.F. and W.W. Chambers, *Regeneration in the spinal cord of the cat and dog.* J Comp Neurol, 1950. **93**(2): p. 241-57.
297. Silver, J. and J.H. Miller, *Regeneration beyond the glial scar.* Nat Rev Neurosci, 2004. **5**(2): p. 146-56.
298. Anderson, M.A., et al., *Astrocyte scar formation aids central nervous system axon regeneration.* Nature, 2016. **532**(7598): p. 195-200.
299. Okada, S., et al., *Conditional ablation of Stat3 or Socs3 discloses a dual role for reactive astrocytes after spinal cord injury.* Nat Med, 2006. **12**(7): p. 829-34.
300. Zamanian, J.L., et al., *Genomic analysis of reactive astrogliosis.* J Neurosci, 2012. **32**(18): p. 6391-410.
301. Anderson, M.A., Y. Ao, and M.V. Sofroniew, *Heterogeneity of reactive astrocytes.* Neurosci Lett, 2014. **565**: p. 23-9.
302. Pekny, M. and M. Pekna, *Astrocyte reactivity and reactive astrogliosis: costs and benefits.* Physiol Rev, 2014. **94**(4): p. 1077-98.

303. Buttini, M. and H. Boddeke, *Peripheral lipopolysaccharide stimulation induces interleukin-1β messenger RNA in rat brain microglial cells.* Neuroscience, 1995. **65**(2): p. 523-530.
304. Qin, L., et al., *Systemic LPS causes chronic neuroinflammation and progressive neurodegeneration.* Glia, 2007. **55**(5): p. 453-62.
305. Han, R.Q., et al., *Postischemic brain injury is attenuated in mice lacking the beta2-adrenergic receptor.* Anesth Analg, 2009. **108**(1): p. 280-7.
306. Yamashita, K., et al., *Monitoring the temporal and spatial activation pattern of astrocytes in focal cerebral ischemia using in situ hybridization to GFAP mRNA: comparison withsgp-2 andhsp70 mRNA and the effect of glutamate receptor antagonists.* Brain Research, 1996. **735**(2): p. 285-297.
307. Liddelow, S.A., et al., *Neurotoxic reactive astrocytes are induced by activated microglia.* Nature, 2017. **541**(7638): p. 481-487.
308. Clarke, L.E., et al., *Normal aging induces A1-like astrocyte reactivity.* Proc Natl Acad Sci U S A, 2018. **115**(8): p. E1896-E1905.
309. Guttenplan, K.A., et al., *Neurotoxic Reactive Astrocytes Drive Neuronal Death after Retinal Injury.* Cell Rep, 2020. **31**(12): p. 107776.
310. Kohler, S., U. Winkler, and J. Hirrlinger, *Heterogeneity of Astrocytes in Grey and White Matter.* Neurochem Res, 2021. **46**(1): p. 3-14.
311. Kuehn, M.H., et al., *Retinal synthesis and deposition of complement components induced by ocular hypertension.* Exp Eye Res, 2006. **83**(3): p. 620-8.
312. Tezel, G., et al., *Oxidative stress and the regulation of complement activation in human glaucoma.* Invest Ophthalmol Vis Sci, 2010. **51**(10): p. 5071-82.
313. Wilhelmsson, U., et al., *Redefining the concept of reactive astrocytes as cells that remain within their unique domains upon reaction to injury.* Proc Natl Acad Sci U S A, 2006. **103**(46): p. 17513-8.
314. Tsai, H.H., et al., *Regional astrocyte allocation regulates CNS synaptogenesis and repair.* Science, 2012. **337**(6092): p. 358-62.
315. Perez-Nievas, B.G. and A. Serrano-Pozo, *Deciphering the Astrocyte Reaction in Alzheimer's Disease.* Front Aging Neurosci, 2018. **10**: p. 114.
316. Reichenbach, A. and A. Bringmann, *New functions of Muller cells.* Glia, 2013. **61**(5): p. 651-78.
317. Chidlow, G., et al., *Glial cell and inflammatory responses to retinal laser treatment: comparison of a conventional photocoagulator and a novel, 3-nanosecond pulse laser.* Invest Ophthalmol Vis Sci, 2013. **54**(3): p. 2319-32.
318. Wang, R., P. Seifert, and T.C. Jakobs, *Astrocytes in the Optic Nerve Head of Glaucomatous Mice Display a Characteristic Reactive Phenotype.* Invest Ophthalmol Vis Sci, 2017. **58**(2): p. 924-932.
319. Lye-Barthel, M., D. Sun, and T.C. Jakobs, *Morphology of astrocytes in a glaucomatous optic nerve.* Invest Ophthalmol Vis Sci, 2013. **54**(2): p. 909-17.
320. Weinreb, R.N., et al., *Primary open-angle glaucoma.* Nat Rev Dis Primers, 2016. **2**: p. 16067.
321. Lewis, G.P., et al., *The fate of Muller's glia following experimental retinal detachment: nuclear migration, cell division, and subretinal glial scar formation.* Mol Vis, 2010. **16**: p. 1361-72.
322. Orellana, J.A., et al., *Modulation of brain hemichannels and gap junction channels by pro-inflammatory agents and their possible role in neurodegeneration.* Antioxid Redox Signal, 2009. **11**(2): p. 369-99.
323. Retamal, M.A., et al., *Cx43 hemichannels and gap junction channels in astrocytes are regulated oppositely by proinflammatory cytokines released from activated microglia.* J Neurosci, 2007. **27**(50): p. 13781-92.
324. Bedner, P., et al., *Astrocyte uncoupling as a cause of human temporal lobe epilepsy.* Brain, 2015. **138**(Pt 5): p. 1208-22.

325. Nagy, J.I., et al., *Elevated connexin43 immunoreactivity at sites of amyloid plaques in alzheimer's disease.* Brain Research, 1996. **717**(1-2): p. 173-178.
326. Kerr, N.M., et al., *Gap junction protein connexin43 (GJA1) in the human glaucomatous optic nerve head and retina.* J Clin Neurosci, 2011. **18**(1): p. 102-8.
327. Shigetomi, E., et al., *Aberrant Calcium Signals in Reactive Astrocytes: A Key Process in Neurological Disorders.* Int J Mol Sci, 2019. **20**(4).
328. Kisler, K., et al., *Cerebral blood flow regulation and neurovascular dysfunction in Alzheimer disease.* Nat Rev Neurosci, 2017. **18**(7): p. 419-434.
329. Wareham, L.K. and D.J. Calkins, *The Neurovascular Unit in Glaucomatous Neurodegeneration.* Front Cell Dev Biol, 2020. **8**: p. 452.
330. Moran, E.P., et al., *Neurovascular cross talk in diabetic retinopathy: Pathophysiological roles and therapeutic implications.* Am J Physiol Heart Circ Physiol, 2016. **311**(3): p. H738-49.
331. Garhöfer, G., et al., *Response of Retinal Vessel Diameters to Flicker Stimulation in Patients with Early Open Angle Glaucoma.* Journal of Glaucoma, 2004. **13**(4): p. 340-344.
332. Gugleta, K., et al., *Dynamics of retinal vessel response to flicker light in glaucoma patients and ocular hypertensives.* Graefes Arch Clin Exp Ophthalmol, 2012. **250**(4): p. 589-94.
333. Hernandez, M.R., H. Miao, and T. Lukas, *Astrocytes in glaucomatous optic neuropathy*, in *Glaucoma: An Open Window to Neurodegeneration and Neuroprotection*. 2008. p. 353-373.
334. Heuser, K., et al., *Ca2+ Signals in Astrocytes Facilitate Spread of Epileptiform Activity.* Cereb Cortex, 2018. **28**(11): p. 4036-4048.
335. Saito, K., et al., *Aberrant astrocyte Ca(2+) signals "AxCa signals" exacerbate pathological alterations in an Alexander disease model.* Glia, 2018. **66**(5): p. 1053-1067.
336. Kuchibhotla, K.V., et al., *Synchronous hyperactivity and intercellular calcium waves in astrocytes in Alzheimer mice.* Science, 2009. **323**(5918): p. 1211-5.
337. Rakers, C. and G.C. Petzold, *Astrocytic calcium release mediates peri-infarct depolarizations in a rodent stroke model.* J Clin Invest, 2017. **127**(2): p. 511-516.
338. Jiang, R., et al., *Dysfunctional Calcium and Glutamate Signaling in Striatal Astrocytes from Huntington's Disease Model Mice.* J Neurosci, 2016. **36**(12): p. 3453-70.
339. Jones, E.V. and D.S. Bouvier, *Astrocyte-secreted matricellular proteins in CNS remodelling during development and disease.* Neural Plast, 2014. **2014**: p. 321209.
340. Muir, E.M., et al., *Matrix metalloproteases and their inhibitors are produced by overlapping populations of activated astrocytes.* Molecular Brain Research, 2002. **100**(1-2): p. 103-117.
341. Bajetto, A., et al., *Chemokines and their receptors in the central nervous system.* Front Neuroendocrinol, 2001. **22**(3): p. 147-84.
342. Jha, M.K., et al., *Diverse functional roles of lipocalin-2 in the central nervous system.* Neurosci Biobehav Rev, 2015. **49**: p. 135-56.
343. Naude, P.J., et al., *Lipocalin 2: novel component of proinflammatory signaling in Alzheimer's disease.* FASEB J, 2012. **26**(7): p. 2811-23.
344. Xing, C., et al., *Neuronal production of lipocalin-2 as a help-me signal for glial activation.* Stroke, 2014. **45**(7): p. 2085-92.
345. Yan, L., et al., *The high molecular weight urinary matrix metalloproteinase (MMP) activity is a complex of gelatinase B/MMP-9 and neutrophil gelatinase-associated lipocalin (NGAL). Modulation of MMP-9 activity by NGAL.* J Biol Chem, 2001. **276**(40): p. 37258-65.
346. Lee, S., et al., *Lipocalin-2 is an autocrine mediator of reactive astrocytosis.* J Neurosci, 2009. **29**(1): p. 234-49.
347. Flo, T.H., et al., *Lipocalin 2 mediates an innate immune response to bacterial infection by sequestrating iron.* Nature, 2004. **432**(7019): p. 917-21.

348. Stephan, A.H., B.A. Barres, and B. Stevens, *The complement system: an unexpected role in synaptic pruning during development and disease.* Annu Rev Neurosci, 2012. **35**: p. 369-89.
349. Bonneh-Barkay, D., et al., *In vivo CHI3L1 (YKL-40) expression in astrocytes in acute and chronic neurological diseases.* J Neuroinflammation, 2010. **7**: p. 34.
350. Craig-Schapiro, R., et al., *YKL-40: a novel prognostic fluid biomarker for preclinical Alzheimer's disease.* Biol Psychiatry, 2010. **68**(10): p. 903-12.
351. Lananna, B.V., et al., *Chi3l1/YKL-40 is controlled by the astrocyte circadian clock and regulates neuroinflammation and Alzheimer's disease pathogenesis.* Sci Transl Med, 2020. **12**(574).
352. Forger, N.G., et al., *Cardiotrophin-Like Cytokine/Cytokine-Like Factor 1 is an Essential Trophic Factor for Lumbar and Facial MotoneuronsIn Vivo.* The Journal of Neuroscience, 2003. **23**(26): p. 8854-8858.
353. Das, S., et al., *Meta-analysis of mouse transcriptomic studies supports a context-dependent astrocyte reaction in acute CNS injury versus neurodegeneration.* J Neuroinflammation, 2020. **17**(1): p. 227.
354. Bonneh-Barkay, D. and C.A. Wiley, *Brain extracellular matrix in neurodegeneration.* Brain Pathol, 2009. **19**(4): p. 573-85.
355. George, N. and H.M. Geller, *Extracellular matrix and traumatic brain injury.* J Neurosci Res, 2018. **96**(4): p. 573-588.
356. Bradbury, E.J. and E.R. Burnside, *Moving beyond the glial scar for spinal cord repair.* Nat Commun, 2019. **10**(1): p. 3879.
357. Crocker, S.J., A. Pagenstecher, and I.L. Campbell, *The TIMPs tango with MMPs and more in the central nervous system.* J Neurosci Res, 2004. **75**(1): p. 1-11.
358. Welser-Alves, J.V., S.J. Crocker, and R. Milner, *A dual role for microglia in promoting tissue inhibitor of metalloproteinase (TIMP) expression in glial cells in response to neuroinflammatory stimuli.* J Neuroinflammation, 2011. **8**: p. 61.
359. De Stefano, M.E. and M.T. Herrero, *The multifaceted role of metalloproteinases in physiological and pathological conditions in embryonic and adult brains.* Prog Neurobiol, 2017. **155**: p. 36-56.
360. Vicuna, L., et al., *The serine protease inhibitor SerpinA3N attenuates neuropathic pain by inhibiting T cell-derived leukocyte elastase.* Nat Med, 2015. **21**(5): p. 518-23.
361. Knight, B.E., et al., *TIMP-1 Attenuates the Development of Inflammatory Pain Through MMP-Dependent and Receptor-Mediated Cell Signaling Mechanisms.* Front Mol Neurosci, 2019. **12**: p. 220.
362. McKeon, R.J., et al., *Reduction of neurite outgrowth in a model of glial scarring following CNS injury is correlated with the expression of inhibitory molecules on reactive astrocytes.* The Journal of Neuroscience, 1991. **11**(11): p. 3398-3411.
363. Pena, J.D., et al., *Enhanced tenascin expression associated with reactive astrocytes in human optic nerve heads with primary open angle glaucoma.* Exp Eye Res, 1999. **68**(1): p. 29-40.
364. Reinhard, J., L. Roll, and A. Faissner, *Tenascins in Retinal and Optic Nerve Neurodegeneration.* Front Integr Neurosci, 2017. **11**: p. 30.
365. Yamaguchi, Y., *Lecticans: organizers of the brain extracellular matrix.* Cell Mol Life Sci, 2000. **57**(2): p. 276-89.
366. Song, I. and A. Dityatev, *Crosstalk between glia, extracellular matrix and neurons.* Brain Res Bull, 2018. **136**: p. 101-108.
367. McKeon, R.J., M.J. Jurynec, and C.R. Buck, *The Chondroitin Sulfate Proteoglycans Neurocan and Phosphacan Are Expressed by Reactive Astrocytes in the Chronic CNS Glial Scar.* The Journal of Neuroscience, 1999. **19**(24): p. 10778-10788.
368. Siebert, J.R., A. Conta Steencken, and D.J. Osterhout, *Chondroitin sulfate proteoglycans in the nervous system: inhibitors to repair.* Biomed Res Int, 2014. **2014**: p. 845323.

369. Galea, I., I. Bechmann, and V.H. Perry, *What is immune privilege (not)?* Trends Immunol, 2007. **28**(1): p. 12-8.
370. Geyer, S., M. Jacobs, and N.J. Hsu, *Immunity Against Bacterial Infection of the Central Nervous System: An Astrocyte Perspective.* Front Mol Neurosci, 2019. **12**: p. 57.
371. Colonna, M. and O. Butovsky, *Microglia Function in the Central Nervous System During Health and Neurodegeneration.* Annu Rev Immunol, 2017. **35**: p. 441-468.
372. Wilson, E.H., W. Weninger, and C.A. Hunter, *Trafficking of immune cells in the central nervous system.* J Clin Invest, 2010. **120**(5): p. 1368-79.
373. Tang, D., et al., *PAMPs and DAMPs: signal 0s that spur autophagy and immunity.* Immunol Rev, 2012. **249**(1): p. 158-75.
374. Zindel, J. and P. Kubes, *DAMPs, PAMPs, and LAMPs in Immunity and Sterile Inflammation.* Annu Rev Pathol, 2020. **15**: p. 493-518.
375. Jack, C.S., et al., *TLR signaling tailors innate immune responses in human microglia and astrocytes.* J Immunol, 2005. **175**(7): p. 4320-30.
376. Okun, E., K.J. Griffioen, and M.P. Mattson, *Toll-like receptor signaling in neural plasticity and disease.* Trends Neurosci, 2011. **34**(5): p. 269-81.
377. Johnson, G.B., et al., *Receptor-mediated monitoring of tissue well-being via detection of soluble heparan sulfate by Toll-like receptor 4.* J Immunol, 2002. **168**(10): p. 5233-9.
378. Okamura, Y., et al., *The extra domain A of fibronectin activates Toll-like receptor 4.* J Biol Chem, 2001. **276**(13): p. 10229-33.
379. Termeer, C., et al., *Oligosaccharides of Hyaluronan activate dendritic cells via toll-like receptor 4.* J Exp Med, 2002. **195**(1): p. 99-111.
380. Gorina, R., et al., *Astrocyte TLR4 activation induces a proinflammatory environment through the interplay between MyD88-dependent NFkappaB signaling, MAPK, and Jak1/Stat1 pathways.* Glia, 2011. **59**(2): p. 242-55.
381. Liu, X., V.S. Chauhan, and I. Marriott, *NOD2 contributes to the inflammatory responses of primary murine microglia and astrocytes to Staphylococcus aureus.* Neurosci Lett, 2010. **474**(2): p. 93-8.
382. Braun, B.J., et al., *The formyl peptide receptor like-1 and scavenger receptor MARCO are involved in glial cell activation in bacterial meningitis.* J Neuroinflammation, 2011. **8**(1): p. 11.
383. Alarcon, R., et al., *Expression of scavenger receptors in glial cells. Comparing the adhesion of astrocytes and microglia from neonatal rats to surface-bound beta-amyloid.* J Biol Chem, 2005. **280**(34): p. 30406-15.
384. Ousman, S.S. and P. Kubes, *Immune surveillance in the central nervous system.* Nat Neurosci, 2012. **15**(8): p. 1096-101.
385. Neefjes, J., et al., *Towards a systems understanding of MHC class I and MHC class II antigen presentation.* Nat Rev Immunol, 2011. **11**(12): p. 823-36.
386. Rock, K.L., E. Reits, and J. Neefjes, *Present Yourself! By MHC Class I and MHC Class II Molecules.* Trends Immunol, 2016. **37**(11): p. 724-737.
387. Banchereau, J., et al., *Immunobiology of dendritic cells.* Annu Rev Immunol, 2000. **18**: p. 767-811.
388. Ellwardt, E., et al., *Understanding the Role of T Cells in CNS Homeostasis.* Trends Immunol, 2016. **37**(2): p. 154-165.
389. Korn, T. and A. Kallies, *T cell responses in the central nervous system.* Nat Rev Immunol, 2017. **17**(3): p. 179-194.
390. Rothhammer, V. and F.J. Quintana, *Control of autoimmune CNS inflammation by astrocytes.* Semin Immunopathol, 2015. **37**(6): p. 625-38.

391. Flavia, T., A. Maria, and L. Cristina, *Chemokines: Key Molecules that Orchestrate Communication among Neurons, Microglia and Astrocytes to Preserve Brain Function.* Neuroscience, 2020. **439**: p. 230-240.
392. Giovannoni, F. and F.J. Quintana, *The Role of Astrocytes in CNS Inflammation.* Trends Immunol, 2020. **41**(9): p. 805-819.
393. Rot, A. and U.H. von Andrian, *Chemokines in innate and adaptive host defense: basic chemokinese grammar for immune cells.* Annu Rev Immunol, 2004. **22**: p. 891-928.
394. McKimmie, C.S. and G.J. Graham, *Astrocytes modulate the chemokine network in a pathogen-specific manner.* Biochem Biophys Res Commun, 2010. **394**(4): p. 1006-11.
395. Dufour, J.H., et al., *IFN-gamma-inducible protein 10 (IP-10; CXCL10)-deficient mice reveal a role for IP-10 in effector T cell generation and trafficking.* J Immunol, 2002. **168**(7): p. 3195-204.
396. Gschwandtner, M., R. Derler, and K.S. Midwood, *More Than Just Attractive: How CCL2 Influences Myeloid Cell Behavior Beyond Chemotaxis.* Front Immunol, 2019. **10**: p. 2759.
397. Michinaga, S. and Y. Koyama, *Dual Roles of Astrocyte-Derived Factors in Regulation of Blood-Brain Barrier Function after Brain Damage.* Int J Mol Sci, 2019. **20**(3).
398. Sofroniew, M.V., *Astrocyte barriers to neurotoxic inflammation.* Nat Rev Neurosci, 2015. **16**(5): p. 249-63.
399. Joly, E., L. Mucke, and M.B. Oldstone, *Viral persistence in neurons explained by lack of major histocompatibility class I expression.* Science, 1991. **253**(5025): p. 1283-5.
400. Elmer, B.M. and A.K. McAllister, *Major histocompatibility complex class I proteins in brain development and plasticity.* Trends Neurosci, 2012. **35**(11): p. 660-70.
401. Barcia, C., et al., *T cells' immunological synapses induce polarization of brain astrocytes in vivo and in vitro: a novel astrocyte response mechanism to cellular injury.* PLoS One, 2008. **3**(8): p. e2977.
402. Hamo, L., et al., *Distinct regulation of MHC molecule expression on astrocytes and microglia during viral encephalomyelitis.* Glia, 2007. **55**(11): p. 1169-77.
403. Corriveau, R.A., G.S. Huh, and C.J. Shatz, *Regulation of Class I MHC Gene Expression in the Developing and Mature CNS by Neural Activity.* Neuron, 1998. **21**(3): p. 505-520.
404. Shatz, C.J., *MHC class I: an unexpected role in neuronal plasticity.* Neuron, 2009. **64**(1): p. 40-5.
405. Shrikant, P. and E.N. Benveniste, *The central nervous system as an immunocompetent organ: role of glial cells in antigen presentation.* The Journal of Immunology, 1996. **157**(5): p. 1819-1822.
406. Guerrero-García, J.J., *The role of astrocytes in multiple sclerosis pathogenesis.* Neurología (English Edition), 2020. **35**(6): p. 400-408.
407. Rostami, J., et al., *Astrocytes have the capacity to act as antigen-presenting cells in the Parkinson's disease brain.* J Neuroinflammation, 2020. **17**(1): p. 119.
408. de Hoz, R., et al., *Retinal Macroglial Responses in Health and Disease.* Biomed Res Int, 2016. **2016**: p. 2954721.
409. Hermann, J.S., *Transforming growth factors type β1 and β2 suppress rat astrocyte autoantigen presentation and antagonize hyperinduction of class II major histocompatibility complex antigen expression by interferon-γ and tumor necrosis factor-α.* Journal of Neuroimmunology, 1990. **27**(1): p. 41-47.
410. Barna, B.P., et al., *Interferon-β impairs induction of HLA-DR antigen expression in cultured adult human astrocytes.* Journal of Neuroimmunology, 1989. **23**(1): p. 45-53.
411. Lee, S.C., et al., *Glutamate differentially inhibits the expression of class II MHC antigens on astrocytes and microglia.* The Journal of Immunology, 1992. **148**(11): p. 3391-3397.
412. Mallat, M., J.L. Marin-Teva, and C. Cheret, *Phagocytosis in the developing CNS: more than clearing the corpses.* Curr Opin Neurobiol, 2005. **15**(1): p. 101-7.

413. Galloway, D.A., et al., *Phagocytosis in the Brain: Homeostasis and Disease.* Front Immunol, 2019. **10**: p. 790.
414. Anderson, S.R., et al., *Complement Targets Newborn Retinal Ganglion Cells for Phagocytic Elimination by Microglia.* J Neurosci, 2019. **39**(11): p. 2025-2040.
415. Fu, R., et al., *Phagocytosis of microglia in the central nervous system diseases.* Mol Neurobiol, 2014. **49**(3): p. 1422-34.
416. Sokolowski, J.D. and J.W. Mandell, *Phagocytic clearance in neurodegeneration.* Am J Pathol, 2011. **178**(4): p. 1416-28.
417. Neher, J.J., et al., *Phagocytosis executes delayed neuronal death after focal brain ischemia.* Proc Natl Acad Sci U S A, 2013. **110**(43): p. E4098-107.
418. Fourgeaud, L., et al., *TAM receptors regulate multiple features of microglial physiology.* Nature, 2016. **532**(7598): p. 240-244.
419. Davis, C.H., et al., *Transcellular degradation of axonal mitochondria.* Proc Natl Acad Sci U S A, 2014. **111**(26): p. 9633-8.
420. Chung, W.S., et al., *Astrocytes mediate synapse elimination through MEGF10 and MERTK pathways.* Nature, 2013. **504**(7480): p. 394-400.
421. Ponath, G., et al., *Myelin phagocytosis by astrocytes after myelin damage promotes lesion pathology.* Brain, 2017. **140**(2): p. 399-413.
422. Gomez-Arboledas, A., et al., *Phagocytic clearance of presynaptic dystrophies by reactive astrocytes in Alzheimer's disease.* Glia, 2018. **66**(3): p. 637-653.
423. Chung, W.S., et al., *Novel allele-dependent role for APOE in controlling the rate of synapse pruning by astrocytes.* Proc Natl Acad Sci U S A, 2016. **113**(36): p. 10186-91.
424. Konishi, H., et al., *Astrocytic phagocytosis is a compensatory mechanism for microglial dysfunction.* EMBO J, 2020. **39**(22): p. e104464.
425. Tham, Y.C., et al., *Global prevalence of glaucoma and projections of glaucoma burden through 2040: a systematic review and meta-analysis.* Ophthalmology, 2014. **121**(11): p. 2081-90.
426. Sivak, J.M., *The aging eye: common degenerative mechanisms between the Alzheimer's brain and retinal disease.* Invest Ophthalmol Vis Sci, 2013. **54**(1): p. 871-80.
427. Weinreb, R.N., T. Aung, and F.A. Medeiros, *The pathophysiology and treatment of glaucoma: a review.* JAMA, 2014. **311**(18): p. 1901-11.
428. Kersey, J.P. and D.C. Broadway, *Corticosteroid-induced glaucoma: a review of the literature.* Eye (Lond), 2006. **20**(4): p. 407-16.
429. Aboobakar, I.F., et al., *Major review: Exfoliation syndrome; advances in disease genetics, molecular biology, and epidemiology.* Exp Eye Res, 2017. **154**: p. 88-103.
430. Danesh-Meyer, H.V. and L.A. Levin, *Glaucoma as a neurodegenerative disease.* J Neuroophthalmol, 2015. **35 Suppl 1**: p. S22-8.
431. Quigley, H.A., et al., *Morphologic Changes in the Lamina Cribrosa Correlated with Neural Loss in Open-Angle Glaucoma.* American Journal of Ophthalmology, 1983. **95**(5): p. 673-691.
432. Downs, J.C. and C.A. Girkin, *Lamina cribrosa in glaucoma.* Curr Opin Ophthalmol, 2017. **28**(2): p. 113-119.
433. Vecino, E., et al., *Glia-neuron interactions in the mammalian retina.* Prog Retin Eye Res, 2016. **51**: p. 1-40.
434. Bussow, H., *The astrocytes in the retina and optic nerve head of mammals: a special glia for the ganglion cell axons.* Cell Tissue Res, 1980. **206**(3): p. 367-78.
435. Ramirez, J.M., et al., *Structural specializations of human retinal glial cells.* Vision Res, 1996. **36**(14): p. 2029-36.
436. Sun, D., S. Moore, and T.C. Jakobs, *Optic nerve astrocyte reactivity protects function in experimental glaucoma and other nerve injuries.* J Exp Med, 2017. **214**(5): p. 1411-1430.

437. Guo, X., et al., *PGC-1alpha signaling coordinates susceptibility to metabolic and oxidative injury in the inner retina.* Am J Pathol, 2014. **184**(4): p. 1017-1029.
438. Quigley, H.A. and A.T. Broman, *The number of people with glaucoma worldwide in 2010 and 2020.* Br J Ophthalmol, 2006. **90**(3): p. 262-7.
439. Foster, P.J. and G.J. Johnson, *Glaucoma in China: how big is the problem?* Br J Ophthalmol, 2001. **85**(11): p. 1277-82.
440. Rein, D.B., et al., *The economic burden of major adult visual disorders in the United States.* Arch Ophthalmol, 2006. **124**(12): p. 1754-60.
441. Varma, R., et al., *An assessment of the health and economic burdens of glaucoma.* Am J Ophthalmol, 2011. **152**(4): p. 515-22.
442. Zhao, D., et al., *The association of blood pressure and primary open-angle glaucoma: a meta-analysis.* Am J Ophthalmol, 2014. **158**(3): p. 615-27 e9.
443. Zhou, M., et al., *Diabetes mellitus as a risk factor for open-angle glaucoma: a systematic review and meta-analysis.* PLoS One, 2014. **9**(8): p. e102972.
444. Mitchell, P., et al., *The relationship between glaucoma and myopia.* Ophthalmology, 1999. **106**(10): p. 2010-2015.
445. Leske, M.C., et al., *Factors for glaucoma progression and the effect of treatment: the early manifest glaucoma trial.* Arch Ophthalmol, 2003. **121**(1): p. 48-56.
446. Quigley, H.A., *New paradigms in the mechanisms and management of glaucoma.* Eye (Lond), 2005. **19**(12): p. 1241-8.
447. Almasieh, M., et al., *The molecular basis of retinal ganglion cell death in glaucoma.* Prog Retin Eye Res, 2012. **31**(2): p. 152-81.
448. Sigal, I.A., et al., *Predicted extension, compression and shearing of optic nerve head tissues.* Exp Eye Res, 2007. **85**(3): p. 312-22.
449. Hernandez, M.R. and J.D. Pena, *The optic nerve head in glaucomatous optic neuropathy.* Arch Ophthalmol, 1997. **115**(3): p. 389-95.
450. Michelson, G., et al., *Visual field defect and perfusion of the juxtapapillary retina and the neuroretinal rim area in primary open-angle glaucoma.* Graefes Arch Clin Exp Ophthalmol, 1998. **236**(2): p. 80-5.
451. Pease, M.E., et al., *Obstructed Axonal Transport of BDNF and Its Receptor TrkB in Experimental Glaucoma.* Investigative Ophthalmology & Visual Science, 2000. **41**(3): p. 764-774.
452. Nickells, R.W., et al., *Under pressure: cellular and molecular responses during glaucoma, a common neurodegeneration with axonopathy.* Annu Rev Neurosci, 2012. **35**: p. 153-79.
453. Howell, G.R., et al., *Axons of retinal ganglion cells are insulted in the optic nerve early in DBA/2J glaucoma.* J Cell Biol, 2007. **179**(7): p. 1523-37.
454. Kerrigan, L.A., et al., *TUNEL-positive ganglion cells in human primary open-angle glaucoma.* Arch Ophthalmol, 1997. **115**(8): p. 1031-5.
455. Cordeiro, M.F., et al., *Real-time imaging of single nerve cell apoptosis in retinal neurodegeneration.* Proc Natl Acad Sci U S A, 2004. **101**(36): p. 13352-6.
456. Fricker, M., et al., *Neuronal Cell Death.* Physiol Rev, 2018. **98**(2): p. 813-880.
457. Skriapa Manta, A., et al., *Optic Disc Coloboma in children - prevalence, clinical characteristics and associated morbidity.* Acta Ophthalmol, 2019. **97**(5): p. 478-485.
458. Deiner, M.S., et al., *Netrin-1 and DCC Mediate Axon Guidance Locally at the Optic Disc: Loss of Function Leads to Optic Nerve Hypoplasia.* Neuron, 1997. **19**(3): p. 575-589.
459. Yu, D.Y., et al., *Retinal ganglion cells: Energetics, compartmentation, axonal transport, cytoskeletons and vulnerability.* Prog Retin Eye Res, 2013. **36**: p. 217-46.
460. Flammer, J., et al., *The impact of ocular blood flow in glaucoma.* Progress in Retinal and Eye Research, 2002. **21**(4): p. 359-393.

461. Morgan, J.E., *Circulation and axonal transport in the optic nerve.* Eye (Lond), 2004. **18**(11): p. 1089-95.
462. TriviÑO, A., et al., *Immunohistochemical Study of Human Optic Nerve Head Astroglia.* Vision Research, 1996. **36**(14): p. 2015-2028.
463. Nguyen, J.V., et al., *Myelination transition zone astrocytes are constitutively phagocytic and have synuclein dependent reactivity in glaucoma.* Proc Natl Acad Sci U S A, 2011. **108**(3): p. 1176-81.
464. Wang, L., et al., *Immunohistologic evidence for retinal glial cell changes in human glaucoma.* Invest Ophthalmol Vis Sci, 2002. **43**(4): p. 1088-94.
465. Nikolskaya, T., et al., *Network analysis of human glaucomatous optic nerve head astrocytes.* BMC Med Genomics, 2009. **2**: p. 24.
466. Neufeld, A.H., M.R. Hernandez, and M. Gonzalez, *Nitric oxide synthase in the human glaucomatous optic nerve head.* Arch Ophthalmol, 1997. **115**(4): p. 497-503.
467. Neufeld, A.H., *Nitric Oxide.* Survey of Ophthalmology, 1999. **43**: p. S129-S135.
468. Calabrese, V., et al., *Nitric oxide in the central nervous system: neuroprotection versus neurotoxicity.* Nat Rev Neurosci, 2007. **8**(10): p. 766-75.
469. Liu, B. and A.H. Neufeld, *Activation of epidermal growth factor receptor signals induction of nitric oxide synthase-2 in human optic nerve head astrocytes in glaucomatous optic neuropathy.* Neurobiology of Disease, 2003. **13**(2): p. 109-123.
470. Liu, B., et al., *Epidermal growth factor receptor activation: an upstream signal for transition of quiescent astrocytes into reactive astrocytes after neural injury.* J Neurosci, 2006. **26**(28): p. 7532-40.

Chapter II

Isolation of Retinal Astrocytes for Experimentation and Analysis

Background & Rationale

In biology and biomedical research, experiments frequently target the behavior of discrete classes of cells as part of an ongoing effort to better understand the physiological and pathological functions of the organism as a whole. The isolation of cells of interest - either individually or en masse - enables the activity of specific cell types to be examined without the confounding effects of neighboring cell populations. The nature of this isolation may vary widely depending on experimental requirements and available techniques, from prospective sorting of cells for *in vitro* experimentation to post hoc bioinformatic separation of specific cell populations after *in vivo* experiments [1-7]. My approaches to isolate retinal astrocytes, both pre- and post- experimentally, have been in large part shaped by the intrinsic properties of the retina and the astrocytes themselves.

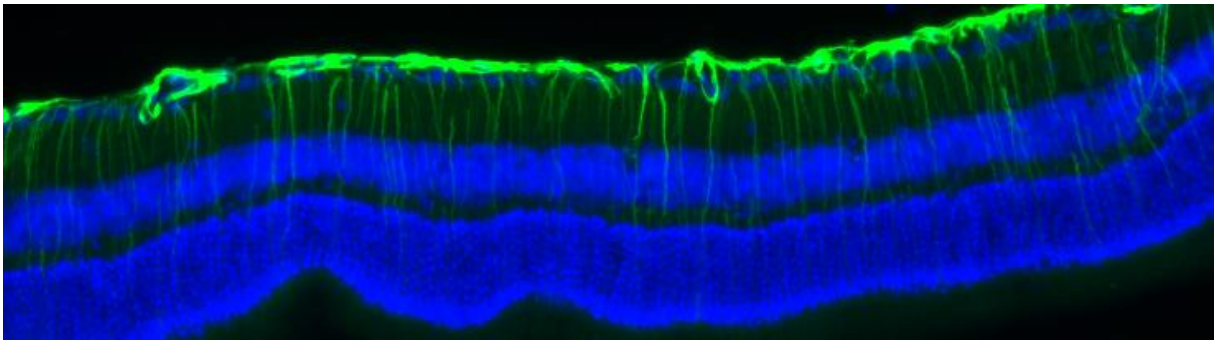

Figure 1: Mouse Retina: The bright green layer at the surface of the retina consists of retinal astrocytes stained with the astrocytic marker GFAP, which also stains the transverse Muller cells to a lesser degree. Although Muller cells are typically only weakly GFAP+, these come from a retina exposed to a model of glaucoma and as a result have upregulated expression of the protein.

Owing to the lamination (or layering) discussed in Chapter I, the distinct population of astrocytes that emerges from the optic nerve during development is present in only a single layer of the retina, where it tiles the vitreal surface, interfacing with both the superficial retinal vasculature as well as the retinal ganglion cells and their axons [8-10]. Unlike the densely packed transverse cells of the retina – such as photoreceptors or Müller cells – retinal astrocytes have broad domains and exist only in this narrow layer; as a consequence, while a 1 mm^2 region of the mouse retina contains approximately 16,000 Müller cells and greater than 400,000 rod photoreceptors, the same region may only have between 250 and 450 astrocytes, depending on proximity to the optic disc [11-13]. With an average size of ~16mm^2, this means that the mouse eye has approximately 4,000-7,000 astrocytes out of over 6.5x10^6 cells, indicating that they make up approximately 0.1% of all retinal cells [12]. This leads to significant challenges in isolating these cells in sufficient quantities for many applications, and – along with

the presence of the more prevalent Müller cells – precludes the use of many conventional approaches such as western blotting to study acutely isolated retinal astrocytes.

Historically, the low density of these cells mean that two distinct approaches have been utilized to study retinal astrocytes – primary cell culture and histology. The first of these, primary cell culture, involves selectively culturing cells isolated by enzymatic dissociation of the retina [14, 15]. This approach has the advantage of allowing cell populations to grow over a dramatically increased area, facilitating the accumulation of much larger numbers of cells suitable for a wide variety of cell and molecular biology experiments. However, primary culture is a time-consuming process in which aspects of the original cells' behavior may be muted or lost, and concerns persist about the purity of the original cell population [16, 17]. Conversely, with histological techniques – especially immunofluorescence – astrocytes can typically be identified unambiguously due to their immunoreactivity and morphology. However, only very limited classes of experimental study can be performed, typically involving the presence (or lack thereof) and localization of specific proteins or RNA fragments [18, 19]. Owing to the non-stochiometric nature of immunohistochemical staining, the results of such experiments are typically qualitative, rather than quantitative. Furthermore, most interventions can only be performed *in vivo* – or *ex vivo* on intact retinas – constraining the ability to query astrocytes independently of their neighboring cells [20, 21].

For my research, I aim to study the changes retinal astrocytes undergo in response to stimuli that mimic some aspects of glaucoma, such as induced ocular hypertension, as well as any differences between retinal astrocytes and those of the optic nerve and brain. Broad understanding of these phenomena would be greatly improved by a comprehensive analysis of accompanying transcriptional change, as revealed by RNA sequencing (RNAseq) [22, 23]. This approach involves the creation of a cDNA library from sample mRNA in order to utilize next generation sequencing to produce a wealth of transcriptional information, revealing what genes are being expressed (and to what degree) within the target cell sample [24].

Although a powerful technique, it has a number of limitations – loss of localization information, (relatively) rapid alteration of transcription in response to changing stimuli, and a need for many cells to detect genes transcribed at low levels – with accompanying strategies to offset them. Prospectively isolating the cells of interest by generating a purified or highly enriched population can offset the loss of localization information when cells are destroyed in RNA isolation. Doing so in a rapid manner, typically while chilling the cells to slow behavioral responses, can further prevent transcriptional changes unrelated to experimental parameters. For some applications, these two aims can instead be achieved by using a technique known as single cell RNAseq, in which separate cDNA libraries are prepared for each cell from the sample [25, 26]. However, single cell RNAseq is inherently noisier than bulk RNAseq, a problem exacerbated by the low density of astrocytes in the retina; previous attempts to perform single cell RNAseq on human retinal cells yielded only a small number of astrocytes (<50), resulting in

comparatively shallow information [27-29]. Instead, a method to acutely isolate and rapidly purify a larger number of retinal astrocytes is required.

In order to bypass the limitations of the existing methods, I have investigated two approaches that aim to acutely isolate and purify, or at least dramatically enrich, retinal astrocytes. The more traditional of these approaches – antigen-based sorting – combines the complete enzymatic dissociation of the retina with labeling of astrocytic cell surface antigens to purify astrocytes from the resulting cell suspension. By targeting astrocyte specific antigens with antibodies conjugated to either fluorescent probes or magnetic beads, fluorescence-assisted or magnet-assisted cell sorting (FACS or MACS) can facilitate the purification of astrocytes; both FACS and MACS have been used extensively for the isolation of brain astrocytes [2, 3, 30]. FACS in particular has the added benefit of being compatible with a variety of transgenic mouse strains expressing GFP or other fluorescent proteins via cell-type specific promoters, such as the Aldh1l1-eGFP mouse line in which astrocytes and Muller cells express a brighter version of green fluorescent protein (GFP). However, attempts to combine these intrinsically fluorescent cells with the retinal astrocyte specific marker PDGFRα (for positive selection), or CD29 – a marker found on the surface of Muller cells but not astrocytes (negative selection) – delivered inconclusive results; there were simply too few cells present after sorting to properly characterize their purity (figure 2).

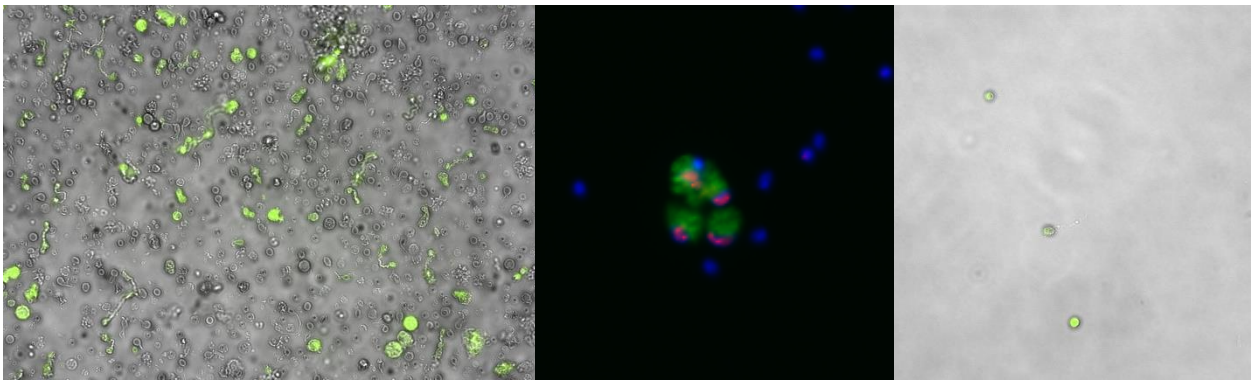

Figure 2: Dissociated retinal cells from Aldh1l1-eGFP mice. Left: GFP expression in unsorted cells. Center: GFAP+ (green) and Pax-2+ (red) astrocytes in unsorted dissociation. Right: Cells sorted by GFP signal intensity.

Alongside attempts at FACS/MACS - based sorting, I also developed an unusual approach that depends primarily upon the anatomical lamination of the retina. This approach, which I have termed ‘astrocyte pull-off’, combines a mild enzymatic treatment meant to partially disaggregate the anatomical the layers of the retina, followed by mechanical separation of the superficial astrocyte layer from the bulk of the retina, and is derived from decades-old attempts to isolate retinal ganglion cells in a similar fashion [31, 32]. In this method, retinas are treated enzymatically to disrupt the extracellular matrix holding together their disparate layers, and then the most superficial layers, home to the retinal vasculature, astrocytes, and retinal ganglion cells, are ‘pulled off’ from the bulk of the retina via adhesion to a substrate. This approach to isolation also achieves the salutary effect of massive enrichment for retinal astrocytes, as higher density cell types such as rod and cone photoreceptors, bipolar cells, and

Müller cells are left behind in the remaining retina. Although attempts at using earlier iterations of this approach targeted retinal ganglion cells, rather than astrocytes, I immediately recognized the potential implications for my work. Retinal astrocytes are located even more vitreally than the RGCs, as they intertwine with the axons of the nerve fiber layer [8, 10]. As a result, they are more readily accessible than retinal ganglion cells utilizing this class of technique. Finally, the comparatively brief post-mortem interval (<1 hr) and the retention of astrocyte end-feet – which can be lost during conventional dissociation approaches but have been shown to possess distinct transcriptomes – represent additional advantages of the pull-off approach [33].

Method Development

Fundamentally, although they target separate populations of cells, the aim of the original retinal ganglion cell pull-off approaches and my astrocyte pull-off are the same: the isolation of a highly enriched sample of a sparse cell population from the retina. So too is the foundational principle: due to retinal lamination, most cell populations are confined to well-defined retinal layers; therefore, positive or negative selection of a cell type or types can be achieved by removal of the appropriate layer(s). In order to discuss the development of the method, a brief overview of the required steps is necessary; a more detailed protocol can be found in the following section.

Briefly, after euthanasia and enucleation, the anterior segment of the eye is removed and the retina is dissected out, with relieving cuts made at 90° intervals to allow the tissue to be flattened. The tissue – either a whole retina from a mouse or a single 'quarter' from a rat's – is then flattened on a porous membrane with the vitreal side up, and an uncoated glass coverslip is placed atop to create a glass-retina-membrane stack. This stack is then inverted, collagenase (type II) is applied to the membrane, and a small weight is added to ensure the retina is pressed against the glass. The retinal stack is then incubated at 37°c in a humidified incubator for ~22-25 minutes, followed by removal of the weight and inversion and brief drying of the sample. The glass coverslip is gently pulled off, and if done correctly a network of blood vessels and astrocytes will adhere to it and be liberated from the retina. While the general outline of the technique is similar to earlier retinal ganglion cell isolation approaches, great care was required to render the approach suitable for astrocytes, as these earlier methods essentially relied on retinal astrocytes and the ILM – which are located vitreally relative to the rest of the retina – as an expendable 'buffer' to protect RGCs during handling.

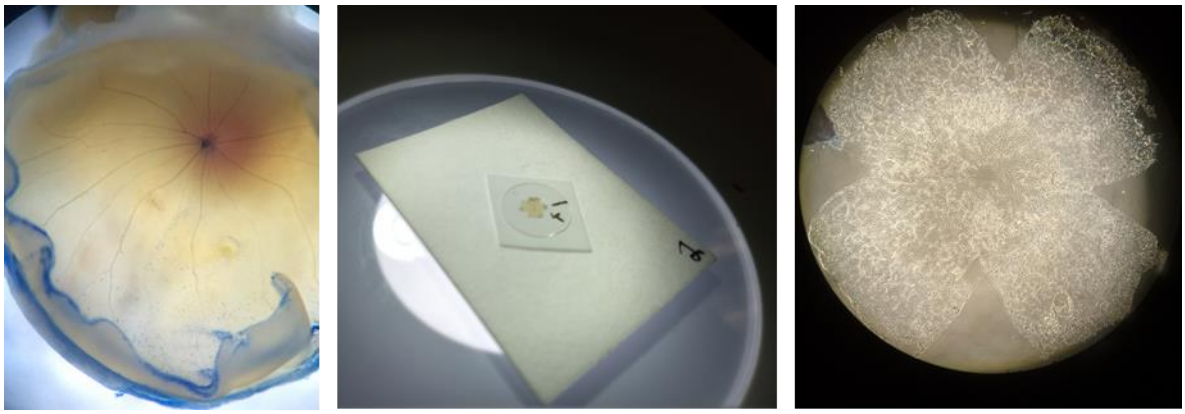

Figure 3: Select images illustrating the pull-off technique. Left: Eye with anterior segment, lens, and vitreous removed. Residual trypan blue can be seen along the edge of the tissue in the lower half of the photo. Center: Stack of filter paper, retina (facing RGC side up) and cover glass sitting on blotting paper after incubation. The astrocyte layer is isolated by gently lifting the glass with forceps. Right: Isolated astrocyte layer photographed in brightfield after separation.

Although published versions of the related retinal ganglion cell pull-off technique were developed primarily in rats, mice are increasingly used for retina research due to the availability of transgenic strains and other specialized genetic tools. Therefore, my initial development of this astrocyte isolation method was performed in rats, which have larger eyes that are easier to work with, but after I had reached a satisfactory level of consistency with the approach I transitioned to testing it in mice. My experience showed that only modest changes in dissection technique – whole retina in the mouse versus ~13mm^2 quarters in the rat – and enzyme volume were required, suggesting that the technique may be a viable approach to isolate retinal astrocytes regardless of the species of tissue origin.

Key Factors

When I first began developing this method, I encountered significant issues with the rate of successful isolation and problems with reproducibility despite the use of consistent methods and reagents. Although modification of enzyme concentration and/or incubation time could alter the thickness of the 'pull-off' by modulating the extent of dissociation, ensuring the adherence of the sample to the glass proved more challenging, and success or failure at this task was largely stochastic. Early attempts to improve adhesion by coating the coverslips with 100µg/ml of poly-d-lysine prior to the procedure were unsuccessful at improving reliability (data not shown), and extensive refinement of the technique improved the quality of successful isolations while having a minimal impact on the rate at which these occurred.

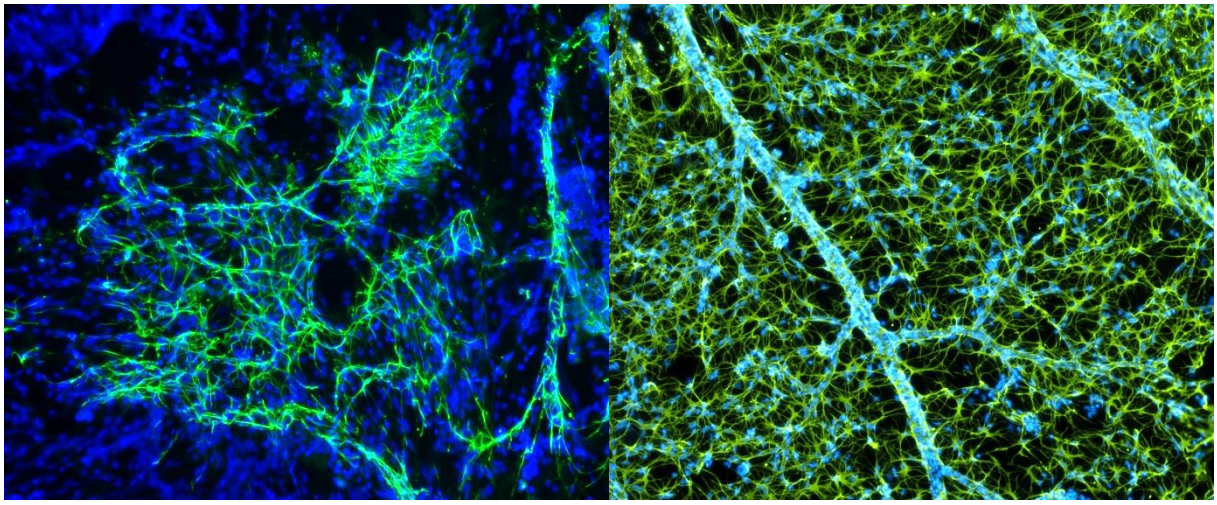

Figure 4: 20x images, GFAP in green, Hoechst nuclear stain in blue. Left, an early pull-off attempt with loss of structure and excess non-astrocytic cells. Right, pull-off after the technique was refined, consisting primarily of structurally intact vasculature and astrocytes.

However, as I continued isolating samples, I began to notice two broad trends. The first of these was an increasing probability of successful adherence the later a given tissue sample was in a sequence of isolations; that is, the 3rd and 4th quarter samples from a rat retina adhered to the glass more frequently than the 1st and 2nd quarters did. The second trend showed correlation with vitreal removal – samples from eyes in which the vitreous was removed intact adhered more frequently, regardless of their place in preparation order, than those from which the

vitreous fragmented and needed to be removed piecemeal. Initially, I suspected these observations reflected unintentional operator biases, with the improvement over the course of an experiment representing a sort of practice effect, while the relative ease or difficulty in removing the vitreous had a corresponding influence on confidence during an early stage of the experiments.

Although the effect of practice served as a convincing explanation for the influence of sample order on success during the earliest phases of method development, as time went on it became increasingly inadequate. Preparing samples daily for a week scarcely improved adhesion rates, which hovered between 25 and 50%, while equal durations without practice were not correlated with greater frequency of failure. However, I instead observed that the presence or absence of condensation on the inner door of the cell culture incubator – an indicator of humidity levels that typically decreased over the course of a multiple sample sequence – was generally predictive of subsequent adherence. In order to test this, I installed a hygrometer in the incubator and simulated the changes in humidity that would occur over the processing of a series of samples; this was accomplished by opening the door for 10 seconds at a time every ten minutes, an approximation of the pace at which individual samples could be processed.

This produced a trend of rapid drops in humidity coinciding with the opening of the door, followed by more gradual rebounds; by measuring the humidity during the 3rd and 4th simulated incubations, I concluded that a relative humidity of 75-85% would improve my sample adhesion. By contrast, normal operating humidity in a properly functioning cell culture incubator is >95%. Subsequent testing with retinal samples, accomplished by briefly 'airing out' the incubator to lower humidity before the addition of samples, yielded an immediate improvement, such that retinas that previously produced 1-2 viable samples were now consistently producing 3-4; I found this improvement too self-evident to merit further testing of the original conditions.

However, while monitoring and control of the relative humidity inside the incubator led to an improved rate of sample capture, eliminating one source of variation highlighted another: the correlation between challenging vitreal removals and failed isolations. Failure to completely remove elements of vitreous from the inner retinal surface led not only to issues with adhesion during the final pull-off step, but also resulted in movement of the coverslip during sample preparation, including instances in which the glass simply fell off during the pre-incubation inversion of the stack. These disrupted samples were typically non-recoverable. The difficulty in ensuring successful vitreal removal is a direct result of the function of this tissue; for high acuity vision to work, the vitreous must be optically clear. Furthermore, removal of the vitreous during dissection occurs in an aqueous solution to protect the ILM and retinal astrocytes, which are located at the surface of the retina, from excess drying and damage during handling; the refractive index of the vitreous is 1.336, nearly identical to water's 1.333, rendering it functionally invisible when submerged.

Investigation of the literature regarding human vitrectomies, a necessary element of vitreoretinal surgery, revealed that ophthalmological surgeons frequently employ vital dyes to aid in visualization of the vitreous, such as brilliant blue or indocyanine green [34]. Although these dyes are carefully chosen to eliminate the possibility of long-term damage to the sensitive neural tissue of the retina, the requirements for my tissue isolation were less strict; I found that the use of 0.4% trypan blue (a common dye for visualizing cell viability) was suitable for this purpose after further dilution to improve transparency. Essentially, the dye mixes more readily with the aqueous dissection buffer than the vitreous, resulting in clear contrast at the surface of any residual vitreous. Routine successful removal of the vitreous further improved the success rate of the isolations, to the extent that the primary remaining cause of failed sample capture is human error during the final mechanical separation of the inner retinal layer.

A discussion of the role of humidity is completely absent in the original retinal ganglion cell protocols, although the method as written includes extended exposure of the sample to air, which would have the effect of drying the inner retina surface [31]. Furthermore, with regards to removal of the vitreous, the experimenter is directed to simply remove it from the flattened retina with blunt forceps, again while the sample is exposed to air. Attempts to use these simpler methods to control for sample moisture and remove the vitreous resulted in failure, however, when tested in the isolation of retinal astrocytes. I suspect the viability of this approach is largely a consequence of the aforementioned use of the ILM and astrocytes as a buffer, which is unsuitable when retinal astrocytes are the target of the isolation.

Although the success of the overall procedure is predicated on the success of sample adhesion, the retina itself must also be sufficiently dissociated. This dissociation is the result of exposure to collagenase, an enzyme that breaks down elements of the retinal extracellular matrix. The extent of this process can be controlled by altering the exposure of the ECM to collagenase – by modifying the enzymes concentration and, to a lesser extent, the volume used – as well as the duration of the incubation. However, both volume and duration interact in complex ways with the process of adhesion, as they influence the moisture content of the sample at the moment of mechanical separation, which is the key determinant of successful adhesion. Instead, adjustment of enzyme concentration proved to be the most direct method of altering dissociation in a predictable, reproducible way. A peculiarity of the approach is that the enzyme is applied - through filter paper - to the back of the retina, generating a concentration gradient that may in part explain why the astrocytes detach from the underlying tissue but not the inner limiting membrane, which lies furthest from the site of enzyme application. Increasing the concentration of enzyme can result in less adhesion of blood vessels and non-astrocyte retinal cells, while lower concentrations can increase the presence of vasculature but also yields a more complete astrocyte network. I use higher collagenase concentrations (~150 U/ml) for applications such as RNAseq in which tissue integrity is less important than minimizing the presence of non-astrocyte cells, while lower concentrations (~75 U/ml) are more suitable for isolating samples for immunofluorescence, which benefit from the context added by vasculature.

Detailed Method

Instruments

Spring scissors: Cohan Vannas (FST 15000-01) or Vannas-Tübingen (FST 15004-08)
Forceps: Angled, blunt or serrated (for holding tissue);
Curved, sharp (MC40B for vitreal removal, Almedic 7 for pull-off step)
#11 scalpel blades or ~25G needle (for globe puncture)
200mg weights
Dissection Microscope (preferably with backlit surface and overhead lamp)
10 ul pipette (for Trypan Blue and Collagenase)
200 ul pipette (for adding liquid for 'droplet' incubation)
1 ml pipette (for adding fixative)
Humidified incubator @ 37c

Consumables

35 mm dish for dissecting retina
.2 um aPES membrane (~14x14 mm, 1 per quarter [rat] or retina [mouse])
12 mm glass coverslips ('German glass', Bellco Glass 1943-10012A)
Filter paper (Bio-rad 'Mini Trans Blot' #1703932)
Transfer pipette, trimmed to ~1cm below bulb
Kimwipes

Reagents

PBS (w/o Mg/Cl) for dissection
HBSS for keeping enucleated eyes until dissection
75 - 150 U/ml Collagenase II (Worthington, Lakewood, NJ, USA)
HBSS for Collagenase II dilution

Pre-Prep:

1. Remove aPES filter from kit by removing plastic reservoir and cutting along inner rim of filter. Cut into 14 x 14 mm rectangular sections, 1 per sample. Pre-soak in room temperature water for 30 min – 2 hrs, while storing extra filter for later use.
2. Prepare blotting paper by cutting two 3 x 3 cm squares per sample, as well as putting aside an additional sheet for sample drying.
3. Label coverslips with orientation mark and numbering.
4. Thaw and dilute aliquot of collagenase II and use HBSS to make 75U/ml-150U/ml working solution. Optimal strength must be determined empirically for each lot and depends on downstream application for samples, but generally speaking a higher concentration leads to thinner samples, with lower concentrations producing thicker samples. The working solution can be kept at room temperature during the process.
5. Set aside 50ml of room temperature PBS (no Mg^{2+}/Cl^{2+}), use this for washing eyes and dissection dish. Cut a 2 x 1 cm strip of Kimwipe, then fold it in half and place in 35mm dissection dish. Add PBS until dish is nearly full.
6. Ensure incubator has water in pan and relative humidity is in the low 80s. This is more straightforward with a small benchtop model, but humidity in a large floor model can be reduced by opening the door for 10-15 seconds at a time, then waiting several minutes for changes to stabilize. Repeat as necessary.

Dissection:

1. Euthanize the animals according to protocol and enucleate with the curved forceps, taking special care not to puncture the globe. Chilling the eyes can make vitreous removal more difficult, but enucleated eyes should not sit for an extended period at room temperature. Therefore, samples should be processed one animal at a time. If isolating only treated eyes and there is just one per animal, two animals at a time can be used.
2. Place the eye in the 35mm dissection dish, using the Kimwipe to stabilize its location. Small blunt forceps – such as suture tying forceps – are also necessary, and should be used to hold extra-orbital muscles or the optic nerve. However, the optic nerve is fragile, and once grasped with forceps may tear if released.
3. Puncture the orb directly posterior to the ora seratta or limbus, using a #11 scalpel blade or a ~25G needle can be used. Use spring scissors to cut around circumference and remove anterior segment and lens with forceps.
4. **Vitrectomy**: This step is more complicated in rats; with mice the vitreous is often largely removed with the lens and only a small amount of additional cleanup is necessary. In rats, utilize 5-10ul of Trypan blue to visualize vitreous. Begin vitrectomy by tugging vitreous loose with forceps, if possible, from around the rim of the eye cup. Vitreous may come out as one solid lump, which is optimal; otherwise remove as much as possible, using repeat applications of Trypan blue to visualize remaining tissue.

5. Once vitreous is removed, use blunt forceps or probe to loosen retina from rest of eyecup. Try to loosen around the anterior rim before moving towards ONH to scoop out retina. Once the retina is detached except at ONH, use spring scissors to make cuts from edge of retina to ~1 mm from optic nerve head at 90 intervals. Once cuts are made, carefully, remove Kimwipe from dish before cutting or pinching the optic nerve behind the retina to detach. If using rats, the retina needs to be further quartered, with each quarter being handled separately; in this case one section should be processed at a time, with the other sections remaining attached at the optic nerve head to preserve orientation. In this case, use the modified transfer pipette to place the remaining retina in another dish with room temperature PBS to prevent drying.

Mounting Retinal Tissue & Incubation:

1. Place a 14 x 14 mm section of aPES filter matte (non-glossy) side up in the dissection dish, taking care to avoid adherence of the retina. Using blunt forceps, center the tissue as best as possible relative to the filter paper.
2. Remove liquid with a 1ml pipette until the retina/quarter lies flat on aPES with the RGC/NFL layer facing up and the photoreceptor layer facing down towards the paper. During this process you will most likely need to carefully unroll and flatten the edges of the retina, particularly if using whole mouse retina. Use blunt forceps or the probe to gently unroll the edges so the whole tissue remains flat, this may require a careful balance between removing enough liquid for the outer retina to begin to adhere to the filter, while leaving enough liquid to avoid tissue damage during handling (1-2mm). If the peripheral edge is ragged or otherwise of particular concern, you can add liquid back in to float tissue off the filter, then use spring scissors to cut .5-1mm to trim the edge.
3. Once liquid is removed and the retinal sample mounted, lift the filter (the retina should not move) and place on dry blotting paper. The blotting paper should be smooth(er) side up, and you may need to press edges of filter into blotting paper to improve drying, use the tips of gloved fingers rather than forceps to avoid warping the aPES. Inspect tissue for signs of residual vitreous – reflection of light from dissection scope should be slightly blurred, while a sharp reflection likely indicates residual vitreous that may result in failure to adhere cells to glass coverslip. However, do not let the sample itself dry excessively.
4. After drying aPES, use forceps to gently lower glass to form the stack, keeping tissue towards center.
5. With glass firmly attached, invert stack using forceps and place on 3x3 cm blotting paper piece. Glass should not pivot/rotate during this step. If it does, that means there was an excess of vitreous. Sometimes the sample can be rescued by removing the coverslip and replacing with a new one, as typically the excess vitreous comes off with the coverslip, but other times the sample cannot be salvaged. Successful removal of the vitreous essentially eliminates the risk of this issue.

6. **Applying Collagenase**: The amount of enzyme to be used will be dictated by the size and type of the samples and must be determined empirically. Typically, 6-7 ul per application is appropriate for whole mouse retina, while 5 ul is better suited for rat retinal quarters. Using the backlight to silhouette the retinal tissue, apply the collagenase II solution gently (1-2 ul/ second) to the glossy surface of the aPES directly over the tissue, covering it evenly. If stack is appropriately dry, absorption should be very rapid (<5-10 seconds). Then apply a second volume, using the same amount as before, which will absorb more slowly.
7. Once glossy surface is dry, gently add 200mg weight in center of tissue with forceps, and use filter paper to carry to incubator. Make note of incubator humidity, briefly venting if the humidity is too high (>85%), and place filter and stack either directly on incubator rack or on plastic rack. Leave in incubator for 22-25 minutes – a longer incubation can help thoroughly liberate the blood vessel / astrocyte matrix, but too long may damage the tissue. The precise humidity and duration will need to be determined empirically for given equipment and applications, but a relative humidity of > 85% risks non-adhesion of the sample, while a lower RH (<75%) will typically dry the sample excessively. However, when titrating humidity to ensure sample adherence it is more straightforward to begin with low humidity – essentially guaranteeing adhesion – and then begin working upwards until the optimal balance of adhesion and sample quality is reached.
8. While the initial sample is incubating, proceed to process the remaining tissue in the same manner. With whole retinas, there will be time to dissect the second eye and mount the retina, while a series of quarter retinas may prove challenging to process during this interval for new users.

Pull-off:

1. After tissue has incubated for appropriate duration, remove from incubator (taking note of the ending humidity). Transfer stack and filter to dissection microscope and gently remove weight. Invert stack (flip to glass side up) while avoiding pressure on glass or retina. Transfer to dry blotting paper and allow to sit for 1-2 minutes, briefly pressing down on filter (but not glass) to maximize contact with blotting paper and subsequent drying.
2. Transfer stack to new, dry 3 x 3 blotting paper. Begin tamping down filter with forceps, beginning at peripheral edge with. With whole retina, tamp at ~90° intervals, centered on each of the four lobes, before making additional presses at 30° intervals between the initial sites of pressure. With a quarter retina sample, press at peripheral edge, then midway along each of the two cut edges; afterwards, perform additional tamping as with the whole retina. This step serves to initiate the pull-off by separating the most peripheral 100-200um of adherent inner retina and glass from the bulk of the retina and filter paper, as well as improving sample adhesion by increasing drying. There should be

minimal to no visible moisture, ideally the glass should adopt a frosted appearance indicating adhesion of the thin layer.

3. Using a pair of curved, fine forceps, slide one tip between the coverslip and filter paper while holding the forceps horizontally. For whole retinas, slide the tip in several 1-2 mm past the edge of the glass, then rotate the underlying blotting paper while keeping the forceps steady. Slowly move the forceps closer to the sample while rotating, until the forceps are nearly at the edge of the sample. At this point, the adherent inner retina should be largely detached from the underlying tissue, and the coverslip can be carefully removed by hand for processing. For quarter retinas, instead loosen along the peripheral edge while moving closer to the sample, the adherent tissue should largely separate without the need for moving the forceps along the cut edges. As with the whole retina samples, once the edge of the sample is reached the coverslip should be gently removed by hand for processing.
4. As the sample will dry rapidly after separation, move quickly to add the required buffer for further processing. I treat the sample with 4% PFA for 10-15 minutes at room temperature for fixation prior to immunostaining, or with buffer RLT from Qiagen RNA isolation kits for downstream applications utilizing RNA. In both cases, 50 ul of liquid should be sufficient.

Notes: As discussed previously, residual vitreous and excess sample moisture are the two primary causes of failure. The moisture/humidity issue can prove particularly challenging, as changes in room temperature and relative humidity can disrupt previously optimized parameters. This issue can be corrected for by small adjustments to the volume of enzyme used for treatment, changes to incubation humidity, and/or increases in the post-incubation drying time before mechanical dissociation. Careful documentation of relative humidity in the incubator at the beginning and end of incubation is extremely helpful in catching these issues quickly and with a minimum of troubleshooting.

Results

Although the use of the pull-off technique to isolate retinal astrocytes is relatively sensitive to ambient factors such as temperature and humidity, when these are controlled for the method can produce highly reproducible results, suitable for both immunostaining and RNA-work. After developing a detailed protocol for the isolation of these cells from rat retinas, I was able – with minimal alteration – to modify the approach so that it performed similarly with tissue from mice.

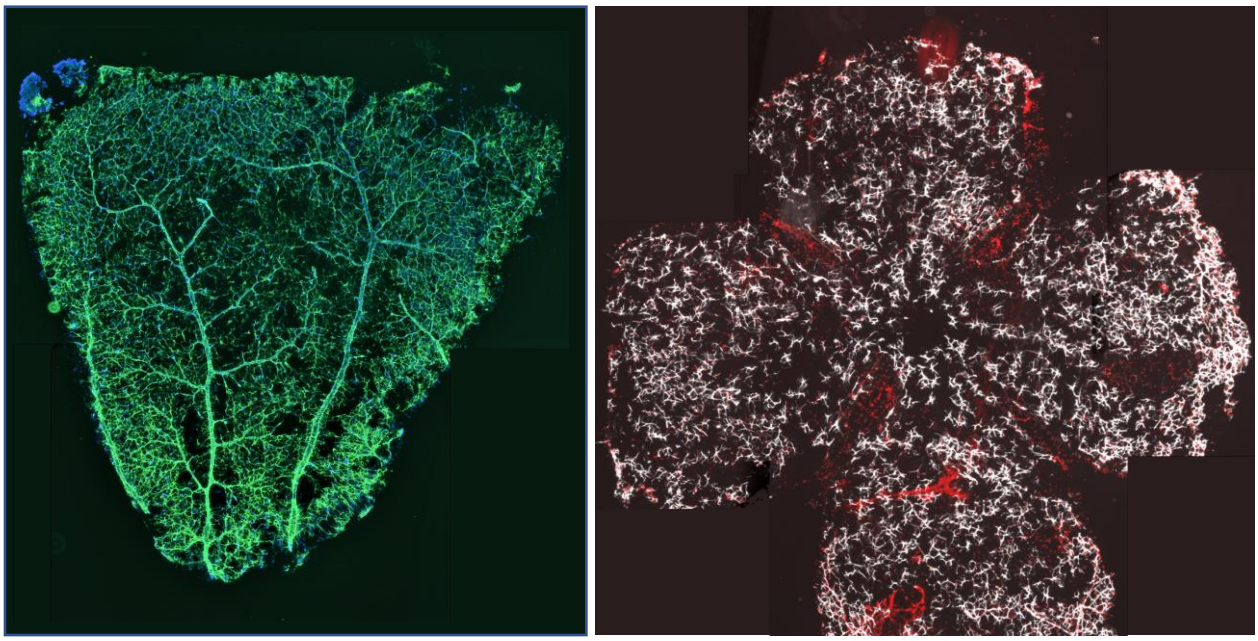

Figure 4: Composite images showing immunostained astrocytes isolated by the pull-off technique. Left: One section of a quartered rat retina, stained with GFAP (green) and Hoechst nuclear stain (blue). A lower concentration of collagenase was used, resulting in a thicker sample containing intact vasculature. Note the small area in the top left where separation from the rest of the retina was incomplete; this is representative of the density of non-astrocyte cells in the retina. Right: An isolation from a full mouse retina, with GFAP (white) and Hoechst nuclear stain (red). The absence of blood vessels is a function of the use of more highly concentrated collagenase.

While the retinas of mice and rats differ greatly in terms of surface area (~15mm^2 for mouse vs ~57mm^2 for rat), the individual quarter-sections processed for rat retinas are quite similar in area to the whole mouse retina, although a small amount of rat tissue (2-3mm$^{2)}$ is lost because the optic nerve head is excluded from the quartered samples [12, 35]. The overlapping incubation conditions for these species, with regards to time of incubation and concentration of collagenase, suggests that these parameters may be relatively constant across mammalian retinas of similar thickness. Conversely, the isolation of the marginally smaller quarter retinas from rats worked best with slightly lower volume ranges (5-6 ul vs 6-7 ul), suggesting that this parameter may be area dependent and require scaling for different sized tissue samples; anecdotally, I found this to be the case when adjusting for instances of partial tissue loss during the method development.

Although I have been unable to precisely quantify the percentage of the isolated cells that are astrocytes, owing to the dense clustering of remaining non-astrocytic nuclei (from the

vasculature and small pockets of deeper retinal layers that can occur), comparing even the thicker samples used for immunostaining with the density of retinal nuclei indicates a >99% reduction in non-astrocytic cells. My previous quantification of pulloff samples (n=9) showed my technique yielding a mean of 249/mm^2 retinal astrocytes at the mid periphery, suggesting that I am collecting nearly all of the retinal astrocytes in these regions and therefore enriching these cells in excess of 100-fold.

Thick Sections and Immunostaining

When lower concentrations of collagenase II are utilized (75 – 90 u/mL), retinal astrocytes and the superficial retinal vasculature retain their histological association, and can be isolated together with minimal disruption. This is particularly useful for immunostaining applications, as retinal astrocytes are polarized cells with functional differences in protein levels in distinct cell regions. For example, astrocytes are coupled to each other and to the retinal vasculature through gap junctions formed by Cx43, an association that was readily apparent in immunostaining of these tissue samples [36]. Furthermore, this confirmed the observation that the retinal astrocytes of mice and rats are predominantly associated with the vasculature, whereas reports from humans and other larger mammals suggest that some percentage of these cells associate exclusively with retinal ganglion cell axons [8].

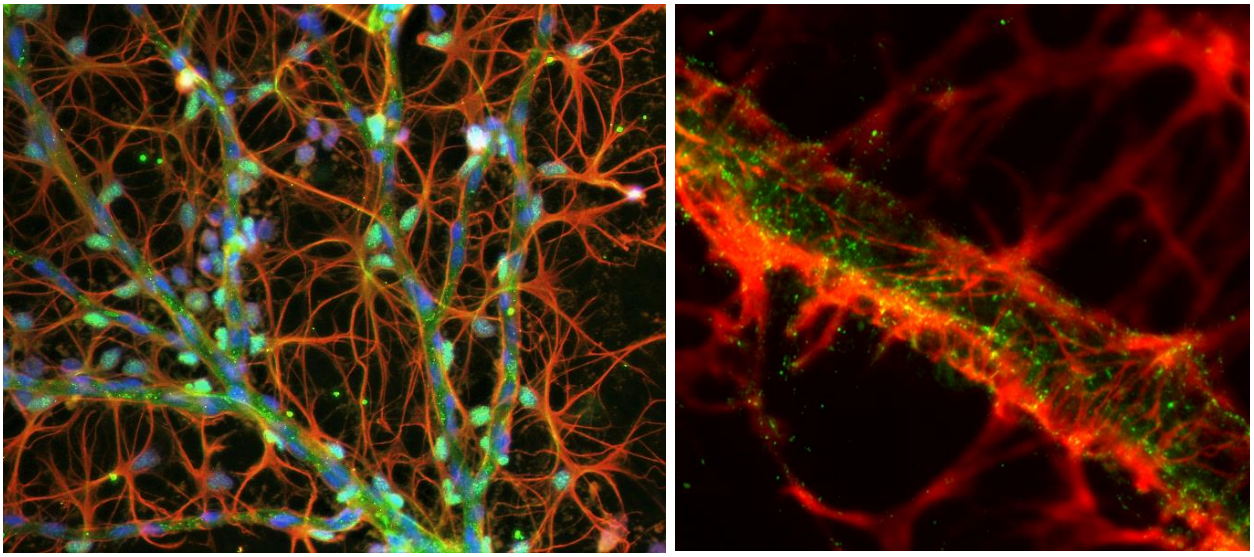

Figure 5: Left, Retinal astrocytes associating closely with the superficial vasculature (GFAP in red, Pax-2 in green, Hoecsht nuclear stain in blue). Right, Astrocyte end-feet (GFAP in red) ensheathing a retinal blood vessel, with punctate staining of gap junctions formed by Cx43 in green.

Although these sections are thicker than those isolated with higher collagenase concentrations, they are thin enough (<20um) that they can be imaged with parameters and equipment suitable for thin histological sections or cultured cells, yet due to the enzymatic nature of the dissociation they retain structural connectivity that would be lost in sectioned tissue. However, the large number of endothelial cells associated with the retinal vasculature means that these

thick samples are less suitable for applications such as RNA-sequencing, in which contributions from other cell types are to be minimized.

Thin Sections and RNA Isolation

Relative to isolations performed with lower levels of collagenase, those performed with 125-150 U/ml produced thinner samples (estimated ~10um thick), typically without adherent vasculature. Although these samples are less well suited for the repeated washes necessary for immunostaining, they are thin enough for phase contrast microscopy immediately after fixation without staining. In these images, as many as 1/3 of all cells are identifiable as astrocytes, although some of the nuclei without recognizable cell bodies may be from astrocytes as well.

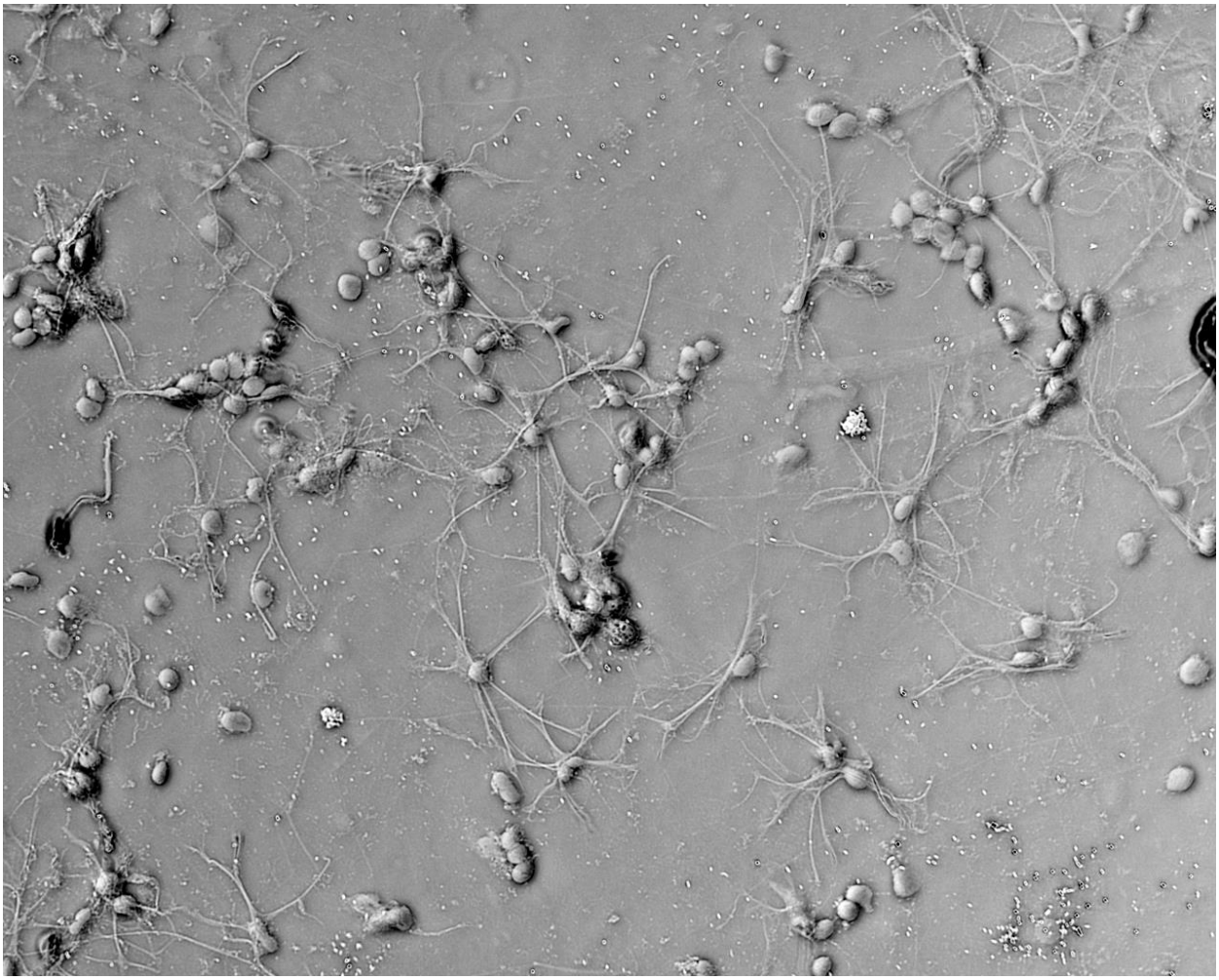

Figure 6: Retinal astrocytes from a 'thin' sample, imaged in brightfield immediately after fixation.

Although samples isolated under these conditions were more fragile, the reduction in adherent blood vessels and other non-astrocyte cells makes them more suitable for RNA-sequencing and other quantitative bulk tissue applications. Despite the relatively small number of cells isolated

in these thin samples, which I estimate to be 10,000 or less, 50ng or more RNA can be isolated from each sample by using a micro scale RNA isolation kit such as the Qiagen RNeasy Micro Kit. Purification of RNA yielded high quality samples with RNA integrity scores ranging from 8.6-9.4 (n=8) as measured via Bioanalyzer 2100. Pooling 3-4 samples per replicate was sufficient for cDNA library generation and downstream sequencing applications, which are discussed at length in Chapter III.

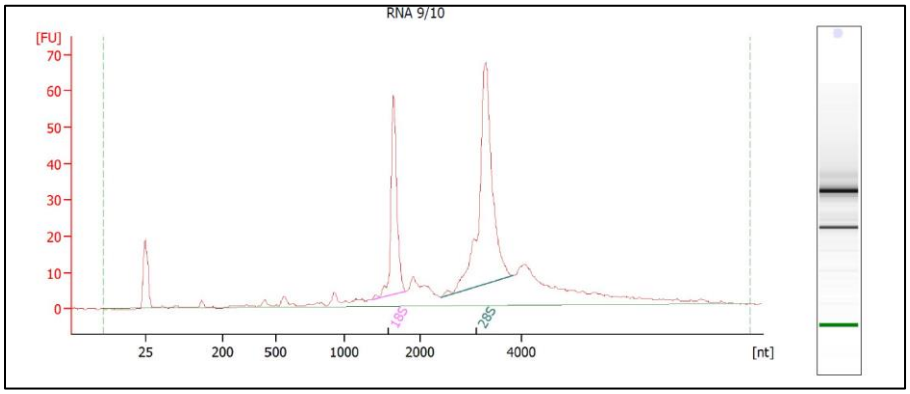

Figure 7: Bioanalyzer trace, showing high RNA integrity. The peaks labeled 18S and 28S represent intact ribosomal RNA, while the unlabeled smaller peak at 25 nt represents degraded RNA. The relative sizes shown here indicate a sample with an RNA integrity number of 9.4, considered very high quality for a tissue sample.

Discussion

Here I have demonstrated the development and application of a technique for isolating enriched populations of retinal astrocytes, a sparse and spatially restricted population of cells unique to the mammalian retina and essential for the development and function of retinal vasculature. As currently developed, this technique produces enrichment of two orders of magnitude or greater, and is suitable for common immunostaining and molecular biology applications. Although this technique does not yield a pure population of retinal astrocytes, it possesses three key benefits over fluorescence-assisted cell sorting (FACS), which is to my knowledge, the only extant method by which pure or nearly pure populations of these cells could be isolated. The first of these is the relatively brief post-mortem interval; FACS-based sorting of sparse cells from solid tissue can take 2 hours or more following an hour-long dissection and dissociation process. However, this entire technique takes less than one hour from live animal to fixed cells or isolated RNA, thus reducing transcriptional changes that can be triggered by cell isolation and confound downstream experiments.

The second benefit is that this technique can function in non-mouse models. The ubiquity of transgenic mouse strains and antibodies validated for mice enables relatively advanced cell-sorting strategies; however, these tools frequently do not exist, even for closely related models such as rats. While mice are frequently used as a model of human eye disease such as glaucoma, factors such as the small size of their eyes mean that results from these studies typically have to be replicated on the eyes of larger mammals such as pigs and non-human primates. Although I have not attempted the application of this technique to larger eyes, the straightforward principles involved and its adaptability suggest that simply cutting a small section from a larger retina may allow for retinal astrocyte isolation from other species, such as non-human primates or human donor tissue.

Finally, the cell sorters required for FACS-based isolation are prohibitively expensive for all but the largest or most specialized labs, necessitating reliance on a core facility and the accumulation of associated usage costs. In contrast, this isolation technique utilizes similar dissection tools and reagents to those necessary for pre-FACS dissociation, with the only additional required supplies being specialized filter paper and microscopy coverslips. These factors not only make it a highly economical method of astrocyte isolation, but one that is technically relatively straight forward.

In addition to the applications I have described and validated above, I have had some success with utilizing these samples for lipidomic analysis by mass-spectrometry, and there are some indications that these cells are culturable (data not shown). However, live-cell functional applications such as these are highly sensitive to even moderate over-drying, which in contrast has not impacted the immunostaining and RNA-based assays. Although I suspect the isolation of culturable astrocytes via this technique – which would represent a major improvement on current approaches to culture astrocytes – is feasible, the factors that would make these isolations reproducible and routine have yet to been identified. Regardless, the straightforward

nature of the technique and its utility for common research applications have already shown the value of its development, and bode well for the potential of future modifications to broaden the approach's applicability for additional research purposes.

References

1. Barres, B.A., et al., *Immunological, Morphological, and Electrophysiological Variation among Retinal Ganglion-Cells Purified by Panning.* Neuron, 1988. **1**(9): p. 791-803.
2. Holt, L.M. and M.L. Olsen, *Novel Applications of Magnetic Cell Sorting to Analyze Cell-Type Specific Gene and Protein Expression in the Central Nervous System.* PloS one, 2016. **11**(2): p. e0150290-e0150290.
3. Yang, Y., et al., *Molecular comparison of GLT1+ and ALDH1L1+ astrocytes in vivo in astroglial reporter mice.* Glia, 2011. **59**(2): p. 200-7.
4. McCarthy, K.D. and J. de Vellis, *Preparation of separate astroglial and oligodendroglial cell cultures from rat cerebral tissue.* J Cell Biol, 1980. **85**(3): p. 890-902.
5. Choi, H.J., R. Wang, and T.C. Jakobs, *Single-Cell Dissociation and Characterization in the Murine Retina and Optic Nerve*, in *Glaucoma: Methods and Protocols*, T.C. Jakobs, Editor. 2018, Springer New York: New York, NY. p. 311-334.
6. Burbach, G.J., et al., *Laser microdissection of immunolabeled astrocytes allows quantification of astrocytic gene expression.* J Neurosci Methods, 2004. **138**(1-2): p. 141-8.
7. Avila Cobos, F., et al., *Computational deconvolution of transcriptomics data from mixed cell populations.* Bioinformatics, 2018. **34**(11): p. 1969-1979.
8. Vecino, E., et al., *Glia-neuron interactions in the mammalian retina.* Prog Retin Eye Res, 2016. **51**: p. 1-40.
9. Selvam, S., T. Kumar, and M. Fruttiger, *Retinal vasculature development in health and disease.* Prog Retin Eye Res, 2018. **63**: p. 1-19.
10. Ogden, T.E., *Nerve fiber layer astrocytes of the primate retina: morphology, distribution, and density.* Invest Ophthalmol Vis Sci, 1978. **17**(6): p. 499-510.
11. Wang, J., et al., *Anatomy and spatial organization of Muller glia in mouse retina.* J Comp Neurol, 2017. **525**(8): p. 1759-1777.
12. Jeon, C.J., E. Strettoi, and R.H. Masland, *The major cell populations of the mouse retina.* J Neurosci, 1998. **18**(21): p. 8936-46.
13. Punal, V.M., et al., *Large-scale death of retinal astrocytes during normal development is non-apoptotic and implemented by microglia.* PLoS Biol, 2019. **17**(10): p. e3000492.
14. Nahirnyj, A., et al., *ROS detoxification and proinflammatory cytokines are linked by p38 MAPK signaling in a model of mature astrocyte activation.* PLoS One, 2013. **8**(12): p. e83049.
15. Lukas, T.J. and A.L. Wang, *Isolation and Culture of Astrocytes from the Retina and Optic Nerve*, in *Astrocytes: Methods and Protocols*, R. Milner, Editor. 2012, Humana Press: Totowa, NJ. p. 105-115.
16. Foo, L.C., et al., *Development of a method for the purification and culture of rodent astrocytes.* Neuron, 2011. **71**(5): p. 799-811.
17. Wolfes, A.C., et al., *A novel method for culturing stellate astrocytes reveals spatially distinct Ca2+ signaling and vesicle recycling in astrocytic processes.* J Gen Physiol, 2017. **149**(1): p. 149-170.
18. Mudhar, H.S., et al., *PDGF and its receptors in the developing rodent retina and optic nerve.* Development, 1993. **118**(2): p. 539-52.
19. Uemura, A., et al., *Tlx acts as a proangiogenic switch by regulating extracellular assembly of fibronectin matrices in retinal astrocytes.* J Clin Invest, 2006. **116**(2): p. 369-77.
20. Tao, C. and X. Zhang, *Retinal Proteoglycans Act as Cellular Receptors for Basement Membrane Assembly to Control Astrocyte Migration and Angiogenesis.* Cell Rep, 2016. **17**(7): p. 1832-1844.
21. Duan, L.J., et al., *Retinal Angiogenesis Regulates Astrocytic Differentiation in Neonatal Mouse Retinas by Oxygen Dependent Mechanisms.* Sci Rep, 2017. **7**(1): p. 17608.

22. Clarke, L.E., et al., *Normal aging induces A1-like astrocyte reactivity.* Proc Natl Acad Sci U S A, 2018. **115**(8): p. E1896-E1905.
23. Boisvert, M.M., et al., *The Aging Astrocyte Transcriptome from Multiple Regions of the Mouse Brain.* Cell Rep, 2018. **22**(1): p. 269-285.
24. Wang, Z., M. Gerstein, and M. Snyder, *RNA-Seq: a revolutionary tool for transcriptomics.* Nat Rev Genet, 2009. **10**(1): p. 57-63.
25. Tang, F., et al., *mRNA-Seq whole-transcriptome analysis of a single cell.* Nat Methods, 2009. **6**(5): p. 377-82.
26. Muller, S., et al., *Single-cell profiling of human gliomas reveals macrophage ontogeny as a basis for regional differences in macrophage activation in the tumor microenvironment.* Genome Biol, 2017. **18**(1): p. 234.
27. Haque, A., et al., *A practical guide to single-cell RNA-sequencing for biomedical research and clinical applications.* Genome Med, 2017. **9**(1): p. 75.
28. Lukowski, S.W., et al., *A single-cell transcriptome atlas of the adult human retina.* EMBO J, 2019. **38**(18): p. e100811.
29. Chen, G., B. Ning, and T. Shi, *Single-Cell RNA-Seq Technologies and Related Computational Data Analysis.* Front Genet, 2019. **10**: p. 317.
30. Pan, J. and J. Wan, *Methodological comparison of FACS and MACS isolation of enriched microglia and astrocytes from mouse brain.* J Immunol Methods, 2020. **486**: p. 112834.
31. Simon, P. and S. Thanos, *Combined methods of retrograde staining, layer-separation and viscoelastic cell stabilization to isolate retinal ganglion cells in adult rats.* J Neurosci Methods, 1998. **83**(2): p. 113-24.
32. Shiosaka, S., H. Kiyama, and M. Tohyama, *A simple method for the separation of retinal sublayers from the entire retina with special reference to application for cell culture.* J Neurosci Methods, 1984. **10**(3): p. 229-35.
33. Boulay, A.C., et al., *Translation in astrocyte distal processes sets molecular heterogeneity at the gliovascular interface.* Cell Discov, 2017. **3**: p. 17005.
34. Rodrigues, E.B., et al., *The use of vital dyes in ocular surgery.* Surv Ophthalmol, 2009. **54**(5): p. 576-617.
35. Danias, J., et al., *Cytoarchitecture of the Retinal Ganglion Cells in the Rat.* Investigative Ophthalmology & Visual Science, 2002. **43**(3): p. 587-594.
36. Danesh-Meyer, H.V., et al., *Connexin43 in retinal injury and disease.* Prog Retin Eye Res, 2016. **51**: p. 41-68.

Chapter III

Transcriptomic and Immunohistochemical Analysis of Retinal Astrocytes in an Acute *in vivo* Model of Ocular Hypertension

Introduction

Glaucoma, a neuropathology of the retina characterized by degeneration and death of retinal ganglion cells and accompanying loss of visual field, is a major neurodegenerative disorder and the leading cause of irreversible blindness worldwide, affecting an estimated 76 million individuals [1, 2]. Although several categories of glaucoma exist and possess distinct etiologies, the most prevalent type is Primary Open Angle Glaucoma (POAG), with aging and raised intraocular pressure acting as major risk factors [3]. Current treatments are often effective at slowing disease progression, but they are not universally effective; moreover, no current therapies are able to replace the lost neurons or restore the compromised visual function [4, 5].

While the precise mechanisms driving POAG remain poorly understood, decades of research implicate the optic nerve head – where the axons of retinal ganglion cells exit the retina – as an early site of damage to these cells [3, 6-9]. Both at the optic nerve head and in the retinal nerve fiber layer, the axons of RGCs are supported by cells that emerge from the optic nerve during development and form a unique population – retinal astrocytes – found only in mammals [10, 11]. These astrocytes are part of a broader class of support cells – glia – found throughout the central nervous system, where they are responsible for both the maintenance of homeostasis under physiological conditions and response to neurological insult. Astrocytes in particular protect neurons from sudden fluxes of ions and neurotoxic transmitters, mediate the flow of blood and oxygen to regions of high neuronal activity, and contribute to the responses to both physical injury and pathogen infiltration of the central nervous system [12-14]. Evidence from animal models of glaucoma, as well as human tissue isolated from glaucomatous eyes, suggests a role for these cells in disease progression, but the net balance of their positive and negative contributions to neuroprotection remains unknown [15-18].

Of the various factors impeding a greater understanding of the role of retinal and optic nerve head astrocytes, perhaps the most significant is the relative sparseness of these cells. Of an estimated > 6.5 million neurons and glia in the retina of an adult mouse, previous studies and our own results suggest that 6,000 or fewer are retinal astrocytes, indicating that these cells represent less than 0.1% of the retina [19, 20]. Various methods, such as cell culture and fluorescence-activated cell sorting (FACS), have been employed to purify populations of retinal astrocytes for study; however, the former induces a loss of *in vivo* characteristics due to the long culture time required, while the latter is not well suited for the separation of astrocytes from the more abundant Müller glia of the retina [21]. More recently, single cell RNA-sequencing of retinas has shed some light on the behavior of these astrocytes, yet these studies are quite expensive and provide limited data from such rare cell types [22].

In order to circumvent the limitations of existing techniques and facilitate the study of transcriptional changes undergone by retinal astrocytes in response to *in vivo* models, we have developed a novel approach to rapidly isolate astrocytes from the retinas of mice and rats. Unlike existing methods, our approach utilizes the localization of these astrocytes to the inner surface of the retina, and by isolating these cells via a mix of enzymatic and biomechanical dissociation that causes minimal disruption of their structural integrity, we are able to confirm their astrocyte identity on the basis of their highly characteristic morphology. Our isolation method is rapid – with a post-mortem interval of less than an hour – and inexpensive, requiring little in the way of specialized equipment beyond a lab incubator and surgical tools. The primary drawback of our approach is that it enriches, rather than purifies, retinal astrocytes; however, by enriching these cells by 2-3 orders of magnitude (and, in particular, removing the more abundant Müller glia), it renders feasible the bio-informatic isolation of astrocytic gene expression changes from the bulk transcriptomic data. Furthermore, the technique is highly suited for the immunohistochemical study of isolated astrocytes, which can in many cases be directly identified even in brightfield microscopy due to the thinness of the tissue layer isolated and the retention of *in vivo* morphology.

Here we utilize this method to study, both by RNA-sequencing and immunohistochemistry, the changes undergone by retinal astrocytes in response to an *in vivo* model of ocular hypertension, which mimics some of the changes induced by glaucoma via elevated intraocular pressure (IOP). This model employs laser-induced photocoagulation in the episcleral veins, leading to a rise in IOP and an accompanying loss of retinal ganglion cells that is detectable within one week of treatment [23]. This rise in IOP is accompanied by an induction of reactivity in retinal astrocytes, which were then isolated for transcriptional study. As the risk of altered function in contralateral eyes have been previously demonstrated, our controls instead consisted of untreated eyes from age-, sex-, and strain-matched animals [24, 25] .

In order to assess the aggregate response of retinal astrocytes in our bulk transcriptomics data, we employ a panel of markers widely used to examine the reactivity of astrocytes in the brain. Furthermore, we exploit the spatially restricted nature of our isolated samples to examine the role of other cell types that may be involved in RGC neurodegeneration/neuroprotection – such as microglia/macrophages – on the basis of their presence at the vitreal surface of the retina. Finally, we utilize immunohistochemistry to confirm the expression of proteins corresponding to a number of genes of interest, derived from our top-10 differentially expressed genes (by adj p-value), the astrocyte markers published by Barres et al., and genes associated with human neurodegenerative disorders such as glaucoma and Alzheimer's disease and their associated animal models [26-29]. By establishing a clearer picture of the response of retinal astrocytes to conditions that result in the loss of retinal ganglion cells, we hope to identify additional targets for neuroprotection in glaucoma and other debilitating neurodegenerative diseases.

Materials & Methods

Animal care and laser photocoagulation

All animals used in this study were treated in accordance with the ARVO statement for the use of animals in ophthalmic and vision research, and all procedures utilized were approved by the Animal Care and Use Committee of the University of California, Berkeley. Male C57BL/6J mice between 9 and 12 weeks of age were purchased from Jackson Laboratories (Bar Harbor, Maine, USA) and allowed to acclimate for one week to the housing facility prior to treatment. Animals were kept on a 12h/12h cycle of light and darkness, and at all times before and after treatment food and water were freely available. After acclimation, laser-based photocoagulation to cauterize episcleral veins was performed as previously described [23].

Briefly, male C57BL/6J mice between 10 and 13 weeks of age were anesthetized with a mixture of 100mg/kg ketamine and 10mg/kg xylazine via intraperitoneal injection; stable body temperature was maintained during the procedure via a veterinary heating pad and topical treatment with the anesthetic proparacaine hydrochloride (0.5%, Akorn, Lake Forest, Il) was applied to the right eye prior to treatment. The right eye then was treated with a 532 nm OcuLight Tx laser (Iridex Corporation, Mountain View, Ca), undergoing 120-130 spot treatments at 80mW (0.5s each) to achieve photocoagulation of the episcleral veins. Afterwards, antibiotic ointment (Ak-Poly-Bac, Akorn, Lake Forest, IL) was applied to the treated eye to aid in recovery. Controls consisted of eyes from untreated, age, strain, and sex matched animals.

Assessing of model efficacy in C57BL/6J mice and IOP exclusion criteria

Although we have previously utilized this model, a small pilot group was used to verify parameters, as the previous work occurred in mice of a different strain. IOP measurements were taken immediately after laser photocoagulation treatment, and then daily under light anesthesia (2% isoflurane) with non-invasive Tonolab tonometer (Icare Lab, Helsinki, Finland). Animals that did not reach 30mm Hg following treatment were excluded from the study. After one week, animals were euthanized, and both the treated right eye and untreated left eye were enucleated and fixed in 4% paraformaldehyde. The eye was then rinsed with PBS, and the retina dissected and flat mounted. Goat-derived anti-Brn3a primary antibody (Santa Cruz Biotechnology, Santa Cruz, CA) was used to target surviving retinal ganglion cells, while AlexaFluor donkey anti-goat IgG (Jackson ImmunoResearch Laboratories, West Grove, PA) was used for visualization. Statistical analysis of RGC density and IOP changes was assessed via Prism software (GraphPad, La Jolla, CA, USA) using un-paired Student's t-test. IOP readings at day 1 post-treatment were found to be predictive of outcome after 1 week, and so tonometry readings for animals in study experiments were conducted only at this time point, with animals that did not reach 30mm Hg being excluded.

Astrocyte isolation

Astrocyte isolation was performed using pull-off method described in detail in Chapter II. Briefly, after euthanasia and enucleation, the anterior segment of the eye is removed and the retina is dissected out, with relieving cuts made at 90° intervals to allow the tissue to be

flattened. The retina is then flattened on a porous membrane with the vitreal side up, and an uncoated glass coverslip is placed atop to create a glass-retina-membrane stack. This stack is then inverted, type II collagenase (Worthington, Lakewood NJ, USA) is applied to the membrane, and a small weight is added to ensure the retina is pressed against the glass. The retinal stack is then incubated at 37°c in a humidified incubator for ~22-25 minutes, followed by removal of the weight and inversion and brief drying of the sample. The glass coverslip is gently pulled off, with astrocytes and elements of the superficial retina adherent. Samples were immediately treated with buffer RLT (Qiagen, Hilden, Germany) for RNA-isolation, or 4% paraformaldehyde for fixation and immunostaining. Individual samples were excluded if <50% of retinal surface area was successfully isolated, and pooled groups were excluded if less than 3 samples were included. N=4 pooled samples / replicates were generated for both the control and treatment groups.

RNA-isolation, cDNA library generation, and RNA sequencing

After adding buffer RLT to individual samples, these were allowed to incubate for approximately 1 minute, then stored on ice for pooling. 3-5 samples were combined, followed by vortexing at maximum speed for 30 seconds. RNA was then isolated from pooled samples per manufacturer's directions using the Qiagen RNeasy Micro Kit (Qiagen, Hilden, Germany) by following protocol for purification of total RNA from microdissected cryosections. RNA quantification was performed via nanodrop, and samples were stored at -80° C. After isolation of all samples, samples were checked for quality via Bioanalyzer 2100. cDNA libraries were generated via KAPA mRNA hyper prep kit (Roche Sequencing and Life Science, Indianapolis, IN, USA) according to manufacturer's instructions. RNA sequencing was performed on a single lane using the NovaSeq 6000, and reads were aligned to the *Mus musculus* reference assembly (GRCm38-mm10).

Bioinformatic analysis

Reads were aligned to the Mus musculus reference genome assembly GRCm38 (mm10) using Spliced Transcripts Alignment to a Reference (STAR) aligner (version 2.7.1a). Count data was analyzed with Hypergeometric Optimization of Motif EnRichment (HOMER) software (version 4.10.4 ; http://homer.ucsd.edu/homer/ngs/index.html) which uses the R package DESeq2 (version 1.22.2) to perform differential gene expression analysis. Genes were filtered by adjusted p value (adjusted $p < 0.05$) and log2-fold change in expression (greater than 1.0 for upregulated and less than -1.0 for downregulated genes). Lists of differentially expressed genes were input into Metascape to determine enriched biological themes within the gene lists.

Cryosectioning & Immunostaining

After enucleation, eyes were fixed in 4% PFA for 10 minutes at 4°C. A 25G needle was then used to puncture the orb at the limbus, and eyes were fixed for an additional 40 minutes. Fixative was removed by wash with PBS, and eyes were sequentially equilibrated in 10% and 30% sucrose for cryoprotection before flash-freezing with -78°C isopentane to embed in optimal temperature compound. Eyes were sectioned and sections were then post-fixed with 4% PFA at room temperature for 10 minutes, then rinsed in PBS before blocking and permeabilization for

1 hour at room temperature in 0.1% PBS-Triton X-100 with 10% donkey serum. Both sections and pull-off samples were then stained overnight with primary antibodies in 0.1% PBS-Triton X-100 with 3% donkey serum (see Appendix A for table of antibodies and concentrations). Stained sections were rinsed three times with PBS, then incubated for 1 hour with 1:250 of appropriate secondary antibodies in 0.1% PBS-Triton X-100 with 3% donkey serum. After additional PBS rinses to remove secondary antibodies, nuclear counterstaining was performed with 1µg/ml Hoechst stain for 20 minutes before a final PBS wash. Images were captured with a Nikon Eclipse-Ti confocal microscope.

Results

Characterizing the model

Although our group has previously utilized this model of laser-based episcleral vein cauterization to induce elevated intraocular pressure and the death of retinal ganglion cells, we nonetheless ran a preliminary batch of 4 mice to confirm that previously employed parameters were valid on our chosen mice (10 - 14-week-old male C57Bl/6J) [23, 30]. Four animals received laser treatment in their right eye, with the left eye acting as a contralateral control, and subsequent tonometry indicated that all animals surpassed the threshold for inclusion one day after treatment (IOP > 30mm Hg). Pressure measurements continued daily for 1 week, with IOP returning to baseline 6-7 days after treatment.

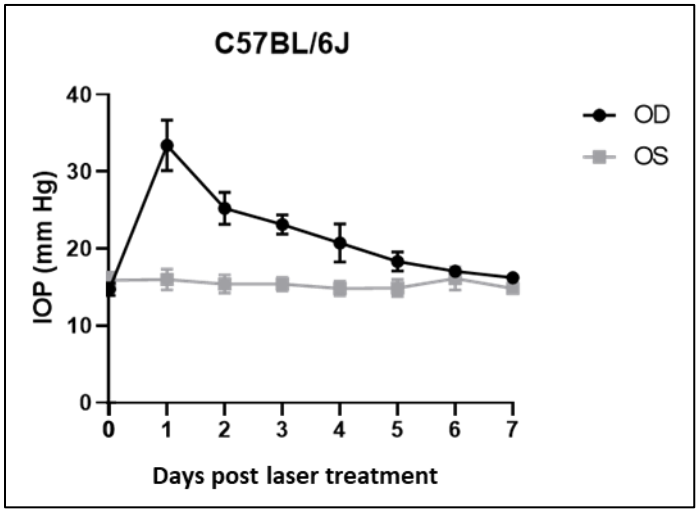

Figure 1: IOP measurements from treated (OD) and untreated fellow (OS) eyes for the C57BL/6J pilot. Plotted figures represent the mean values of all eyes within replicate.

After 1 week, animals were euthanized and their eyes extracted; of these, 3 treated eyes were used for assessment of retinal ganglion cell loss via BRN3A immunostaining with untreated contralateral eyes serving as controls, while the 4th treated eye was used to confirm the feasibility of performing the *pull-off* method on a treated retina. Counting of BRN3A positive cells in treated and control eyes confirmed a loss of approximately 20% of RGCs in the treated retina.

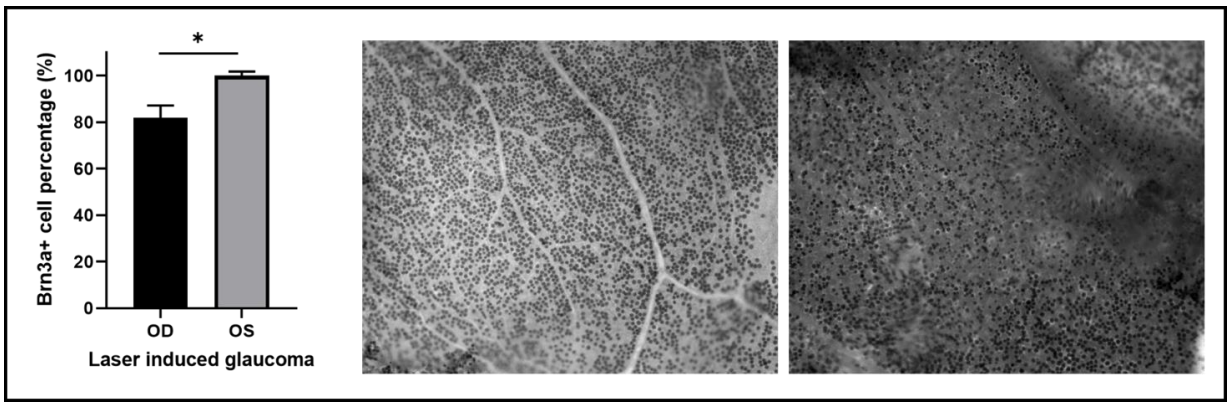

Figure 2: Left: Chart showing statistically significant (p-value <.05) decrease in Brn3a+ RGCs in treated (OD) versus control (OS) one week after treatment. Center: Untreated eye, intact RGCs stained via retrograde transport of trypan blue from cut at optic nerve. Right: Treated eye, showing reduced transport due axonal damage and loss of RGCs.

Subject Inclusion Rate and Sample Acquisition Results

Based on previous studies by our group and the results from the pilot, we established an inclusion threshold of IOP > 30mm Hg on the day after treatment [23, 30]. Of a total of 23 animals treated in 4 groups, 17 remained above 30 mm Hg one day after treatment and were included, for an inclusion rate of approximately ~74%; none of the treatment groups produced less than 4 included animals. Control eyes were obtained from untreated, age-, sex-, and strain-matched animals, with 4 eyes used per control replicate. During tissue isolation, the first control group and 3rd treatment group produced unsatisfactory yields, and these samples were marked for exclusion. After purification of RNA, measurement of sample concentration via nanodrop indicated that RNA yield ranged from 200-400ng per pooled group, suggesting a yield of 50-100ng per tissue sample. RNA integrity numbers were generated for each of the pooled samples, and ranged from 8.6 – 9.4, indicating high quality samples.

Initial Results from RNA-seq

Large scale gene expression changes in response to treatment

After adjusting p-values to account for testing multiple hypotheses in parallel and applying a log2-fold change threshold of > 1 for upregulated genes (*i.e.*, 2-fold upregulated) and < -1 for downregulated genes (>50% downregulated), 1173 genes demonstrated statistically significant (adj p-value < 0.05) differential expression in treatment tissue relative to control. Of these, the bulk – 1129 genes (96.2%) – were upregulated, while a smaller number – 44 (3.8%) displayed downregulation.

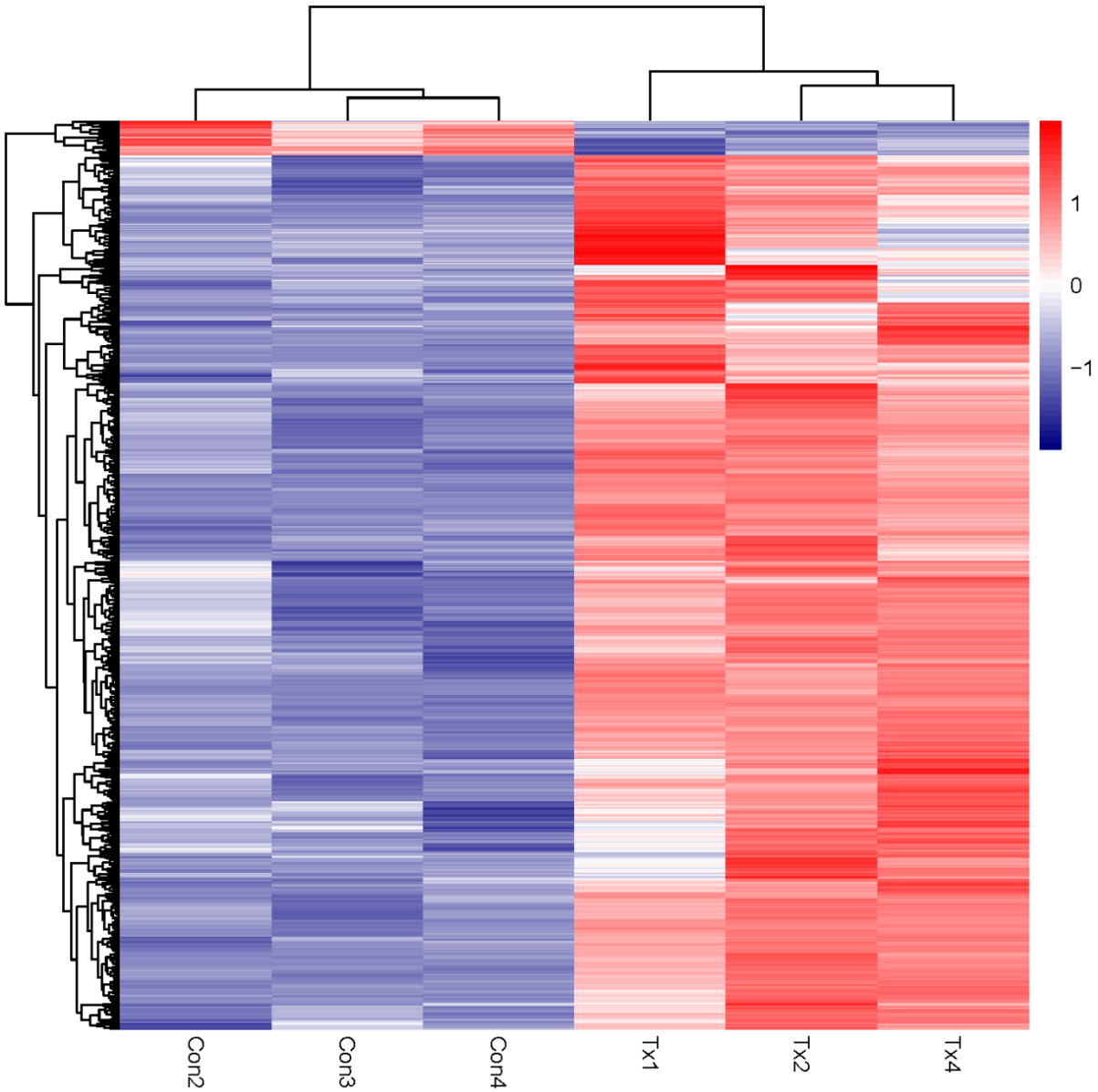

Figure 3: Heatmap of Z-scores for gene expression changes of upregulated and downregulated genes exceeding log2-fold>1 expression change with adj p-value < 0.05.

Assessing Variance between and within Laser Treated OHT Eyes and Controls

Measures were taken to reduce variability during the molecular biology elements of our experiment, such as having library prep and sequencing performed in a single batch to minimize technical variation. However, the use of an *in vivo* model and the sensitive nature of our tissue isolation created opportunities for external factors to influence our experimental outcomes. As discussed previously, the samples from a given control or treatment cohort were pooled at the outset of the RNA isolation, allowing the partial offset of variation between samples without increasing the amount of sequencing required. The transcriptomic data were assessed to ensure that that the variance between pooled samples was primarily driven by gene expression differences between treatment and control. Our principal component analysis indicates that 81% of the variance between samples can be attributed to the differential expression of genes in treatment vs control samples.

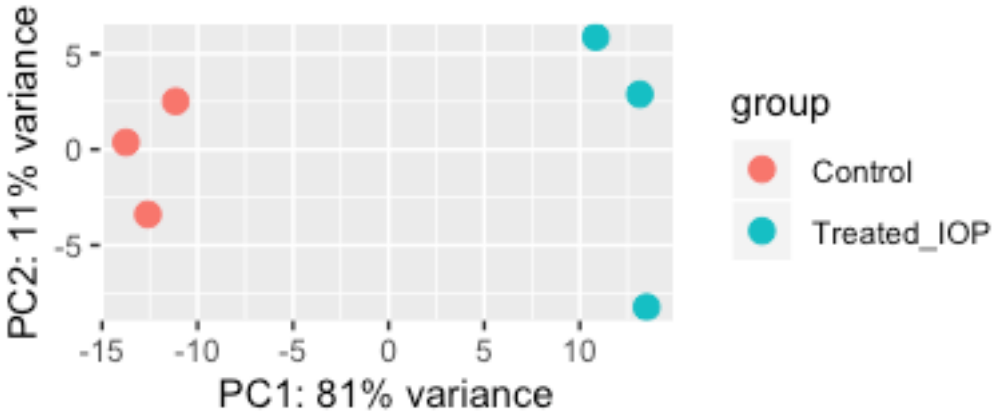

Figure 4: Principal component analysis of variance within and between cohorts.

However, I also had concerns that the treatment itself might influence our transcription data through not only the desired induction of differential gene expression, but also by altering the tissue's physical properties, such that the cellular composition of the samples might differ between treatment and control. Specifically, I wanted to measure changes in markers of cell type that were expected to be insensitive to the treatment, to confirm that gene expression changes were a function of altered cellular behavior, rather than an increase or decrease in a given cell population caused by a change in sensitivity to my isolation methods as a result of the treatment.

Primarily, I was concerned about changing ratios of astrocytes, neurons, Müller glia, and endothelial cells. For markers of retinal astrocytes, I utilized Pax-2 and Pdgfra, which are among a small number of genes known to be expressed in the retina by astrocytes alone, and to our knowledge are insensitive to the induction of reactivity. Conversely, Pax-6 is a marker of all endogenous cells of the neuroretina – including both neurons and Müller cells – while

Cd29/Itgb1 has been proposed as a marker specific to Müller cells in the retina. To detect neurons – primarily retinal ganglion cells – I utilized the neuronal marker NeuN, as well was Rbpms and Brn3a, which are frequently used for RGC staining. Finally, Pecam-1/CD31 is a marker of the endothelial cells that comprise the vasculature.

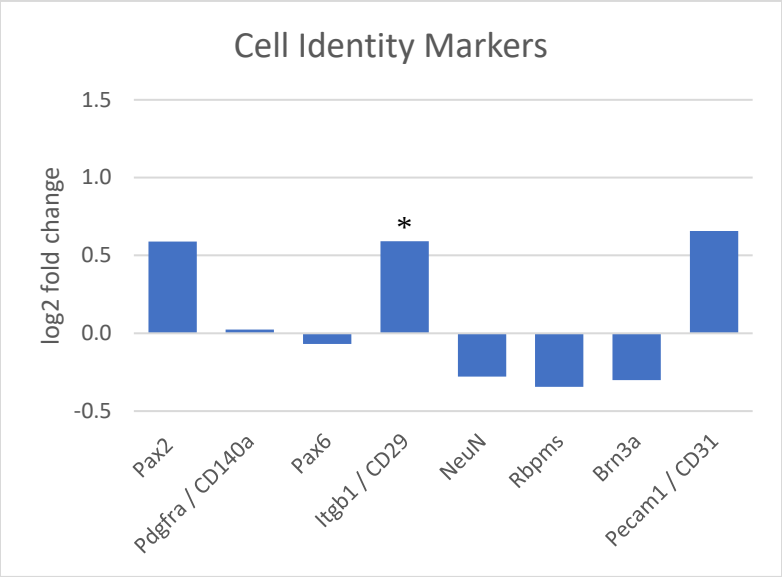

Figure 5: Log2-fold change of markers of cell identity in treated samples relative to controls, (*) indicates statistical significance (adj p-value <.05). Only the Müller cell marker CD29 displayed significant upregulation, but the degree of upregulation was still below the log2-fold threshold of 1.

Of the expression changes in these genes, only that of the Müller cell marker CD29 achieved statistical significance (adjusted p-value <0.005); however, the expression change – an increase of roughly 50% – is below threshold for differential gene expression and roughly comparable to changes in the astrocytic marker Pax2 and endothelial cell marker CD31. Conversely, neuronal/RGC markers showed a consistent decrease of approximately 20%. In comparison, a total of 1129 genes in the study demonstrated both statistical significance and 100% or greater upregulation, suggesting that differential isolation of retinal cell types between control and treatment samples played only a modest role in the assessment of gene expression changes.

Biological Enrichment of Functional Categories

Utilization of Metascape to analyze biologically relevant categories upregulated in the treated tissue revealed that 'inflammatory response' (GO:0006954) and 'regulation of cytokine production'(GO:0001817) were the two most significantly enriched categories, with -log10(P) values of 76 and 60, respectively. Of the remaining categories among the ten most significantly enriched, with -log10(P) values ranging from 45 to 31, six are classified as immune related, while two were related to vascularization (GO:0001568) or extracellular matrix organization (R-MMU-1474344). Owing to the smaller number of genes with reduced expression, fewer categories of biological processes could be identified as being downregulated in the treated samples relative to the controls. Of these, only two – cholesterol biosynthetic process (GO:0006695) and terpenoid metabolic process (GO:0006721) – demonstrated statistical significance, with -log10(P) of 5.6 and 5.1 resepectively.

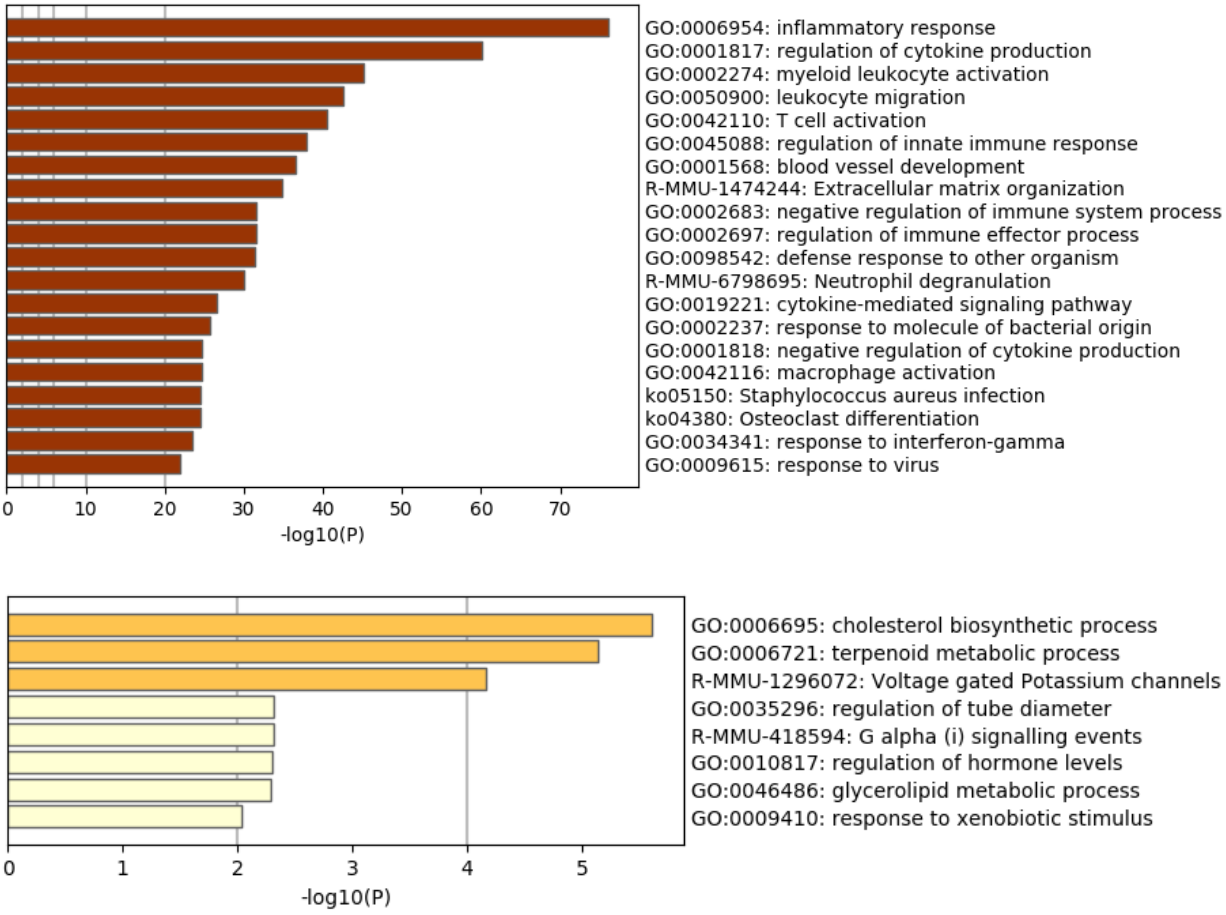

Figure 6: Biological enrichment categories for upregulated (top) and downregulated (bottom) genes. All categories in the top figure are statistically significant, while only the top two categories in the lower figure qualify.

Top 10 most statistically significant changes in gene expression

At the level of individual genes, the top 10 most statistically significant changes were all observed in genes that were upregulated. Of these, 3 – Steap4, Serpina3n and C3 – are considered markers of reactive astrocytes, while three others – Lyz2, Gpnmb, and Lgals3 – are associated with disease-activated (DAM) or neurodegeneration-induced (MGnD) microglia and found in Alzheimer's disease [27-29]. Of the remaining 4 genes, CD74 is a component of MHC II involved in immune surveillance, Mpeg1 and Cybb (Nox2) are involved in the destruction of phagocytosed bacteria, and Col1a1 codes for collagen type 1, a major component of the extracellular matrix [31-34].

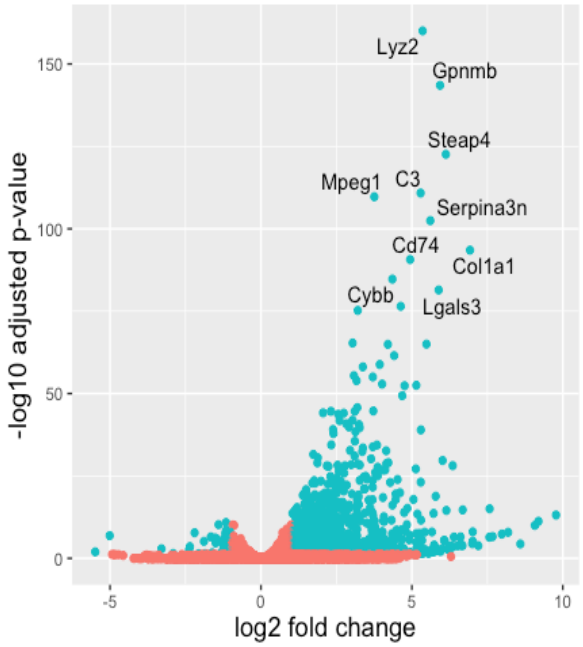

Gene	Significance	Log2 fold	Adj p-val
Lyz2	Antimicrobial, cleaves bacterial cell wall peptidoglycans (DAM)	5.4	9.02E-161
Gpnmb	Microglial regulation of neuroinflammation (DAM)	5.9	3.10E-144
Steap4	Metalloreductase, mediates iron availability during inflammation (RA)	6.1	2.56E-123
C3	Targets pathogens and debris for elimination, involved in synaptic pruning (RA)	5.3	1.46E-111
Mpeg1	Induces pores in phagocytized bacteria, sensitizing them to attack	3.8	1.92E-110
Serpina3n	Inhibitor of immune proteases (RA)	5.6	3.50E-103
Col1a1	Type I collagen	6.9	3.06E-94
Cd74	Major histocompatibility complex II, involved in immune surveillance	4.9	2.20E-91
Cybb	Generates superoxide utilized in the killing of phagocytized pathogens	4.4	1.93E-85
Lgals3	Potential regulator of phagocytosis in both astrocytes and microglia (DAM)	5.9	3.86E-82

Figure 7: Top: Volcano plot of 1129 upregulated and 44 downregulated genes above threshold, top 10 genes by adjusted P-value labeled. Bottom: Table of top 10 genes with functional annotation, log2-fold expression changes, & adjusted P-values. (DAM – Disease associated microglia, RA – reactive astrocytes).

However, a particular challenge in assessing the contributions of reactive astrocytes in heterogenous tissue samples such as these is that there is considerable overlap of markers between reactive astrocytes, the endogenous microglia of the CNS, and infiltrating cells of the peripheral immune system. Therefore, I have utilized previously published panels of reactive astrocyte markers, as well as activated microglia associated with Alzheimer's disease and genes associated with a hereditary model of glaucoma in mice, to investigate broader scale trends in the differential gene expression data.

Markers of Reactive Astrocytes – Barres' Panel

A primary aim of my study was to investigate the extent and features of induced reactivity in retinal astrocytes, however my isolation technique also captures vascular tissue at the vitreal surface of the retina and, to a lesser extent, neurons. Although the use of pooled samples and a cell identity marker panel allowed me to verify that variation between samples remained within acceptable boundaries, the issue of attributing the change in expression of a given gene to a particular cell type remains. While immunostaining approaches can resolve this uncertainty on a marker-by-marker basis, I also utilize an existing panel of astrocyte reactivity markers published by Barres et al. to more broadly assess the responses of these cells[27]. These markers are based on the response of astrocytes to two models of neurological insult, mimicking bacterial infection of the neural parenchyma and stroke respectively, and are categorized as common to both (Pan-reactive), infection-specific (A1), and stroke-specific (A2). Although these designations come with cavaets, as addressed in the Chapter I, they also provide a framework for assessing known astrocyte signals in a mixed tissue sample such as ours.

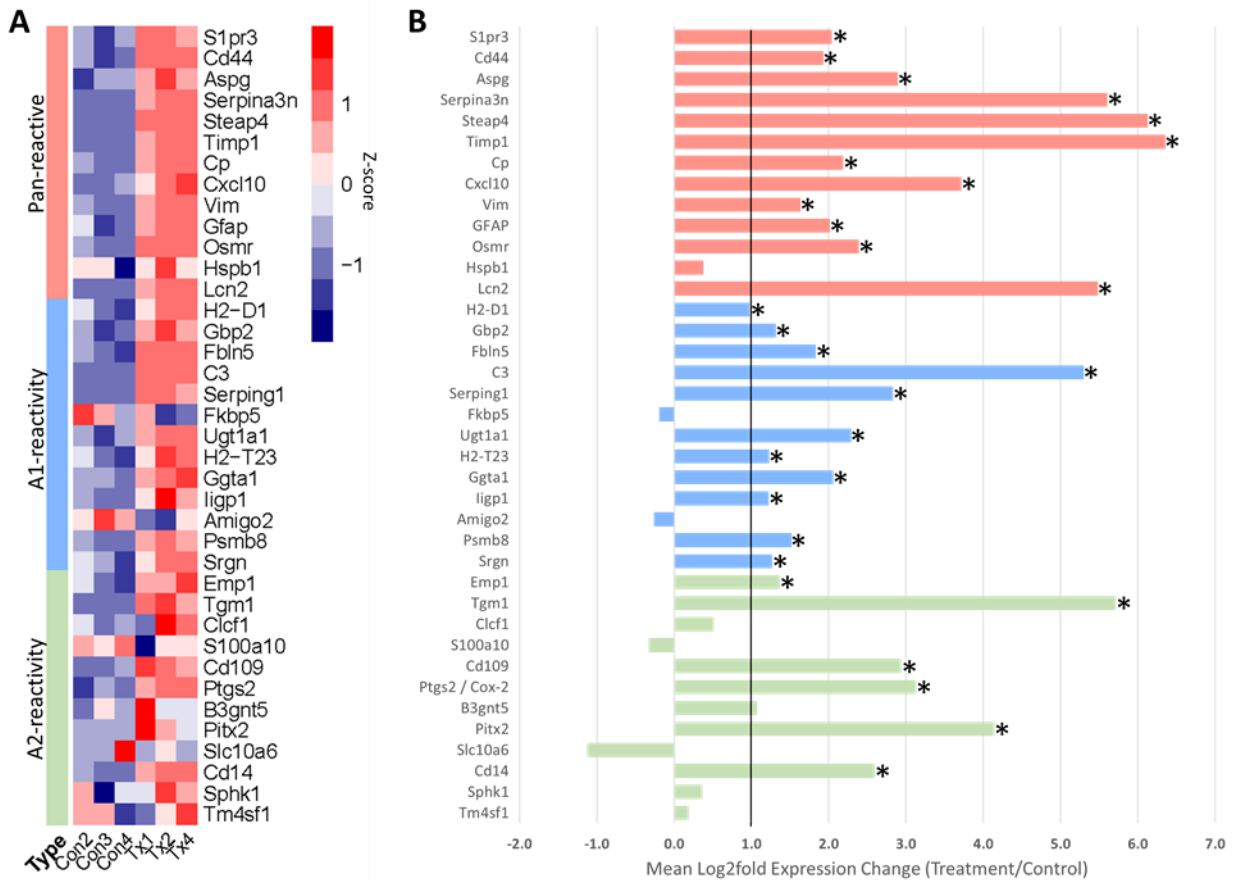

Figure 8: A, Heatmap of differential gene expression of astrocyte reactivity markers proposed by Barres lab. B, Log2-fold expression changes in reactivity markers (* adj. P-value < .05)

Pan Reactive Markers

Of the pan-reactive markers proposed by Barres et al., 12 of 13 (92.3%) underwent statistically significant upregulation in treated samples relative to controls while exceeding the minimum fold increase, compared to 4.5% of all genes in the mouse reference assembly[35]. This indicates that my method of sample isolation is suitable for the detection of reactive astrocyte markers, and that the *in vivo* model generates reactive astrocytes. Of these, Steap4 and Serpina3n are among the top 10 differentially expressed genes by significance in our study, with the former being the 3rd most significantly upregulated and the latter being the 6th most. Steap4 codes for a transmembrane metalloreductase of the same name, which alters the charge of extracellular Fe^{3+} and Cu^{2+} to facilitate the flow of iron and copper into the cell; prior studies have shown it to be upregulated in response to TNF-α signaling [36]. Serpina3n's role in neuroinflammation is the more clearly understood of the two, as it is an inhibitor of immune proteases, including those secreted by T-cells in the onset of neuropathic pain [37].

Table 1: Pan-reactive Markers

Gene Alias / Annotation	Fold Change	Adj P-value
Steap4	69.8	2.56E-123
Serpina3n	48.8	3.50E-103
Lcn2	44.7	1.03E-65
Osmr	5.2	7.90E-40
Timp1	81.7	7.49E-29
Cp	4.6	8.66E-29
S1pr3	4.1	7.27E-19
Cd44	3.8	7.09E-17
GFAP	4.0	3.63E-14
Cxcl10	13.1	1.26E-13
Vim	3.1	3.31E-12
Aspg	7.4	0.000294
Hspb1	1.3	0.240592

In addition to the pan-reactive astrocyte markers, I also detected upregulation of A1 and A2 astrocyte markers, although mostly at lower levels of statistical significance and fold change.

A1 Markers

Of the 12 initial A1 markers, 10 (83.3%) were both statistically significant and at least 2 fold upregulated, as was the additional A1 marker C3. Although initially left off the list of transcriptional markers of A1 astrocytes published by Barres et al, it was included as an immunostaining marker for these cells and later was added as a transcriptional marker [27, 38]. Complement component 3, as the protein product is known, is a major element of the complement system, which marks cellular elements and debris for elimination; it has also been demonstrated to play a role in synaptic pruning [39]. It is the most upregulated, in terms of both significance and fold change, of the A1 astrocyte markers, and is the 4th most upregulated gene in this study overall.

Table 2: A1 Reactive Astrocyte Markers

Gene Alias / Annotation	Fold Change	Adj P-value
C3	39.1	1.46E-111
Serping1	7.1	1.47E-41
Fbln5	3.6	8.58E-14
Gtga1	4.2	9.58E-12
Psmb8	2.9	1.73E-10
Ugt1a1	4.9	2.86E-08
Gbp2	2.5	4.08E-08
H2-D1	2.0	1.51E-06
H2-T23	2.3	0.000317
Iigp1	2.3	0.001258
Srgn	2.4	0.001393
Amigo2	0.8	0.2371
Fkbp5	0.9	0.536051

A2 Markers

Finally, the A2 category of reactive astrocyte markers gave the lowest proportion of above-threshold gene expression changes, with 5 of the 12 genes (41.7%) in this category qualifying, although this is still enriched compared to the upregulation of all tested genes (4.5%). However, I have replaced the marker Pitx3 – a pituitary homeobox gene only lightly expressed (0.2 transcripts per million (TPM)) in the retina – with the retina specific Pitx2 (1.3 TPM); in this modified version of the A2 category 50% of genes are upregulated [40]. Curiously, the A2 marker Slc10a6 was detected at even lower levels (< 0.1 TPM) than the non-retina homeobox gene Pitx3 and only in two samples (one each control and treatment), suggesting that this may also be a region specific marker of astrocytes. However, unlike the aforementioned pituitary homeobox gene, SlC10a6 belongs to the much larger Solute Carrier family of genes, and I am ill-positioned to speculate on the retinal equivalent.

Table 3: A2 Reactive Astrocyte Markers

Gene Alias / Annotation	Fold Change	Adj P-value
Cd14	6.0	2.60E-17
Tgm1	52.7	2.30E-14
Cd109	7.7	1.08E-07
Pitx2	17.7	2.12E-05
Emp1	2.6	0.000162
Ptgs2/Cox-2	8.8	0.002772
S100a10	0.8	0.306943
Sphk1	1.3	0.371147
Clcf1	1.4	0.392199
B3gnt5	2.1	0.412989
Tm4sf1	1.1	0.880538
Slc10a6	0.5	1

Although my investigation is primarily concerned with the detection and assessment of reactive astrocytes in the retina, I am also interested in a number of other genes, namely markers of disease associated microglia (DAM, a category of genes upregulated in microglia in Alzheimer's disease and associated models) as well as the genes with known mutant alleles in the dba/2j mouse strain, a genetic model of glaucoma utilized by many research groups.

Dba/2J Variant Allele Genes

While the markers proposed by Barres et al. provided me with an initial framework to assess astrocyte reactivity in these samples, the panel they form provides only a single lens through which to view these results [27]. Moreover, the majority of these markers are informed by research in the brain and the spinal cord, rather than the retina, while knowledge of glia-specific changes in glaucoma and other retinal disease states remains sparse. However, the most prominent mouse genetic model of glaucoma – the dba/2J strain of mice – has a well established pattern of mutations that contributes to the glaucoma-like phenotype these mice develop during the aging process [41, 42]. Although these genes are not glia specific and I do not expect that the etiology of this chronic hereditary model of glaucomatous stress would closely mirror the acute inducible model, I nonetheless investigated the panel of at least 15 genes whose variant alleles contribute to the dba/2j phenotype for commonalities with my results.

Table 4: Dba/2J Variant Allele Genes

Gene Alias / Annotation	Fold Change	Adj P-value
Gpnmb	61.1	3.10E-144
P2rx7	4.5	4.55E-12
Klrd1	128.0	3.60E-05
Mx1	5.6	0.001437
Gpr84	3.2	0.00383
Cdh23	2.5	0.044239
Ahr	1.5	0.074276
Fscn2	1.4	0.337807
Tyrp1	1.9	0.501204
Myo5a	0.9	0.504402
Cox7a2l	0.9	0.560707
Asp2	1.0	0.976002
Cd5	0.9	0.976967
Taar1	0.0	1
Hc	1.3	1

Of the 15 genes whose variants contribute to the glaucoma-like phenotype of dba/2j mice, 6 (40%) show statistically significant upregulation in the treated samples. Of these, the top three by significance – Gpnmb, P2rx7, and Klrd1 – are of particular note. Gpnmb (adj p-value 3.1E-144), a transmembrane protein often found in pigmented cells, may also play a role in regulating the role of microglia in neuroinflammation, and is found in plaque associated microglia in both mouse models of Alzheimer's and human tissue isolated from deceased patients with the disease [43]. Likewise, the purine receptor P2rx7 is found in microglia as well as astrocytes and Müller glia; relative to other purine receptors it requires exposure to large

concentrations of ATP for activation and several studies suggest it may act as a sensor for damage to nearby neurons [44]. Finally, Klrd1 – a marker of NK-type immune cells – shows a large, statistically significant upregulation in our data, suggesting that infiltration of immune cells may contribute to our experimental data, a possibility also implied by our biological enrichment analysis [45].

Markers of Disease-associated and Neurodegeneration-induced Microglia

Although my main focus is on the response of retinal astrocytes in the model, my data also suggests the presence of microglia in these tissue samples. In particular, several of the most statistically significant upregulated genes are markers of a microglia phenotype (or phenotypes) associated with neurodegenerative diseases, including Alzheimer's. As microglia are known to contribute to astrocyte reactivity, and since a number of groups have previously described commonalities between glaucoma – a disease characterized by neurodegeneration in the retina – and Alzheimer's disease – a neurodegenerative disease of the brain – I have additionaly investigated the aggregate changes in a pair of gene panels identified as markers of disease / neurodegeneration associated microglia [27, 46].

These panels, both published in 2018, primarily characterize the response of microglia in mouse genetic models of Alzheimer's, although specific markers from each were later investigated in human donor tissue from deceased Alzheimer's patients. The first of these two publications utilized the 5XFAD mouse line to model familial Alzheimer's and characterized the observed microglial phenotype as DAM (Disease Associated Microglia); while the second employed the APP-PS1 mouse line, along with models of ALS and MS, and termed the resultant phenotype MGnD (Microglia – neurodegenerative) [28, 29]. Despite the use of distinct mouse models, both groups found their phenotype to be mediated by apoplipoprotein E (Apoe) – a major component of human Alzheimer's progression – and Trem2 – a receptor expressed on microglia. While the DAM phenotype was further subdivided into two stages, the MGnD microglia were not, although a trio of genes from the DAM stage 2 phenotype – Clec7a, Itgax and Trem2 – were also found in MGnD microglia, as was the DAM stage 1 marker Apoe. Although researchers investigating microglia are still studying the extent to which these phenotypes overlap and the degree to which they correlate with microglia in human neurodegeneration, the two categories are sometimes collectively referred to as DAM microglia in the literature [47].

Table 5: Stage 1 Disease-associated Microglia Markers

Gene Alias / Annotation	Fold Change	Adj P-value
Lyz2	41.0	9.02E-161
Apoe	2.0	0.001528
Tyrobp	6.3	4.45E-24
Ctsd	2.7	2.54E-17
Ctsb	1.8	1.06E-08
B2m	2.6	3.66E-06
Fth1	0.9	0.719619

Table 6: Stage 2 Disease-associated Microglia Markers

Gene Alias / Annotation	Fold Change	Adj P-value
Clec7a	18.4	1.18E-65
Itgax	39.3	1.08E-39
Trem2	6.7	1.65E-15
Cst7	16.2	8.23E-09
Lilrb4a	39.2	7.64E-24
Ccl6	6.5	4.37E-13
Axl	2.3	1.17E-08
Csf1	1.5	0.001145
Ctsl	1.4	0.008093
Lpl	1.6	0.01673
Timp2	1.3	0.030387
Cd9	1.4	0.172503

Table 6: Neurodegeneration-induced Microglia Markers

Gene Alias / Annotation	Fold Change	Adj P-value
Gpnmb	61.1	3.10E-144
Lgals3	59.2	3.86E-82
Clec7a	18.4	1.18E-65
Itgax	39.3	1.08E-39
Spp1	3.9	1.56E-17
Trem2	6.7	1.65E-15
Apoe	2.0	0.001528
Ccl2	17.7	0.017704
Fabp5	1.0	0.991845

Markers for both DAM phenotypes, as well as the MGnD phenotype, showed high levels of upregulation and statistical significance, with three genes – Lyz2 (DAM S1, #1), Gpnmb (MGnD, #2), and Lgals3 (MGnD, #10) appearing in the top 10 genes by statistical significance. Lysozyme, the protein encoded by Lyz2, possesses antimicrobial properties but is also present in sterile neurodegenerative disorders; a recent study suggests it may contribute to TLR4 activation in the CNS [48]. Gpnmb and Lgals3, which are both characterized as markers of the MGnD phenotype, are briefly summarized in the preceding section on dba/2j markers and the following section on choosing validating markers, respectively.

Furthermore, the genes common to DAM S2 and MGnD – Clec7a, Itgax, and to a lesser extent, Trem2 – show high levels of enrichment and statistical significance as well, with both Clecl7a (#15) and Itgax (#40) appearing in the top 50 genes by p-value. However, the Clecl7a product Dectin-1 – a pattern recognition receptor involved in responding to fungal infection – and the integrin alpha X chain protein coded by Itgax are also characteristics of peripheral macrophages [49, 50]. Owing to the bulk nature of the sequencing, it is unclear to what degree this outcome is a function of a single population of microglia expressing a mixed phenotype, multiple populations of microglia expressing distinct phenotypes, or contributions from other cell types, particularly infiltrating immune cells.

Although bioinformatic approaches to deconvolute bulk RNA-seq data do exist, like biological enrichment categories they are not particularly well equipped to contend with cell populations for which reference data is sparse (such as retinal astrocytes), or which feature extensively overlapping markers (such as microglia and peripheral immune cells). Instead, using a mix of conventionally sectioned retinal tissue and samples isolated by the same pulloff technique utilized in our RNA-sequencing experiments, I have employed a mix of markers chosen from the previously highlighted results to get a clearer look at the changes in the retina induced by this model.

Validation and Localization of Upregulated Markers Induced by Treatment

Choosing Markers

In choosing to utilize immunostaining to validate our transcriptomic results, I was motivated by a desire to confirm that changes to RNA transcription in the model produced concurrent changes in protein expression and by the capacity of staining techniques to localize the markers of interest to specific cells and cell types. As my primary focus is on the response of retinal astrocytes to this *in vivo* model, with a secondary focus on the response of microglia, emphasis was placed on markers associated with these cell types, particularly among genes with the most consistent upregulation. In particular, I sought markers with relatively well understood functions, which had the potential to clarify the cell types involved in broader gene expression patterns. For example, I chose the marker Lgals3 due to its high upregulation (59.2-fold), statistical significance (adj p-value 3.86E-82), its prior linkage to phagocytic activity in both astrocytes of the optic nerve head and microglia, and its categorization as an MGnD marker in microglia [51, 52]. Additional considerations include biological relevance (*i.e*., whether the gene had well documented roles in relevant human conditions such as glaucoma and Alzheimer's), as well as more practical considerations (such as whether available antibodies for the markers had been previously validated in the brain or retina). As imparting clarity to the transcriptomic results was foremost among my priorities in choosing staining markers, I have continued to utilize the widely used proteins GFAP and Iba-1 as markers of astrocytes and Müller glia respectively, although the latter is also expressed among macrophage-type cells of the immune system more broadly. Next, I selected markers linked to astrocyte reactivity, both in the Barres panel and in the literature more broadly.

Markers of Reactive Astrocyte States

The first of these, Lcn2, is associated with reactive astrocytes in a variety of mouse models and human diseases – including Alzheimer's – and is thought to contribute to both the propagation of reactivity and increased permeability of the blood brain/retinal barrier [35, 53-55]. Regarded as a pan-reactive marker by Barres et al., Lcn2 underwent a >40-fold upregulation with high significance (adj p-value of 1.03E-65) in treated samples[27]. My second marker - complement component C3 - is likewise found in both animal models and human neurodegeneration including glaucoma, where it localizes to the inner layers of the retina in which astrocytes and retinal ganglion cells reside [35, 56]. C3 is an essential component of the complement system, which is involved in targeted phagocytosis of debris and pathogens, as well as specialized roles in the nervous system such as synaptic pruning [39]. Presented as a key marker of A1 astrocyte reactivity by Barres group, C3 displayed approximately 40-fold upregulation and was highly statistically significant (adj p-value 1.46E-111) in this experiment. Finally, the gene Ptgs2 - which codes for the inducible form of the prostaglandin synthesizing enzyme cyclooxygenase - is an A2 reactivity marker per the Barres group classification system and has been previously investigated in a variety of neurodegenerative disorders, although its contributions are clouded

by the role it plays under physiological conditions [57]. Although it displays a more modest 8.8-fold induction (adj p-value 0.0028), I chose this as our representative A2 astrocyte marker in part because of an ongoing investigation of the role of astrocyte secreted lipids our lab is collaborating on.

Additional Microglial and Function-specific Markers

In addition to these representative markers of astrocyte reactivity states, I selected the approximately 60-fold upregulated gene Gpnmb (adj p-value 3.10E-144) as a marker of neurodegeneration associated microglia. Beyond Gpnmb's status as an MGnD microglia marker, it also localizes to microglia surrounding amyloid plaques in Alzheimer's derived donor tissue and in animal models of the disease, as well as being a major contributor the glaucomatous phenotype seen in dba/2j mice [28, 41-43]. I also selected 3 additional markers – Lgals3, Thbs-1, and Ki67 – based on their functional roles and reports of their presence in reactive astrocytes. The highly upregulated marker Lgals3 was chosen for its role in regulating phagocytic activity in both microglia and the astrocytes of the optic nerve (see above). Conversely, Thbs-1 – which codes for the astrocyte-secreted, pro-synaptogenic ECM component thrombospondin-1, was chosen due to its role in promoting survival in intrinsically photosensitive RGCs, which display decreased sensitivity to axonal insult [58-60]. Finally, the marker of proliferation Ki-67 (35-fold upregulated, adj p-value 7.42E-28) was chosen to identify proliferating cells in the treated retina, as we had not expected the model to induce proliferative behavior in the retina yet observed measurable expression in the treated tissue [61].

Immunostaining Results

GFAP & Astrocyte Reactivity Markers

In the healthy retina, GFAP staining is typically restricted to astrocytes at the optic nerve head and in the vitreal boundary region. As with other models of ocular hypertension and neurodegeneration in the retina, I observed additional GFAP expression in the Müller cells of treated retinas, where it forms a single filament running linearly along the long axis of the cell. Although the bulk of GFAP upregulation in my transcriptomic data presumably comes from retinal astrocytes – as Müller cells only intermittently adhere to the pulloff sections, typically at the very edge of the sample – for the most part the relatively modest change in GFAP expression (3-fold increase) is difficult to detect via immunofluorescence due to the non-stochiometric nature of the process. However, isolated regions closer to the periphery of the tissue displayed localized hypertrophy, in which the density of GFAP filaments within astrocytes increases dramatically, a phenomenon readily detected by immunostaining (Fig 9).

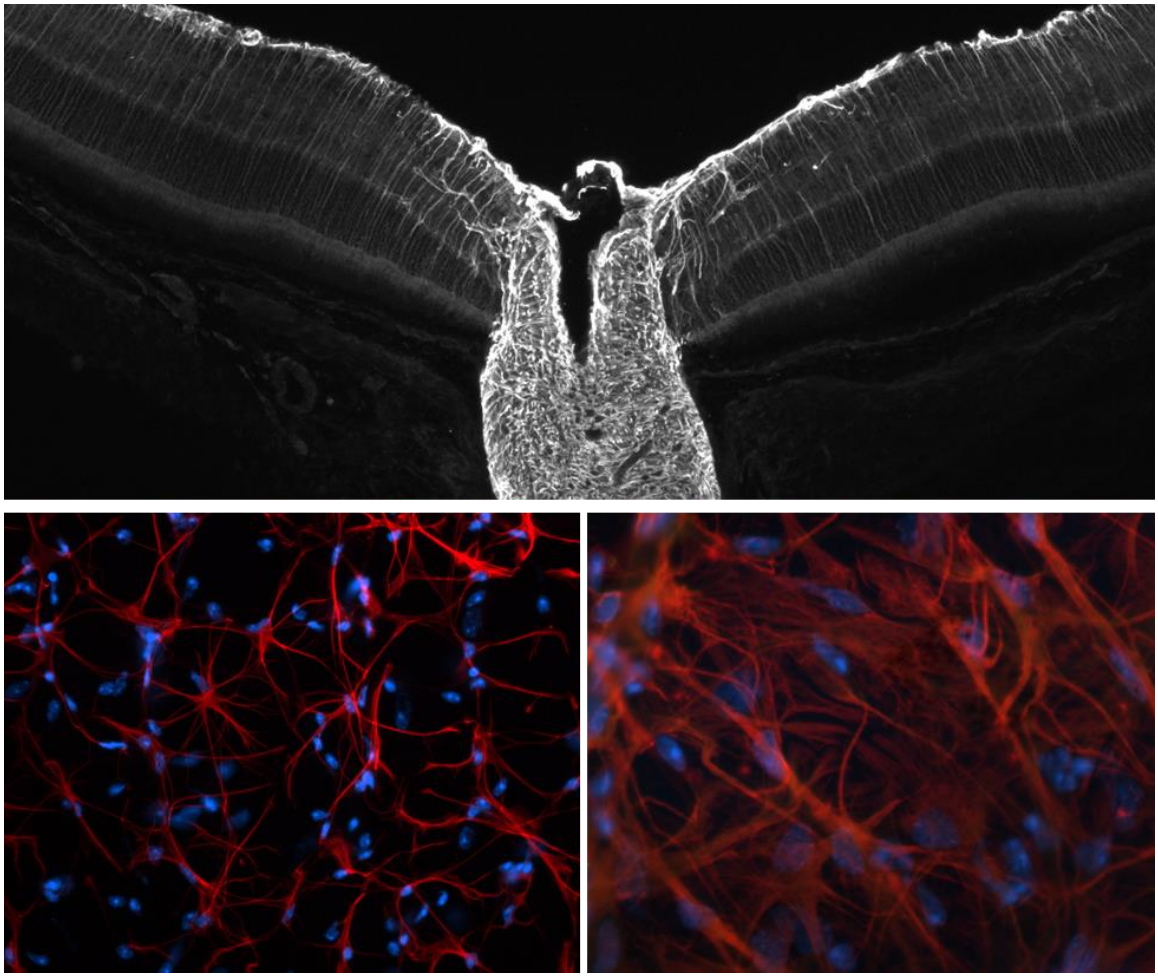

Figure 9: GFAP reactivity in the mouse retina. Top: Cross section of optic nerve head and retina from treated retina, stained for GFAP (white). Müller cells (transverse, parallel to optic nerve) cells to either side of the optic nerve head do not express GFAP in untreated tissue. Lower (Left & Right): Astrocyte GFAP expression (red) with Hoecsht nuclear stain (blue), viewed en face after pull-off isolation. Left: Untreated astrocytes display slender processes. Right: Severely reactive astrocytes showing hypertrophy of processes.

I also utilized a trio of additional astrocyte reactivity markers: Lcn2, C3, and Cox-2. The first of these, the pan-reactive marker Lcn2, was essentially undetectable in the untreated retina and displayed considerable upregulation in the treated retina, as expected. Increases in Lcn2 expression were observed primarily at the vitreal boundary region, especially in proximity to the superficial vasculature, and isolation of tissue by the pulloff approach allowed us to verify that retinal astrocytes indeed express Lcn2 in response to our treatment conditions (Fig 10).

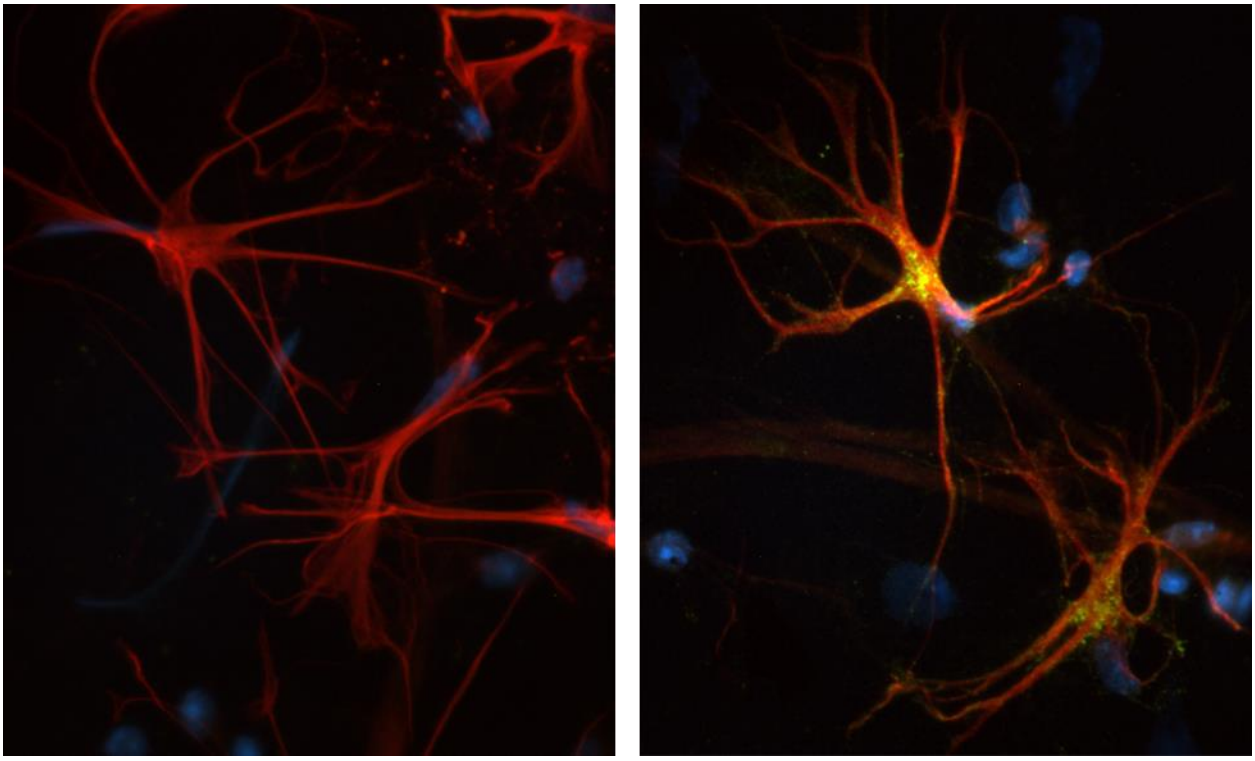

Figure 10: GFAP (red) and Lcn2 (green) in the mouse retina. Astrocyte only express Lcn2 when reactive. Left: Pull-off isolated astrocytes expressing GFAP but not Lcn2. Right: Pull-off isolated astrocytes from treated animals show both GFAP and Lcn2 expression.

Additional cells also expressed Lcn2 in response to treatment, with vasculature associated cells – most likely pericytes – showing expression, along with a small number of intensely stained cells we believe to be neutrophils, which are known to express high levels of the protein. In contrast, neither C3 nor Cox-2 provided detectable staining at the cellular level, with C3 stained pulloff astrocytes displaying only background levels of signal in both treated and untreated tissue. In both cases this is likely to be an issue of antigen masking, as both antibodies can require elaborate antigen retrieval processes (not shown).

Iba-1 and Microglial Markers

As with the GFAP staining of astrocytes, use of the marker Iba-1 can indicate the structure and morphology of microglia, as well as peripheral macrophage immune cells. Under physiological conditions, such as in control retinas, microglia adopt a ramified morphology, in which they extend slender processes to contact adjacent and nearby cells as part of the monitoring of the neural parenchyma. These ramified microglia are also observed in the treated retinas, however I additionally detected amoeboid morphologies, often adopted by phagocytic microglia and macrophages engulfing dead cells and debris. In multiple cases, these cells appeared to be phagocytosing nuclei at the retinal ganglion cell layer and at the retinal surface, consistent with expected clearance of dead and damaged RGCs induced by our treatment model. Rounded cells, with a macrophage-like morphology, were also observed adhering to the retinal surface from the vitreous, although I cannot on the basis of Iba-1 alone differentiate between a microglial origin for these cells rather than a peripheral macrophage one (Fig 11).

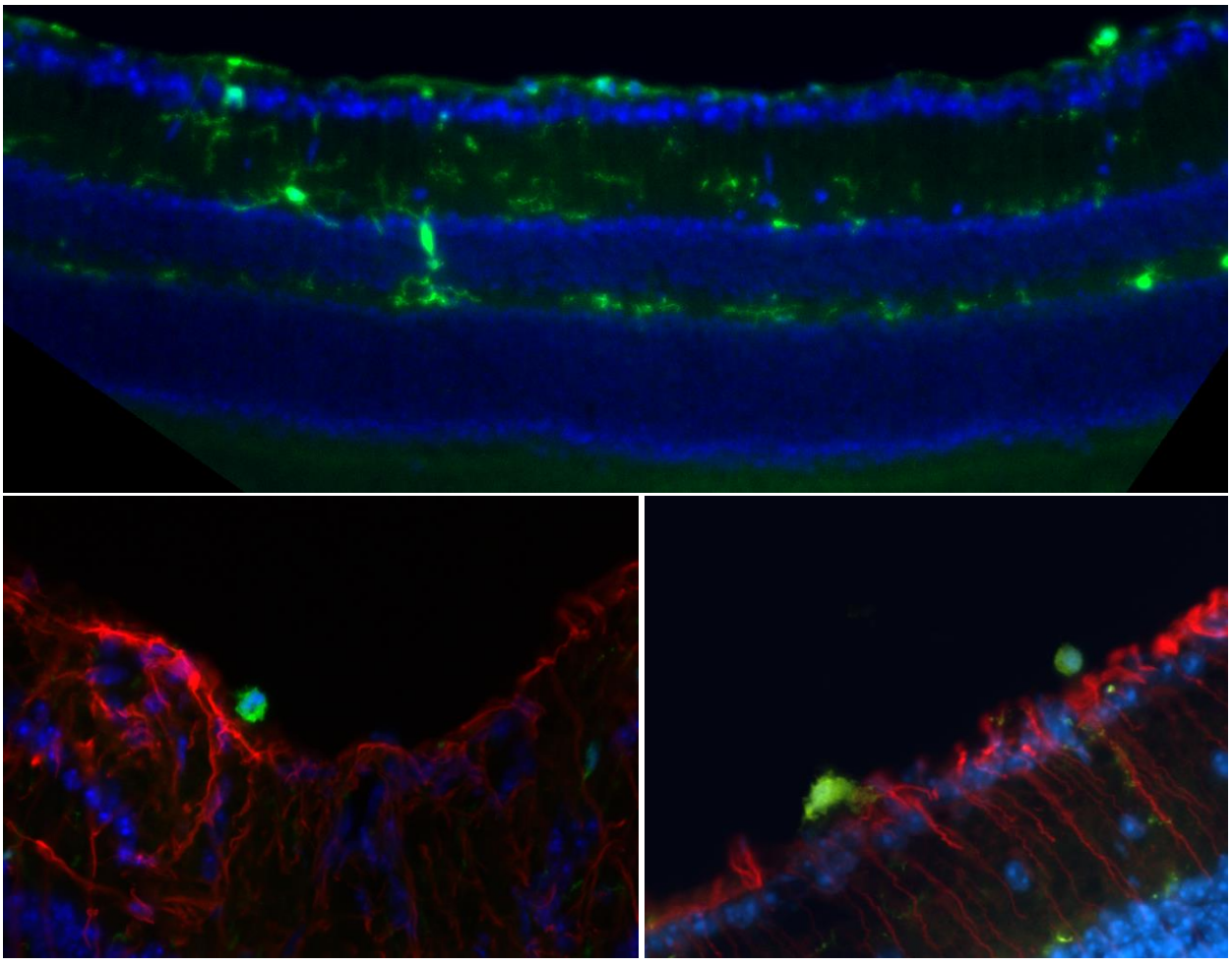

Figure 11: Microglia in treated retinas stained for Iba-1 (green) and Hoecsht nuclear stain (blue) Top: Microglia demonstrate both highly angular, ramified morphologies, as well as rounded and compact amoeboid morphologies that can indicate phagocytic state.
Bottom (both): Amoeboid microglia or macrophages on the retinal surface, with astrocytes stained via GFAP (red) for contrast.
Left: Amoeboid Iba-1+ cell on the retinal surface in the vicinity of the optic nerve head. Right: A pair of amoeboid Iba-1+ cells in the central retina, the morphology of the cell on the left suggests it is engulfing a dying cell – possibly an RGC – on the retinal surface.

I also stained for Lgals3 and Gpnmb, which I expected to detect in retinal microglia. Lgals3 showed expression in the optic nerve posterior to the retina, as previously reported and attributed to astrocytes, but had limited expression in the central retina. A population of rounded cells on the retinal surface, likely overlapping with the Iba-1+ 'macrophages', also expressed Lgals3; these were most abundant in proximity to the optic nerve head (Fig 12). Conversely, Gpnmb staining was only rarely associated with Iba-1+ cells and – unlike Iba-1 and Lgals3 – was not associated with the macrophage like round cells adhering to the retinal surface. Lgals3 and GPNMB will be covered more thoroughly in the coming section on sites of focal injury.

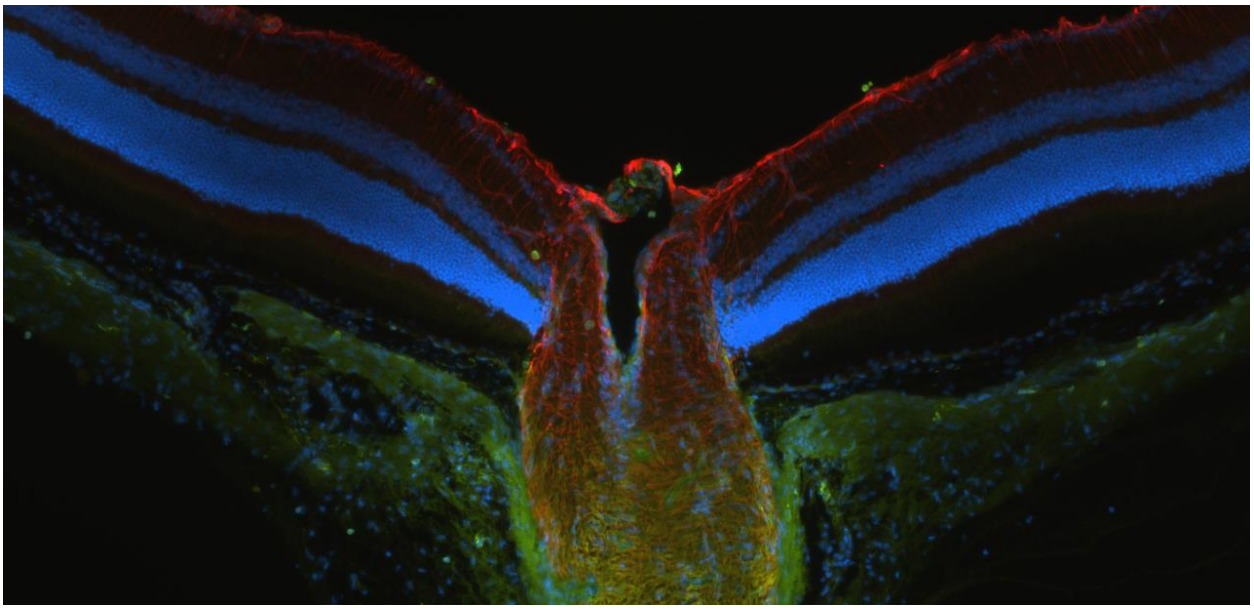

Figure 12: Optic nerve head from treated eye, stained for GFAP (red) and Lgals3 (green) with Hoechst nuclear stain (blue). Retinal and optic nerve astrocytes express GFAP, as do Müller cells. Lgals3 shows as small amoeboid cells – likely macrophages – emerging from the optic nerve head and transversing the retinal surface. Astrocytes in the optic nerve head further from the retina (lower portion) also express Lgals3, an indicator of their role in phagocytosing damaged mitochondria from RGC axons.

Ki-67 and Thrombospondin-1

Our final two immunostaining markers, Ki-67 and thrombospondin-1, were largely absent in the central retina and near peripheral regions. Neuronal and glia cells in the mature retina do not proliferate under physiological conditions, and although we saw marked upregulation of Ki-67 in transcriptomic data, the absolute expression of this gene was still low. In the treated tissue, a small number of cells in both the peripheral retina and the optic nerved head showed clear Ki-67 staining, but these cells may have been endothelial in origin and were too sparse to merit additional investigation. Thrombospondin-1, conversely, localized to vasculature in the central regions of both control and treated retinas at similar levels (data not shown). As such, the source of increased expression of both markers, like that of Gpnmb, appears to lie elsewhere.

Focal Injuries at the Periphery: Scarring and Detachment

While astrocyte reactivity and microglia activation in the central retina – as observed by morphological changes and alteration of immunohistochemical profile – was modest, more dramatic changes were detected at the periphery. These retinal changes – which include detachment and the buildup of scar-like deposits – clearly occurred in the retina during life, rather than during enucleation or dissection. Further supporting this interpretation, a re-investigation of these sites shows widespread loss of photoreceptors (as indicated by the loss of both the outer segment and outer nuclear layers) and broad disruption of the retinal pigment epithelium (RPE), which forms a monolayer separating the outer retina from the choroid in control eyes. As photocoagulation scars are known side effects of exposure of the retina to the class of 532 nm laser used for episcleral vein cauterization, it is apparent that these sites are a direct result of the treatment model, an interpretation consistent with the high degree of localization observed [62].

Of the nine immunostaining markers we investigated in the treated retina, all but one – Cox-2 – showed bright staining in and around the peripheral scar regions. Although several of the scar sites displayed autofluorescence in the outer retina, particularly at the 488nm wavelength used for much of our staining, all the remaining markers except C3 and thrombospondin-1, showed morphologically clear staining of individual cells. Given the high degree of localization of C3 and thrombospondin-1 at the site of injury, and the limited autofluorescence observed in the 594nm and 647nm channels I utilized for detecting these markers, I believe even the signal from these less specific markers represents valid detection.

GFAP & Iba-1 at the Site of Injury

In contrast to the modest upregulation of GFAP in the astrocytes and Müller cells of the central retina, the response of glia at the acute laser injury sites was characterized both by more intense staining and dramatic morphological changes, particularly among Müller cells. Although these glia display a radial morphology both under physiological conditions as well as during moderate reactivity, many of the Müller cells at the sites of injury have adopted a stellate morphology similar to retinal astrocytes and withdrawn their end-feet from the inner retina, extending their processes toward damaged tissue in the outer retina (Fig 13).

Just as the GFAP positive cells at the site of retinal injury display clear morphological signs of reactivity, so to do the Iba-1 positive cells at these locations differ markedly from the homeostatic microglia observed elsewhere in the retina. Ramified morphologies are all but absent; instead, we observe amoeboid morphologies and clear examples of phagocytosis. However, from Iba-1 alone we cannot identify what fraction of these cells represent endogenous microglia, and the high number of iba-1+ cells in these regions suggest recruitment of cells from other areas or the peripheral immune system (Fig 13).

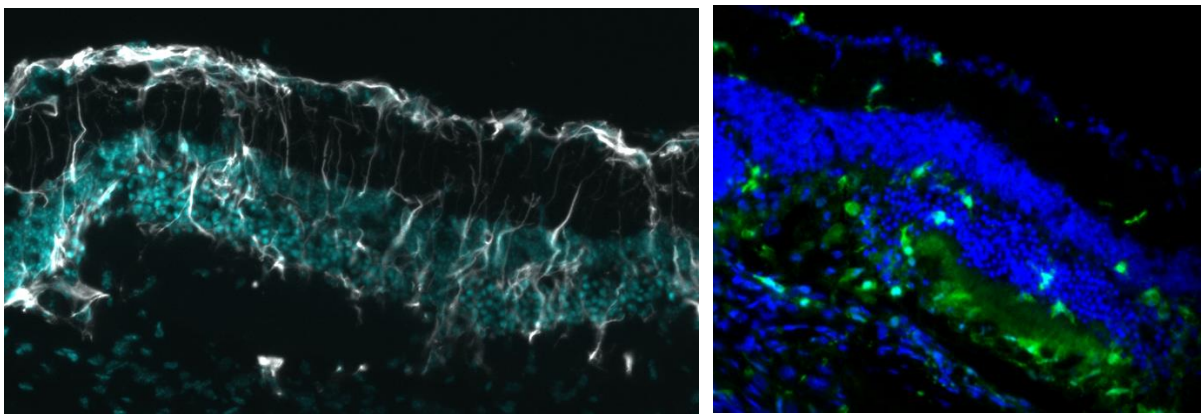

Figure 13: GFAP and Iba-1 expression at scar sites induced by laser injury. Left: Highly reactive Muller cells lose their characteristic linear morphology and adopt multipolar, astrocyte-like forms (GFAP, white; Hoecsht nuclear stain cyan) Right: Iba-1+ (green) cells likely representing a mix of microglia and macrophages cluster at scar site. The scar itself displays modest autofluorescence in the green channel.

Lcn2, Lgals3 and Gpnmb

Combining GFAP or Iba-1 with additional staining against Lcn2, Lgals3, and Gpnmb further reveals the complex cellular response at these sites of laser injury. Although astrocytes in the treated retina show Lcn2 reactivity, bright Lcn2 staining at these locations appears to sporadically stain cells demonstrating complex ramified morphology in detached fragments of the outer retina, which may be Müller cells (Fig 14). As GFAP staining only highlights a narrow area within these cells, even in reactive states, following up with a marker that stains a larger fraction of the Müller cell body such as glutamine synthetase or CRALBP would be necessary to confirm or dismiss this possibility [63]. Regardless, while not Iba-1+ themselves, these ramified cells display close association with Iba-1+ cells at injury sites; whether this proximity is indicative of direct interactions or merely the result of both cell types being recruited to the same location remains unclear. Lgals3, conversely, more clearly colocalizes with Müller cells at some injury sites, as well as some amoeboid cells that are likely immune in nature (Fig14).

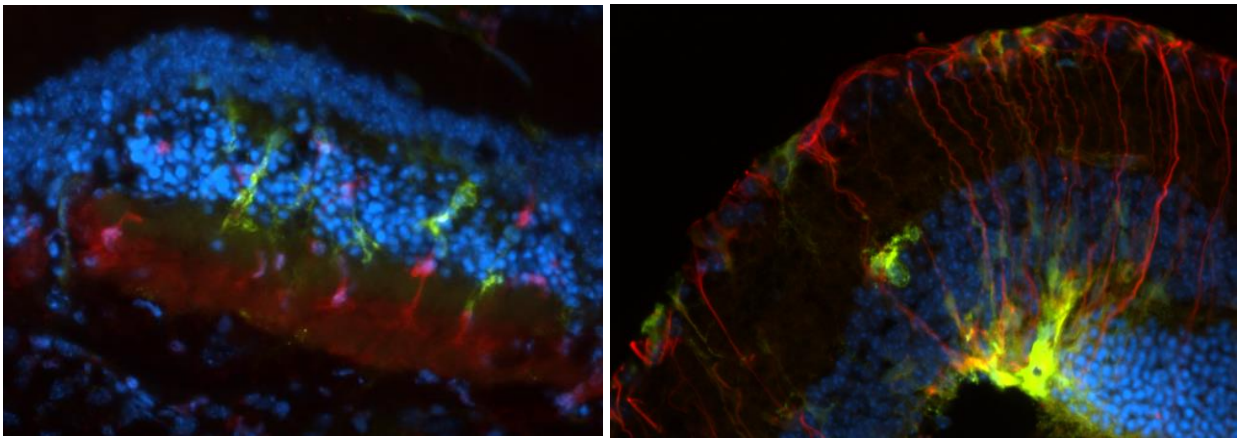

Figure 14: Likely reactive Müller cells at scar sites. Left: Lcn2+ cells (green) with Müller cell-like morphologies near Iba-1+ cells engulfing photoreceptors at a scar site. Right: Gfap+ (red) Müller cells expressing Lgals3 (green), especially at the outer retina. An amoeboid Lgals3+ cell can also be seen within the retina.

Finally, Gpnmb colocalizes only infrequently with Iba-1+ cells at the site of injury, and not at all with GFAP+ cells at these locations. Instead, it is found primarily in a dense aggregation of cells at the outer edge of the injury site, while GFAP+, Iba-1+, Lcn2+, and Lgals3+ cells are found at or near the inner edge of the injury. The localization and high levels of Gpnmb – a marker commonly associated with melanocytes – suggests the potential involvement of RPE cells, which are highly pigmented. By combining brightfield imaging with immunofluorescence, I was able to verify disruption of the RPE layer at retina's outer edge and demonstrate that the Gpnmb+ cells are almost certainly RPE cells (Fig 15).

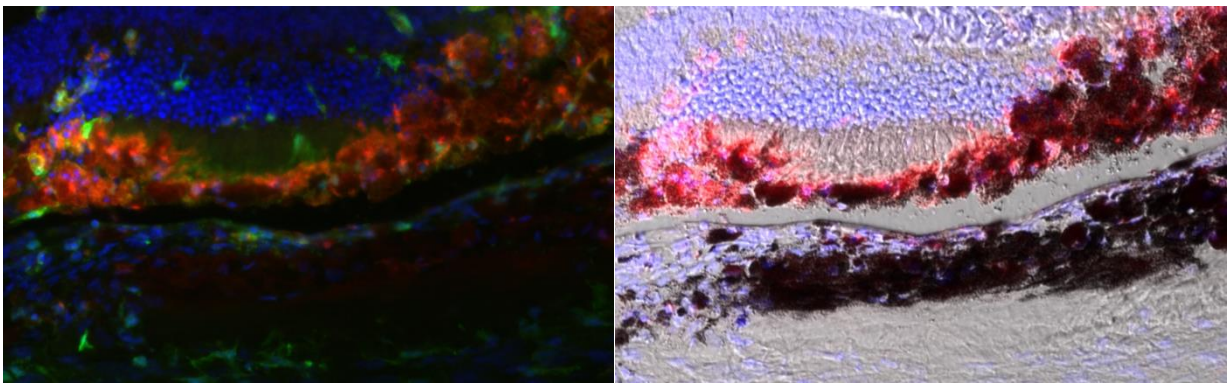

Figure 15: Iba-1+ cells and Gpnmb+ cells congregate at a scar site but these markers are rarely co-expressed. Left: Iba-1 (green) and Gpnmb (red) cells and appear to primarily approach the site of a scar from oppsite sides, with the Gpnmb+ cells in particular localized to the outer, but not inner, side of the scar. A small number of cells, mostly in the upper left, express both markers. Right: By comibing Gpnmb (red) immunofluorescence with brightfield, the Gpnmb+ cells are revealed to be highly pigmented RPE cells from the retinal boundary clustering around the outer segments of detached photoreceptors in the center of the image.

Ki-67 and Thrombospondin-1

While Ki-67 staining was essentially absent in the central retinal regions, we found modest numbers of these cells at the laser injury sites; although the disrupted structure, combined with the intrinsically high density of nuclei in the layer they were found, complicate the issue of determining the identity of these potentially proliferating cells. Thrombospondin-1 showed intense expression at some injury sites but not others. Closer examination, again combined with brightfield imaging, revealed that expression was restricted to the outer segments of detached photoreceptors; expression was absent at locations where the retina remained attached or where damage had progressed to total loss of photoreceptors (Fig 16). Additionally, RPE cells surround the outer edge of these thrombospondin-1+ photoreceptors, maintaining the proximity between these cell types found in healthy tissue. Whether these detached RPE cells are engaging in neuroprotective behavior with regards to these photoreceptors or facilitating their removal is unclear, and elevated Gpnmb expression is observed in neither intact RPE nor in regions where photoreceptor loss is already complete. Although these detached photoreceptors have outlived their peers elsewhere, it is unclear whether any would have survived; while we have not utilized TUNEL staining, I did observe engulfment of a small number of these cells by Iba-1+ cells (Fig 14).

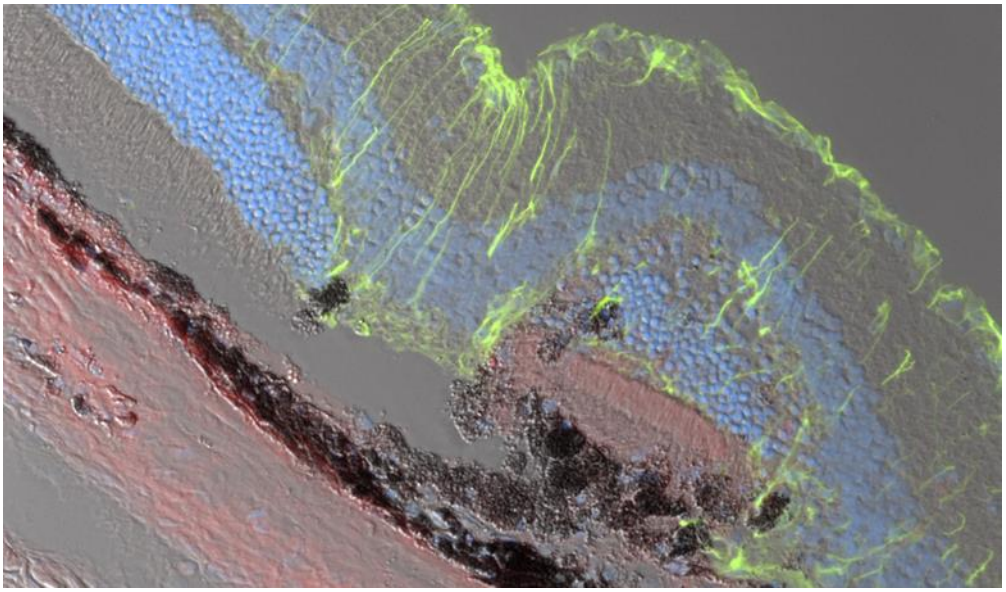

Figure 16: RPE cells surround detached photorecptor outer segments, which colocalize with thrombospond-1. This combination immunofluorescence (GFAP, green; thrombospondin-1, red; hoechst nuclear stain, blue) and brightfield image shows a complex portrait of a scar site, where detached photorecptor outer segments, but not those of still attached photoreceptors (upper left), colocalize with thrombospondin-1. As thrombospondins are extracellular matrix proteins, the identity of the cells responsible for it's secretion remain unclear.

Pull-off IHC: Scars and Macrophage March

Although a number of highly upregulated markers from our transcriptomics data were expressed most strongly at these sites of laser injury, our retinal astrocyte isolation/enrichment technique separates by design the innermost retinal region from the outer layers where injury was most pronounced. This then necessitates inquiry – are the laser sites contributing to our transcriptional data, and if so, how is this occurring? Furthermore, Iba-1 and Lgals3 are also highly expressed in the macrophage like cells on the vitreal surface of the retina, suggesting that these cells may be confounding the signals we have attributed to microglia. Thus, one must ask: what are the relative contributions of astrocytes, retinal surface macrophages, and – potentially – the outer retinal injury sites to our transcriptional data? In order to answer this essential question, I turned once again to the pulloff technique to isolate samples, using immunohistochemistry rather than molecular biology to investigate the characteristics of these tissue samples.

During the initial experiments to isolate tissue for transcriptomics, I observed that retinas from treated animals were more fragile, and were more likely to display only partial adherence to the coverslip during sample isolation. However, on the basis of imaging (and later, the characterization of cell type specific markers in Fig 5) we determined that while this altered the total amount of tissue isolated, it largely did not alter the makeup of that tissue. That is, the surface area of samples acquired from treated tissue differed from those from controls, but the thickness of the samples did not. The one notable exception to this trend were sites that appeared to be damage from dissection tools contacting the retina, which I had previously observed could lead to loss of tissue or imaging artifacts.

However, staining of additional pulloff samples isolated from treated retinas revealed that these instead likely represented the sites of laser-induced injury, which apparently resisted the enzymatic dissociation we employed to separate the innermost layer from the rest of the retina. These sites share a number of key characteristics – a small (200-300um) core surrounded by hypertrophic astrocytes, typically at the edge of isolated tissue, that was difficult to image in brightfield, but which stained for markers such as C3 and Iba-1. Although we observed 1-3 peripheral retinal scars in each of the 6 samples we investigated for this phenomenon, we suspect these may only represent the most central sites of damage, as areas peripherally located relative to these sites typically had poor adhesion during the isolation process. These scars show varying degrees of de-cellularization, ranging from complete absence of detectable cells in the central lesion to patterns of surviving cells that suggest partial sparing of the vasculature. Curiously, despite the ubiquity of highly reactive astrocytes surrounding these sites, none were observed in the lesion's core, in apparent contradiction with many of the sites with outer retinal damage assessed via cryosection. It is unclear whether this is a feature of the majority of injury sites, or only those isolated by the pulloff – that is, the loss of astrocytes in the vitreal boundary region may be a requirement for the adherence of these sites to the coverslip, as these astrocytes would typically form the innermost surface of the retina

and present a barrier to adhesion. It is also possible that the apparent absence of astrocytes, reactive or otherwise, in the lesion core is an artifact of the dense nature of these sites, with antibodies only weakly penetrating to the underlying astrocytes. A clue to the ability of these sites to resist enzymatic dissociation is readily apparent in the transcriptional data, where the gene coding for Collagen 1 is upregulated by two orders of magnitude with high statistical significance. Essentially, the apparently fibrotic scarring at these sites appears to have rendered them resistant to the relatively mild collagenase treatment that readily enables separation of retinal layers, ensuring the enrichment of this gene by promoting the inclusion of tissue that expresses it.

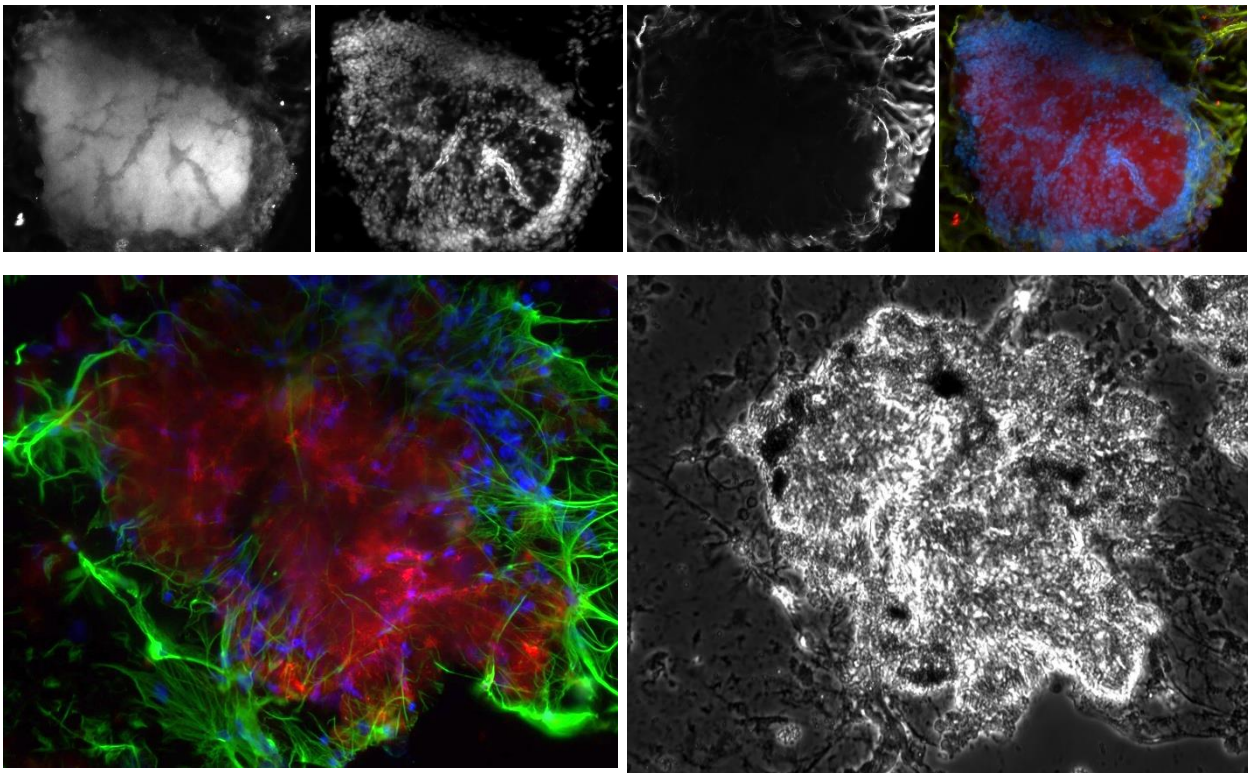

Figure 17: Scar sites adhere to the coverslip during pull-offs. Upper (left to right): A scar site showing high levels of C3 expression, partial decellurization, and absence of glia in the core region. Upper right: Composite image of this scar site, with C3 in red, Hoecsht nuclear stain in blue, and GFAP in green. Lower: Another adherent scar site. Left: Stained with GFAP (green), Iba-1 (red) and Hoecsht nuclear stain (blue). Right: Brightfield.

Although the likely presence of vitreal surface macrophages in our pulloff samples is less mysterious – their adherence to the inner limiting membrane all but assures they would be isolated by such an approach whenever they are present – I nonetheless utilized staining of the pull-offs to gain greater understanding of this phenomenon as well. Although I observed small numbers of these cells on most of the sectioned tissue, their location outside the retina raises the possibility that even careful processing might nevertheless dislodge these cells, masking their presence. Initially we did not observe clear Iba-1+ cells on the pulloff samples from the treated animals, but found strangely large (>100 um) circular regions of modest iba-1 staining.

However, on further examination, we realized that the most likely explanation was that the macrophages on the vitreal side of the ILM were in effect being crushed by the glass coverslips placed to isolate the astrocytes. These cells were found distributed across the retinal surface (Fig 18), not only near the lesion sites, and instances of engulfment by Iba-1+ cells in the RGC layer (Fig 11) and at the retinal surface detected by staining of sections suggests that at least in part these macrophages participate in the elimination of dead and dying retinal ganglion cells.

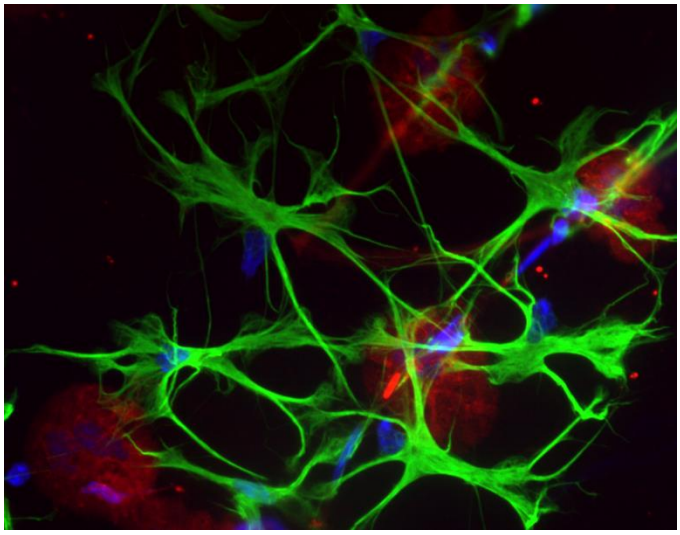

Figure 18: Iba-1+ (red) positive cells, likely macrophages, isolated by pull-off alongside retinal astrocytes (GFAP, green).

Discussion

In order to better understand the response of retinal astrocytes to elevated intraocular pressure, I employed my pulloff method of isolation to enrich for this cell population and minimize confounding contributions to the transcriptomic data from other cell types. While this approach performed as expected on intact, untreated tissue, treated retinas from the *in vivo* model displayed distinct features – retinal surface macrophages and enzyme resistant 'scars' – that resulted in the isolation of additional cell populations not found in the control. Although the additional tissue isolated at sites of scarring is largely an artifact of the treatment mechanism, the presence of surface macrophages is a more complicated matter. Amoeboid macrophages were abundantly present at the sites of injury, yet they were also found in central regions – sometimes engaged in obvious engulfment of cells of the inner retina – distant from the peripherally located lesions. The extent to which these Iba-1+ cells are the result of localized photocoagulation injury versus diffuse, OHT-mediated RGC death remains an open question, and would require the experiment to be reprised with a model that avoids focal scarring. Such an experiment might answer other questions as well – although we have attributed most of the tissue consistency changes we observed to focal damage from laser treatment, the induction of GFAP expression in Müller cells is expected to alter their structural properties. As such an upregulation is observed with slower acting models that are entirely pressure-driven, we cannot say with certainty that changes to the cellular composition of isolated samples would be absent under these conditions.

However, while certain elements of the experiment unfolded in an unexpected manner, we also recognize that in many regards the tissue isolation approach performed as intended. Although neither the surface macrophages nor the photocoagulation scars were expected at the outset of the experiment, the inclusion of these cells in our tissue samples – from which an estimated >99% of retinal cells are excluded – enabled the detection of transcriptional signatures of these events, facilitating their subsequent detection via immunohistochemistry. Furthermore, because the same isolation parameters can be used for both RNA isolation and tissue staining, we were able to verify the adhesion of scar sites, elucidating the most likely mechanism by which markers found mainly in the outer layers of the retina could be detected in a sample consisting primarily of retinal surface cells.

Astrocytic and Müller Cell Response

Transcriptional analysis of isolated tissue samples suggested the clear presence of a reactive astrocyte response. While the reality of these results proved to be more complex – many markers of astrocyte reactivity overlap with those of peripheral immune response, which were also observed in transcriptional and IHC results – severe localized hypertrophy and Lcn2 staining of retinal astrocytes confirm that these cells indeed undergo reactivity in response to the model. Although I was optimistic that the panels published by the Barres group would be

sufficient to detect the signature of astrocyte reactivity even in heterogenous bulk samples, this experience highlights the importance of using multiple approaches in validating results.

Although they were not the population of retinal glia I sought to investigate, I found that a number of our markers – such as Lgals3 and (potentially) Lcn2 – were upregulated more clearly in Müller cells than retinal astrocytes, most likely a function of their proximity to the scar sites. Although Müller cells are closely related to astrocytes, and sometimes referred to as 'astroglia', they possess clear morphological differences and specialization to their highly conserved niche; however, in response to focal injury at the scar sites they underwent severe gliosis and adopted more astrocyte-like morphologies. This phenomenon has been previously documented to occur as a response to photocoagulation, and is apparently a function of the darkly pigmented cells of the RPE absorbing large amounts of the laser's energy, which then diffuses as heat into the retina, inducing cytotoxicity and reactivity [62]. Müller cells only sporadically adhere during pulloff from the untreated retina, and although the Müller cell marker CD29 underwent statistically significant upregulation (adj. p-value 0.005) in treated vs control tissue, the increase was modest enough (~50%) that I discounted the likely impact on our transcriptional results. However, this line of reasoning assumed a relatively uniform response across the retina, rather than the possibility that small numbers of highly reactive Müller cells were driving the increased contribution to the transcriptional signal.

The differential roles of astrocytes and Müller cells remains a major unknown of glial research in the retina. Although the role of astrocytes in the development of the retinal vasculature are well documented, in the mature retina Müller cells are the more completely understood class of glia [64-67]. Generally, the morphology of retinal neurons and glia follows one of two types: narrow, transverse cells including rod and cone photoreceptors, bipolar cells, and Müller cells; and "tiling" cells that run parallel to the retinal surface, such as horizontal cells, retinal ganglion cells, and astrocytes. The latter morphology is well suited for cells that aggregate signals from a larger area, and astrocytes in the brain are known to modulate their homeostatic buffering through large, connected networks [68, 69]. As previous work studying glial connectivity in the retina demonstrated widespread coupling between retinal astrocytes with a unidirectional flow into neighboring Müller cells, it may be that retinal astrocytes play a distinct role in coordinating broader scale responses while Müller cells provide a more focused response in a narrow area, consistent with their highly localized response to focal injury in this model [70, 71]. However, owing to the focal scars induced by the model – which resulted in both severe gliosis in a percentage of Müller cells and an oversampling of those same highly reactive cells – I am unable to isolate an astrocyte specific signal from these results that could contribute to the resolution of these questions.

Microglia Markers

Initially, the highly significant changes in microglial markers, particularly those associated with neurodegenerative diseases in the brain, led me to expect that closely related phenomena were taking place in the treated retinas. Indeed, the enrichment for markers of MgND and DAM

phenotypes exceeded even that of astrocyte reactivity markers. However, the presence of infiltrating immune cells – both at the retinal surface and in the deeper scar tissue – confounds this interpretation. Although many of these markers may really be upregulated in the resident microglia, as per my initial interpretation, determining the validity of this hypothesis would require verification on a gene-by-gene basis via either additional immunostaining or *in situ* hybridization of target mRNA sequences. As with astrocyte markers, these results emphasize the importance of careful technique choice for validation; even without the unexpected contribution of scar tissue and peripheral immune cells, the presence of Lgals3 in the abundant Müller cells of the retina would have confounded analysis by approaches such as RT-qPCR or western blotting.

More unexpected than Lgals3+ Müller cells or infiltrating peripheral immune cells, however, was the localization of Gpnmb. Based on its involvement in the glaucoma-like phenotype of dba/2j mice and more recent reports of its expression by plaque-adjacent microglia in Alzheimer's disease, I had considered this gene to be perhaps the most promising result in the initial data. While I was surprised to find it only infrequently in Iba-1+ cells and instead expressed primarily by RPE cells, the narrow circumstances of its expression – at sites of retinal detachment with still living photoreceptors – hints at a crucial but unknown function for glycoprotein NMB, the protein for which it codes. Although little is known, the protein-protein STRING Interaction Network for this gene shows an association with the class II histocompatibility complexes used in immune surveillance through the member HLA-DRB5, as well as with the well-studied receptor EGFR and its ligand HB-EGF, an essential factor for astrocyte survival [72-74]. I look forward to the field's ongoing work to understand the function of this mysterious gene.

Ambiguous Markers and Overall Thoughts

Finally, I must consider elements of the experiment that gave more ambiguous results. Although both were highly upregulated, neither C3 nor Cox-2 stained individual cells, leaving uncertainty as to the A1 vs A2 polarization of the reactive astrocytes, and as to whether the unexpectedly reactive Müller cells are polarized in a similar fashion. However, this classification schema is itself under careful reconsideration, with a recent consensus statement warning against over-reliance on this framework to draw conclusions about astrocyte behavior [35]. Furthermore, a recent meta-analysis suggests that many of these markers – most of which were significantly upregulated in my results – are more closely linked to the acute neurological injury induced by favored models than they are to the chronic neurodegeneration that characterizes human disease, which would be consistent with the outcome of this experiment [75].

Conversely, while the marker Ki-67 clearly stained a small number of individual nuclei, its relatively limited expression was restricted to sites of focal laser injury; further efforts to identify what populations of cells may have expressed it were not made. The pro-synaptogenic Thrombospondin-1 presented a similar ambiguity, as it was found primarily in the extracellular matrix, revealing localization to detached photoreceptors but not indicating the cell type

responsible for its secretion. Careful investigation of the retinal ganglion cell layer revealed no difference in Thrombospondin expression in this area between control and treated retinas; both the presence at detached photoreceptors and absence among retinal ganglion cells were a surprise, and raise questions about the role of this putatively neuroprotective protein in the damaged retina [59].

Although I was surprised that the combination of the *in vivo* model – which gives satisfactory results for the study of ocular hypertension on the optic nerve – and my cell isolation method – which typically isolates layers as thin as a single cell at the inner retinal surface – did not produce the anticipated clarity regarding the response of retinal astrocytes to elevated IOP, I must admit a certain satisfaction in the clarity my approach provided. Many studies of the retina utilize bulk tissue studied through a particular set of markers and lack the ability to reconstruct the basis for their detection. This is especially problematic given that many of the models frequently employed for the study of glaucoma – such as the injection of microbeads into the anterior chamber – involve their own forms of acute, non-glaucomatous damage. Had I relied on additional bulk tissue approaches such as western blotting or rt-qPCR, the bimodal distribution of injury and reactivity – modest in the central retina, severe at the peripheral scars – that characterizes this model would have been overlooked; instead, these changes would essentially be averaged across the retina, potentially setting future investigators off on the wrong path.

A particular strength of my cell isolation method for retinal astrocytes, as mentioned above, is the ability to use the same protocol and parameters for both quantitative molecular biology assays and for immunostaining. Both approaches have their advantages and disadvantages, and so are frequently employed together for a given study; however, particularly when cell sorting techniques like FACS or MACS are employed, sample preparation typically differs for the two approaches, making direct correlation of results difficult. Although modern technologies like RNA-seq offer tremendous investigatory potential, careful scrutiny is still required – through older, low through-put techniques such as immunostaining – to ensure that interpretation of these large data sets corresponds to the reality.

As discussed at the end of Chapter II, the astrocyte pulloff method demonstrates potential for future work on functional applications; with the prospect of modifying the technique to allow for nearly immediate *in vitro* study of astrocytes a particularly intriguing possibility. However, even more modest aspirations stand to benefit from this method. A variety of models that produce generalized IOP increases – some chronic, some acute – have been used to study elements of glaucoma, but the ability to isolate the changes occurring in the innermost retinal layer and the astrocytes therein is generally lacking. Moreover, existing isolation techniques are even more limited for larger animal models, such as non-human primates, or for donor tissue from truly glaucomatous eyes. Future experiments involving this method may yet provide a key insight to the behavior of retinal astrocytes under pressure.

References

1. Tham, Y.C., et al., *Global prevalence of glaucoma and projections of glaucoma burden through 2040: a systematic review and meta-analysis.* Ophthalmology, 2014. **121**(11): p. 2081-90.
2. Sivak, J.M., *The aging eye: common degenerative mechanisms between the Alzheimer's brain and retinal disease.* Invest Ophthalmol Vis Sci, 2013. **54**(1): p. 871-80.
3. Weinreb, R.N., et al., *Primary open-angle glaucoma.* Nat Rev Dis Primers, 2016. **2**: p. 16067.
4. Weinreb, R.N., T. Aung, and F.A. Medeiros, *The pathophysiology and treatment of glaucoma: a review.* JAMA, 2014. **311**(18): p. 1901-11.
5. Williams, P.R., et al., *Axon Regeneration in the Mammalian Optic Nerve.* Annu Rev Vis Sci, 2020. **6**: p. 195-213.
6. Quigley, H.A., et al., *Morphologic Changes in the Lamina Cribrosa Correlated with Neural Loss in Open-Angle Glaucoma.* American Journal of Ophthalmology, 1983. **95**(5): p. 673-691.
7. Hernandez, M.R. and J.D. Pena, *The optic nerve head in glaucomatous optic neuropathy.* Arch Ophthalmol, 1997. **115**(3): p. 389-95.
8. Sigal, I.A., et al., *Predicted extension, compression and shearing of optic nerve head tissues.* Exp Eye Res, 2007. **85**(3): p. 312-22.
9. Almasieh, M., et al., *The molecular basis of retinal ganglion cell death in glaucoma.* Prog Retin Eye Res, 2012. **31**(2): p. 152-81.
10. Watanabe, T. and M.C. Raff, *Retinal astrocytes are immigrants from the optic nerve.* Nature, 1988. **332**(6167): p. 834-7.
11. Stone, J. and Z. Dreher, *Relationship between Astrocytes, Ganglion-Cells and Vasculature of the Retina.* Journal of Comparative Neurology, 1987. **255**(1): p. 35-49.
12. Barres, B.A., *The mystery and magic of glia: a perspective on their roles in health and disease.* Neuron, 2008. **60**(3): p. 430-40.
13. Sofroniew, M.V., *Astrocyte Reactivity: Subtypes, States, and Functions in CNS Innate Immunity.* Trends Immunol, 2020. **41**(9): p. 758-770.
14. Biesecker, K.R., et al., *Glial Cell Calcium Signaling Mediates Capillary Regulation of Blood Flow in the Retina.* J Neurosci, 2016. **36**(36): p. 9435-45.
15. Sun, D., S. Moore, and T.C. Jakobs, *Optic nerve astrocyte reactivity protects function in experimental glaucoma and other nerve injuries.* J Exp Med, 2017. **214**(5): p. 1411-1430.
16. Hernandez, M.R., *The optic nerve head in glaucoma: role of astrocytes in tissue remodeling.* Progress in Retinal and Eye Research, 2000. **19**(3): p. 297-321.
17. Kerr, N.M., et al., *Gap junction protein connexin43 (GJA1) in the human glaucomatous optic nerve head and retina.* J Clin Neurosci, 2011. **18**(1): p. 102-8.
18. Soto, I. and G.R. Howell, *The complex role of neuroinflammation in glaucoma.* Cold Spring Harb Perspect Med, 2014. **4**(8).
19. Jeon, C.J., E. Strettoi, and R.H. Masland, *The major cell populations of the mouse retina.* J Neurosci, 1998. **18**(21): p. 8936-46.
20. Punal, V.M., et al., *Large-scale death of retinal astrocytes during normal development is non-apoptotic and implemented by microglia.* PLoS Biol, 2019. **17**(10): p. e3000492.
21. Backstrom, J.R., et al., *Phenotypes of primary retinal macroglia: Implications for purification and culture conditions.* Exp Eye Res, 2019. **182**: p. 85-92.
22. Lukowski, S.W., et al., *A single-cell transcriptome atlas of the adult human retina.* EMBO J, 2019. **38**(18): p. e100811.

23. Zhang, L., et al., *Establishment and Characterization of an Acute Model of Ocular Hypertension by Laser-Induced Occlusion of Episcleral Veins.* Invest Ophthalmol Vis Sci, 2017. **58**(10): p. 3879-3886.
24. Tribble, J.R., et al., *When Is a Control Not a Control? Reactive Microglia Occur Throughout the Control Contralateral Pathway of Retinal Ganglion Cell Projections in Experimental Glaucoma.* Transl Vis Sci Technol, 2021. **10**(1): p. 22.
25. Gallego, B.I., et al., *IOP induces upregulation of GFAP and MHC-II and microglia reactivity in mice retina contralateral to experimental glaucoma.* J Neuroinflammation, 2012. **9**: p. 92.
26. Zamanian, J.L., et al., *Genomic analysis of reactive astrogliosis.* J Neurosci, 2012. **32**(18): p. 6391-410.
27. Liddelow, S.A., et al., *Neurotoxic reactive astrocytes are induced by activated microglia.* Nature, 2017. **541**(7638): p. 481-487.
28. Krasemann, S., et al., *The TREM2-APOE Pathway Drives the Transcriptional Phenotype of Dysfunctional Microglia in Neurodegenerative Diseases.* Immunity, 2017. **47**(3): p. 566-581 e9.
29. Keren-Shaul, H., et al., *A Unique Microglia Type Associated with Restricting Development of Alzheimer's Disease.* Cell, 2017. **169**(7): p. 1276-1290 e17.
30. Liu, H.H., et al., *Comparison of laser and circumlimbal suture induced elevation of intraocular pressure in albino CD-1 mice.* PLoS One, 2017. **12**(11): p. e0189094.
31. Bucala, R. and I. Shachar, *The integral role of CD74 in antigen presentation, MIF signal transduction, and B cell survival and homeostasis.* Mini Rev Med Chem, 2014. **14**(14): p. 1132-8.
32. Pang, S.S., et al., *The cryo-EM structure of the acid activatable pore-forming immune effector Macrophage-expressed gene 1.* Nat Commun, 2019. **10**(1): p. 4288.
33. Lam, G.Y., J. Huang, and J.H. Brumell, *The many roles of NOX2 NADPH oxidase-derived ROS in immunity.* Semin Immunopathol, 2010. **32**(4): p. 415-30.
34. Ricard-Blum, S., *The collagen family.* Cold Spring Harb Perspect Biol, 2011. **3**(1): p. a004978.
35. Escartin, C., et al., *Reactive astrocyte nomenclature, definitions, and future directions.* Nat Neurosci, 2021.
36. Scarl, R.T., et al., *STEAP4: its emerging role in metabolism and homeostasis of cellular iron and copper.* J Endocrinol, 2017. **234**(3): p. R123-R134.
37. Vicuna, L., et al., *The serine protease inhibitor SerpinA3N attenuates neuropathic pain by inhibiting T cell-derived leukocyte elastase.* Nat Med, 2015. **21**(5): p. 518-23.
38. Clarke, L.E., et al., *Normal aging induces A1-like astrocyte reactivity.* Proc Natl Acad Sci U S A, 2018. **115**(8): p. E1896-E1905.
39. Stephan, A.H., B.A. Barres, and B. Stevens, *The complement system: an unexpected role in synaptic pruning during development and disease.* Annu Rev Neurosci, 2012. **35**: p. 369-89.
40. Uhlen, M., et al., *Proteomics. Tissue-based map of the human proteome.* Science, 2015. **347**(6220): p. 1260419.
41. Chang, B., et al., *Interacting loci cause severe iris atrophy and glaucoma in DBA/2J mice.* Nat Genet, 1999. **21**(4): p. 405-9.
42. Howell, G.R., et al., *Absence of glaucoma in DBA/2J mice homozygous for wild-type versions of Gpnmb and Tyrp1.* BMC Genet, 2007. **8**: p. 45.
43. Huttenrauch, M., et al., *Glycoprotein NMB: a novel Alzheimer's disease associated marker expressed in a subset of activated microglia.* Acta Neuropathol Commun, 2018. **6**(1): p. 108.
44. Illes, P., et al., *P2X receptors and their roles in astroglia in the central and peripheral nervous system.* Neuroscientist, 2012. **18**(5): p. 422-38.
45. Borrego, F., et al., *The CD94/NKG2 Family of Receptors: From Molecules and Cells to Clinical Relevance.* Immunologic Research, 2006. **35**(3): p. 263-278.

46. Mancino, R., et al., *Glaucoma and Alzheimer Disease: One Age-Related Neurodegenerative Disease of the Brain.* Curr Neuropharmacol, 2018. **16**(7): p. 971-977.
47. Butovsky, O. and H.L. Weiner, *Microglial signatures and their role in health and disease.* Nat Rev Neurosci, 2018. **19**(10): p. 622-635.
48. Yadav, S. and A. Surolia, *Lysozyme elicits pain during nerve injury by neuronal Toll-like receptor 4 activation and has therapeutic potential in neuropathic pain.* Sci Transl Med, 2019. **11**(504).
49. Goodridge, H.S., et al., *Activation of the innate immune receptor Dectin-1 upon formation of a 'phagocytic synapse'.* Nature, 2011. **472**(7344): p. 471-5.
50. Gautier, E.L., et al., *Gene-expression profiles and transcriptional regulatory pathways that underlie the identity and diversity of mouse tissue macrophages.* Nat Immunol, 2012. **13**(11): p. 1118-28.
51. Davis, C.H., et al., *Transcellular degradation of axonal mitochondria.* Proc Natl Acad Sci U S A, 2014. **111**(26): p. 9633-8.
52. Puigdellivol, M., D.H. Allendorf, and G.C. Brown, *Sialylation and Galectin-3 in Microglia-Mediated Neuroinflammation and Neurodegeneration.* Front Cell Neurosci, 2020. **14**: p. 162.
53. Naude, P.J., et al., *Lipocalin 2: novel component of proinflammatory signaling in Alzheimer's disease.* FASEB J, 2012. **26**(7): p. 2811-23.
54. Lee, S., et al., *Lipocalin-2 is an autocrine mediator of reactive astrocytosis.* J Neurosci, 2009. **29**(1): p. 234-49.
55. Jha, M.K., et al., *Diverse functional roles of lipocalin-2 in the central nervous system.* Neurosci Biobehav Rev, 2015. **49**: p. 135-56.
56. Kuehn, M.H., et al., *Retinal synthesis and deposition of complement components induced by ocular hypertension.* Exp Eye Res, 2006. **83**(3): p. 620-8.
57. Minghetti, L., *Cyclooxygenase-2 (COX-2) in inflammatory and degenerative brain diseases.* J Neuropathol Exp Neurol, 2004. **63**(9): p. 901-10.
58. Christopherson, K.S., et al., *Thrombospondins are astrocyte-secreted proteins that promote CNS synaptogenesis.* Cell, 2005. **120**(3): p. 421-33.
59. Bray, E.R., et al., *Thrombospondin-1 Mediates Axon Regeneration in Retinal Ganglion Cells.* Neuron, 2019. **103**(4): p. 642-657 e7.
60. Perez de Sevilla Muller, L., et al., *Melanopsin ganglion cells are the most resistant retinal ganglion cell type to axonal injury in the rat retina.* PLoS One, 2014. **9**(3): p. e93274.
61. Scholzen, T. and J. Gerdes, *The Ki-67 protein: From the known and the unknown.* Journal of Cellular Physiology, 2000. **182**(3): p. 311-322.
62. Chidlow, G., et al., *Glial cell and inflammatory responses to retinal laser treatment: comparison of a conventional photocoagulator and a novel, 3-nanosecond pulse laser.* Invest Ophthalmol Vis Sci, 2013. **54**(3): p. 2319-32.
63. Reichenbach, A. and A. Bringmann, *Müller Cells in the Healthy and Diseased Retina*. Müller Cells in the Healthy and Diseased Retina. Vol. 25. 2010. 1-417.
64. Selvam, S., T. Kumar, and M. Fruttiger, *Retinal vasculature development in health and disease.* Prog Retin Eye Res, 2018. **63**: p. 1-19.
65. Tao, C. and X. Zhang, *Retinal Proteoglycans Act as Cellular Receptors for Basement Membrane Assembly to Control Astrocyte Migration and Angiogenesis.* Cell Rep, 2016. **17**(7): p. 1832-1844.
66. Duan, L.J., et al., *Retinal Angiogenesis Regulates Astrocytic Differentiation in Neonatal Mouse Retinas by Oxygen Dependent Mechanisms.* Sci Rep, 2017. **7**(1): p. 17608.
67. Vecino, E., et al., *Glia-neuron interactions in the mammalian retina.* Prog Retin Eye Res, 2016. **51**: p. 1-40.
68. Giaume, C., et al., *Astroglial networks: a step further in neuroglial and gliovascular interactions.* Nat Rev Neurosci, 2010. **11**(2): p. 87-99.

69. Scemes, E. and D.C. Spray, *The astrocytic syncytium*, in *Non-Neuronal Cells of the Nervous System: Function and Dysfunction*. 2003. p. 165-179.
70. Zahs, K.R. and E.A. Newman, *Asymmetric gap junctional coupling between glial cells in the rat retina.* Glia, 1997. **20**(1): p. 10-22.
71. Newman, E.A. and K.R. Zahs, *Calcium waves in retinal glial cells.* Science, 1997. **275**(5301): p. 844-7.
72. Szklarczyk, D., et al., *STRING v11: protein-protein association networks with increased coverage, supporting functional discovery in genome-wide experimental datasets.* Nucleic Acids Res, 2019. **47**(D1): p. D607-D613.
73. Rock, K.L., E. Reits, and J. Neefjes, *Present Yourself! By MHC Class I and MHC Class II Molecules.* Trends Immunol, 2016. **37**(11): p. 724-737.
74. Puschmann, T.B., et al., *HB-EGF affects astrocyte morphology, proliferation, differentiation, and the expression of intermediate filament proteins.* J Neurochem, 2014. **128**(6): p. 878-89.
75. Das, S., et al., *Meta-analysis of mouse transcriptomic studies supports a context-dependent astrocyte reaction in acute CNS injury versus neurodegeneration.* J Neuroinflammation, 2020. **17**(1): p. 227.

Appendix A

Primary Antibodies

Antigen	Product #	Host Species	Concentration
GFAP	ab53554	Goat	1:1000
GFAP	ab7260	Rabbit	1:1000
Iba-1	ab178847	Rabbit	1:500
C3	ab200999	Rabbit	1:250
Gpnmb	AF2330	Goat	1:500
Thrombospondin-1	sc-59887	Mouse	1:250
Lgals3	AF1197	Goat	1:250
Cox-2	sc-376861	Mouse	1:250
Lcn2	AF1857	Goat	1:250
Ki-67	CST-9129	Rabbit	1:250

A Novel Method Facilitates Acute Isolation of Rat Retinal Astrocytes

4396 - A0287

Paul F Cullen & John G Flanagan
paul.f.cullen@berkeley.edu

Berkeley Optometry & Vision Science

Purpose

To develop a method for the rapid isolation of retinal astrocytes that preserves their *in vivo* characteristics for functional and transcriptional analysis.

Background

As our understanding of astrocytes' essential role in maintaining neuronal health improves, they are increasingly being investigated as mediators of neuroprotection and neurodegeneration in disease states.[1] Recent work suggests that retinal astrocytes secrete factors that are directly neuroprotective in a chronic ocular hypertension model that mimics some aspects of glaucoma.[2] Paradoxically, this protection appears to be diminished in astrocytes exposed to chronic disease states. The lack of a means to acutely isolate retinal astrocytes has stymied efforts to understand the transcriptional and functional alterations that undergird these changes. An unusual approach developed by Simon & Thanos to mechanically isolate retinal ganglion cells from adult rats served as an inspiration for our method.[3]

Results

- Mean astrocyte yield density per quantified region in 9 animals was 249 astrocytes/mm^2 (SD ± 48) and ranged from 162/mm^2 to 309/mm^2.
- In many regions astrocyte coverage was nearly continuous, except for areas occupied by blood vessels, and connections formed by astrocyte processes were preserved.

Conclusion

We show that it is possible to selectively isolate astrocytes from the inner retina, separating them from the bulk of tissue, including Müller cells with which they share the cell surface markers commonly used to prospectively isolate brain astrocytes. This has enabled the investigation of acutely isolated cells for functional and transcriptional studies.

Berkeley UNIVERSITY OF CALIFORNIA

Methods

1. Female Wistar rats from 4 to 6 weeks old were euthanized and their eyes subsequently enucleated and immersed in 4°c PBS. Removal of the anterior segment and vitreous was performed under a dissection microscope, with .4% Trypan blue used to visualize the vitreous and any damage to retinal tissue.

2. Retinas were gently extracted from the eye cup, with 4 relieving cuts made halfway to the optic nerve head to allow for flattening. A 1mm biopsy punch was used to remove the optic nerve head, and the retina was cut into individual quarters mounted on filter paper. A 12mm coverslip was stacked atop the retina for incubation.

3. After assembly, the retinal stack was inverted so that the filter paper rests atop the retina. Type II collagenase was added dropwise to the filter directly above the retina, and a 200mg weight was added to ensure the tissue pressed flat against the coverslip before incubation at 37°c in a humidified incubator.

4. After incubation, the weight was removed and the stack inverted. Gentle lifting of the coverslip separates adherent astrocytes and superficial blood vessels from the underlying retinal tissue.

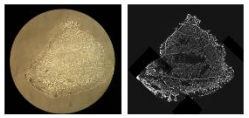

Left: adherent retinal tissue visualized in brightfield, right: the same sample after staining for the astrocyte marker GFAP.

5. For quantification, glass-adherent tissue was fixed in 4% PFA for 20 minutes at room temperature. Subsequently, samples were stained for the astrocyte marker GFAP for quantification of yield, or with additional antibodies to analyze the composition and integrity of the isolated tissue layer. Quantification was performed on 1mm^2 regions of tissue to determine astrocyte density.

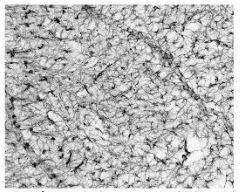

A 1mm^2 section of retina, stained with α-GFAP antibodies and used for quantification.

Alternatively, live adherent tissue can be detached from coverslips by brief incubation in .25% Trypsin with .1mM EDTA for further processing and dissociation.

Representative Images

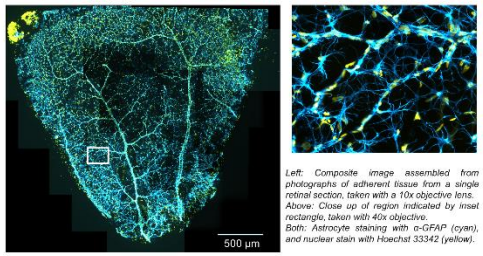

Left: Composite image assembled from photographs of adherent tissue from a single retinal section, taken with a 10x objective lens. Above: Close up of region indicated by inset rectangle, taken with 40x objective. Both: Astrocyte staining with α-GFAP (cyan), and nuclear stain with Hoechst 33342 (yellow).

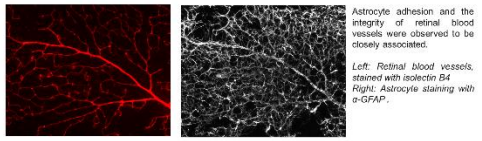

Astrocyte adhesion and the integrity of retinal blood vessels were observed to be closely associated.

Left: Retinal blood vessels, stained with isolectin B4
Right: Astrocyte staining with α-GFAP.

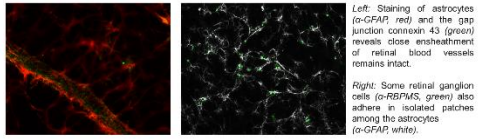

Left: Staining of astrocytes (α-GFAP, red) and the gap junction connexin 43 (green) reveals close ensheathment of retinal blood vessels remains intact.

Right: Some retinal ganglion cells (α-RBPMS, green) also adhere in isolated patches among the astrocytes (α-GFAP, white).

References

1. Pekny M & Pekna M. Astrocyte reactivity and reactive astrogliosis: costs and benefits. *Physiological Reviews*. 2014; 94(4): 1077-1098.
2. Lye-Barthel, Wei J, Liu H-H, et al. Astrocyte-derived lipocalin A4 and S4 prevents neuroprotection from acute and chronic injury. *J Clin Invest*. 2013;123(7):4403-4414.
3. Simon F & Thanos S. Combined methods of retrograde staining, layer-separation and viscoelastic cell stabilization to isolate retinal ganglion cells in adult rats. *J Neuroscience Methods*. 1998; 83(2):113-124.

Berkeley Optometry & Vision Science

A Novel Enrichment Method Reveals Transcriptional Changes in Retinal Astrocytes Exposed to Elevated IOP

Paul F Cullen, Yujia Yang, Sandra Muroy, Lu Chen and John G Flanagan
paul.f.cullen@berkeley.edu

ARVO 2021 Travel Grant Recipient

Purpose

Retinal astrocytes, along with those of the optic nerve, have been shown to play key roles in the survival of retinal ganglion cells (RGCs), particularly in response to glaucomatous stress. The mechanisms regulating this protection, however, are poorly understood, as these cells populate the retina sparsely and are difficult to isolate acutely. By utilizing a novel isolation method and examining the transcriptomic data from retinal astrocytes exposed to elevated intraocular pressure (IOP), we aim to understand the response of these cells to ocular hypertension.

Methods

Adult male C57/B6 mice underwent laser-induced episcleral vein cauterization, resulting in elevated IOP[1]. After one week, treated animals and age-matched controls were euthanized and highly enriched populations of retinal astrocytes were isolated by a combination of enzymatic dissociation and mechanical separation. Purified RNA from these samples was used to generate cDNA libraries for next generation sequencing, and differential gene expression was analyzed after bioinformatic cleanup.

Figure 1: Enzymatic dissociation enables mechanical separation of retinal astrocytes

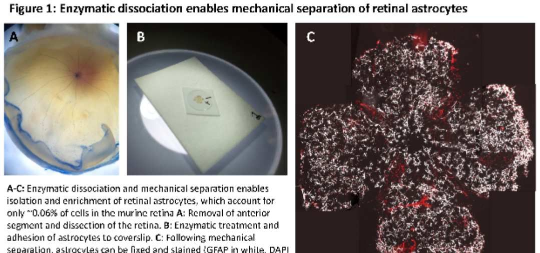

A-C: Enzymatic dissociation and mechanical separation enables isolation and enrichment of retinal astrocytes, which account for only ~0.06% of cells in the murine retina **A:** Removal of anterior segment and dissection of the retina. **B:** Enzymatic treatment and adhesion of astrocytes to coverslip. **C:** Following mechanical separation, astrocytes can be fixed and stained (GFAP in white, DAPI pseudo-colored in red) or transferred to RNA preserving buffer for transcriptomics.

Results

Figure 2: Laser treatment induces elevated intraocular pressure, retinal ganglion cell loss

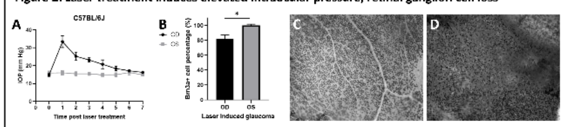

A: Intraocular pressure rises after episcleral vein cauterization, before returning to baseline at day 7. **B:** Retinal ganglion cell survival (OD), as measured by Brn3a+ cell counts, normalized to contralateral controls (OS). **C** and **D:** Retinal ganglion cell loss visualized by retrograde dye filling of surviving RGCs (**C:** control retina; **D:** treated retina)

Figure 3: Large scale gene expression changes in response to treatment

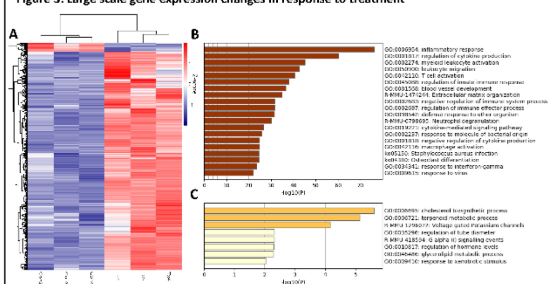

A: Heatmap of gene expression. With thresholds of log2-fold change > 1 and adjusted p-value <0.05, 1129 genes met inclusion criteria for upregulation, while 44 met criteria for downregulation. **B** and **C:** Biological enrichment categories for upregulated (B) and downregulated (C) genes.

Figure 4: Markers of reactive astrocytes[2] and activated microglia[3] over-represented in top 10 genes

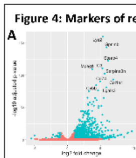

B

Gene	Significance	Log2-fold	Adj P val
Lyz2	Antimicrobial, cleaves bacterial cell wall peptidoglycans (DAM)	5.4	9.02E-161
Gpnmb	Microglial regulation of neuroinflammation (DAM)	5.9	3.13E-144
Steap4	Metalloreductase, mediates iron availability during inflammation (RA)	6.[illegible]	2.55E-128
C3	Targets pathogens and debris for elimination, involved in synaptic pruning (RA)	5.[illegible]	1.45E-111
Mpeg1	Induces pores in phagocytized bacteria, sensitizing them to attack	3.6	1.92E-110
Serpina3n	Inhibitor of immune proteases (RA)	5.6	3.50E-103
Col1a1	Type I collagen	6.9	3.05E-94
Cd74	Major histocompatibility complex II, involved in immune surveillance	4.9	2.20E-91
Cybb	Generates superoxide utilized in the killing of phagocytized pathogens (DAM)	4.4	1.98E-85
Lgals3/Mac2	Potential regulator of phagocytosis in both astrocytes[2] and microglia[3] (DAM)	5.9	3.05E-82

A: Volcano plot of 1129 upregulated and 44 downregulated genes above threshold, top 10 genes by adjusted P-value labeled. **B:** Table of top 10 genes with functional annotation, log2-fold expression changes, & adjusted P-values. (RA – reactive astrocytes[2], DAM – Disease associated microglia[3]).

Figure 5: Markers of astrocyte reactivity[2] induced by laser treatment

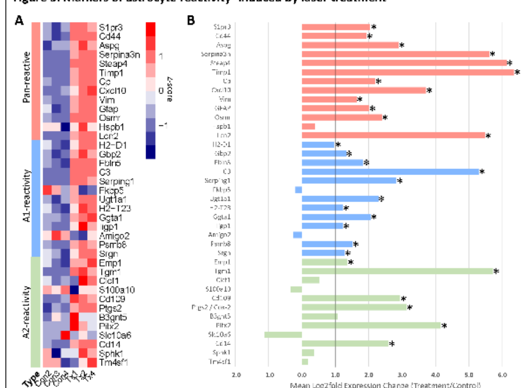

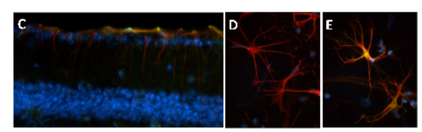

A: Heatmap of differential gene expression of astrocyte reactivity markers proposed by Barres lab[2]. **B:** Log2-fold expression changes in reactivity markers (* adj. p-value < 0.05). **C-E**, Immunofluorescence of retinal astrocytes for GFAP (red) and astrocyte reactivity marker Lcn2 (green). **C:** Cryosection of treated retina. **D-E:** Mechanically isolated astrocytes (**D:** control; **E:** treated).

Conclusions

Our results highlight the induction of reactivity in retinal astrocytes in response to elevated IOP, while also suggesting a role for activated microglia displaying markers of a phenotype associated with Alzheimer's disease[3]. This may illuminate future directions for research into retinal neuroprotection and comports well with previous studies demonstrating parallels between glaucoma and other neurodegenerative diseases.

Berkeley
UNIVERSITY OF CALIFORNIA

Acknowledgements: We would like to thank Prof. Kaoru Saijo for her sage advice and the Functional Genomics Lab at UC Berkeley for their expert handling of our RNA samples.